Dynamic Physical Resource Block Allocation for Fourth Generation Wireless Communication Systems

Thesis submitted in accordance with the requirements of
the University of Liverpool for the degree of Doctor in Philosophy

by

Obilor Nwamadi

April 2011

Declaration

The work in this thesis is based on research carried out at the University of Liverpool. No part of this thesis has been submitted elsewhere for any other degree or qualification and it is all my own work unless referenced to the contrary in the text.

Obilor Nwamadi

Liverpool, United Kingdom.

Abstract

In order to meet the demand for high speed ubiquitous communications, fourth generation (4G) wireless communication systems employ large transmission bandwidth, which needs to be allocated efficiently to all the users in the system. This thesis investigates computationally efficient dynamic physical resource block (PRB) allocation for 4G wireless communication systems using orthogonal frequency division multiple access (OFDMA) and single carrier FDMA (SC-FDMA) techniques. The proposed dynamic PRB allocation schemes, based on greedy algorithms, aim to allocate the available spectrum according to the time and frequency selectivity of different users, and significantly enhance the spectral efficiency (SE) and bit error rate (BER) of the system over the existing allocation algorithms such as the one dimensional (1-D) and two dimensional (2-D) greedy algorithms.

This work contains three main contributions. The first two contributions focus on addressing the inherent bias of the existing greedy algorithms in user ranking, while the third contribution aims to reduce the complexity of the PRB algorithms proposed in the first two contributions.

First, three enhanced ranking PRB allocation algorithms are proposed, which are referred to as the maximum greedy (MG), mean enhanced greedy (MEG) and single mean enhanced greedy (SMEG) algorithms. Simulation results show that the proposed algorithms significantly outperform the existing 1-D and 2-D greedy algorithms in terms of BER and data rate fairness. In particular, the MEG algorithm is shown to achieve an

SE performance close to that achieved by the Hungarian algorithm (optimal algorithm to maximise the required wireless utility), while requiring a much lower computational complexity. In addition, the effects of imperfect channel estimation, root mean square (RMS) delay, Doppler spread and channel estimate feedback delay on performance are investigated. Furthermore, the impact of different optimisation utilities (such as BER and SE) on performance of the allocation algorithms is investigated.

Second, the work in the first contribution is extended to utilise multi-criteria ranking (MCR) for greedy PRB allocation, where different ranking criteria, such as the mean and standard deviation of users utility, are assigned different weights. Simulation results show that the proposed MCR based greedy algorithms can provide near-optimal PRB allocation in terms of BER, SE and outage probability, irrespective of the optimisation utility employed. It is also of interest to see that when MCR is coupled with the channel frequency response (CFR) utility, the BER performance is comparable to case with the BER utility, while at a much lower complexity.

Third, a so-called selective greedy PRB allocation is proposed to reduce the complexity of the algorithms in the first two contributions, where the greedy PRB allocation is applied to a number of selected users with poor rankings, while the rest users with better rankings area allocated PRBs randomly (without optimisation). Simulation results show that the selective mean enhanced greedy (SLMEG) and the selective MCR greedy (SLMCRG) algorithms outperform the 1-D and 2-D greedy algorithms in terms BER and outage probability, especially at high SNR.

Acknowledgements

I have had a wonderful time here in the University of Liverpool. There are many people that have made my time memorable. First of all, I would like the thank my supervisor, Dr. Judy Zhu for giving me the opportunity to pursue my studies. Her hard work, insightfulness and patience have been the key to my success, I am greatly indebted to her. I would also like to thank Professor Asoke Nandi for all his encouragement and support. I am also grateful to the EPSRC for providing all the finance that made the project possible.

I would also like to thank the past members of the SPC group, Dr Sonu Punnose and Dr Luciano Sarperi for convincing me that a research degree is worthwhile and I greatly appreciate their friendship, encouragement and support. I particularly thank Dr Sergio Bravo, for his companionship in the lab. I will not forget all our discussions and yes our singing. Like I said, we should give up research and form a band, I think we will do well. I appreciate the friendship of all the other members of the group, Dr Nazmat Bakinde, Dr Mohammed Musbah, Dr Nan Zhou, Dr Jingbo Gao, Waqar and Hussain.

Many thanks must also go to my family. I have missed all of you a lot. I thank my parents, Mr and Mrs Nwamadi for laying all the right foundations in my early childhood. I am also greatly indebted to my brother, Mr Obasi Nwamadi, none of this would be possible without his encouragement, guidance and financial support, I can never repay you back for everything. You are my hero. I would also thank all

my sisters for their prayers and support. I thank all of you for giving me all the new nieces and nephews. Now that this is finished, I can spend more time with them and not be the "stranger" uncle. I am grateful to my cousins Tony and Colin that helped me settle down quickly in Liverpool, thank you very much for all the wonderful meals I have had in your house. I also thank David Galadima, my roommate and friend of all these years, all your support is greatly appreciated. A big shout out goes out to all my other friends also, you all know who you are.

I would like to thank everybody that has made my time in Liverpool wonderful. Furthermore, I thank all the members of Christ Church Liverpool for their spiritual support. I thank all the tutors of Derby and Rathbone and Roscoe and Gladstone halls for all the fun times we had, and the support through all the sleepless nights caused by "those" first year students.

Finally, I would like to thank all the faculty members of the Eastern Mediterranean University, Cyprus for guiding me in the right direction during my undergraduate degree. I greatly appreciate their teaching, friendship, encouragement and support.

Contents

List of Figures

List of Tables

Mathematical Notations

$(\cdot)^H$	Hermatian Transpose
$(\cdot)^T$	Transpose
x	Scalar value
$\mathbf{x}$	Vector
$\mathbf{X}$	Matrix
$\text{diag}(\mathbf{v})$	a square diagonal matrix whose diagonal elements are entries of vector $\mathbf{v}$
$\text{tr}(\cdot)$	Trace of a square matrix
$E[\cdot]$	Expectation Operator
$F_{M;ik}$	The element in the ith row and kth column of the $(M \times M)$ discrete Fourier transform (DFT) matrix given by $(1/\sqrt{x})\exp(-j2\pi ik/x)$, $i, k = 0, \cdots, (M-1)$
$\mathbf{I}_M$	$M \times M$ identity matrix
$\mathbf{0}_{M\times N}$	$M \times N$ zero matrix

List of Acronyms

1 or 2 - D	1 or 2 - Dimensional
2G	Second Generation
3G	Third Generation
3GPP	Third Generation Partnership Project
4G	Fourth Generation
AHP	Analytic Hierarchy Process
AM	Adaptive Modulation
AMC	Adaptive Modulation and Coding
AMPS	Advance Mobile Phone Service
AWGN	Additive White Gaussian Noise
BER	Bit Error Rate
BLER	BLock Error Rate
CCDF	Complimentary Cumulative Distribution Function
CDF	Cumulative Distribution Function

CDMA	Code Division Multiple Access
CFR	Channel Frequency Response
CIR	Channel Impulse Response
CoMP	Co-ordinated Multi Point
CP	Cyclic Prefix
CSI	Channel State Information
CSM	Collaborative Spatial Multiplexing
dB	decibels
DFT	Discrete Fourier Transform
DMT	Discrete Multi-Tone
Electre	ELimination and Choice Expressing the REality
EDGE	Enhanced Data rates for GSM Evolution
ETACS	European Total Access Communication System
EESM	Effective Exponential SNR Mapping
FDD	Frequency Division Duplex
FDMA	Frequency Division Multiple Access
FEC	Forward Error Correction
FFT	Fast Fourier Transform
FIR	Finite Impulse Response
GPRS	General packet radio service

GSM	Global System for Mobile Communications
HSPA	High Speed Packet Access
IBI	Inter-Block Interference
IDFT	Inverse Discrete Fourier Transform
IFFT	Inverse Fast Fourier Transform
IP	Internet Protocol
IS	International Standard
ISI	Inter-Symbol Interference
ITU	International Telecommunications Union
LDPC	Low Density Parity Check Codes
LOS	Line of Sight
LTE	Long Term Evolution
LTE-A	Long Term Evolution-Advanced
MCR	Multi-criteria Ranking
MCRG	Multi-Criteria Ranking Greedy
SLMCRG	Selective Multiple Criteria Greedy
MCS	Modulation and Coding Scheme
MEG	Mean Enhanced Greedy
MG	Maximum Greedy
MIMO	Multiple Input Multiple Output

MLD	Maximum Likelihood Detection
MMSE	Minimum Mean Square Equalisation
MSE	Mean Square Error
MVT	Minimum Value Threshold
NLOS	Non Line of Sight
OFDMA	Orthogonal Frequency Division Multiple Access
OFDM	Orthogonal Frequency Division Multiplexing
ORI	Outranking Relationship Indicator
OSINR	Output Signal to Interference and Noise Ratio
PAPR	Peak-to-Average Power Ratio
PDP	Power Delay Profile
PRB	Physical Resource Block
Promethee	Preference Ranking Organisation METHod for Enrichment Evaluations
QAM	Quadrature Amplitude Modulation
QoS	Quality of service
QPSK	Quadrature Phase Shift Keying
RC	Ranking Criteria
SLMCRG	Selective Multi-Criteria Ranking Greedy
SLMEG	Selective Mean Enhanced Greedy

RMS	Root Mean Square
SC-FDE	Single Carrier - Frequency Domain Equalisations
SC-FDMA	Single Carrier - Frequency Division Multiple Access
SDMA	Space Division Multiple Access
SE	Spectral Efficiency
SINR	Signal to Interference and Noise Ratio
SMEG	Single Mean Enhanced Greedy
SNR	Signal to Noise Ratio
STD	Standard Deviation
TDD	Time Division Duplex
TDMA	Time Division Multiple Access
TF	Transport Format
TOPSIS	Technique for Order preference by Similarity to Ideal Situation
TTI	Transmission Time Interval
TU	Typical Urban
UMTS	Universal Mobile Telecommunications System
W-CDMA	Wideband Code Division Multiple Access
WiMAX	Worldwide Interoperability for Microwave Access
ZF	Zero Forcing

Chapter 1

Introduction

The need for faster and ubiquitous wireless communications has greatly spurred on the development of the fourth generation (4G) wireless communication systems. The current second generation (2G) and third generation (3G) wireless communication systems are at the limit of their data carrying capacity because of the dramatic increase in the number of personal mobile devices that connect to the internet. This strain on the network often causes customer dissatisfaction due to dropped voice calls or extremely slow data downloads. The increasing uptake of smart phones and mobile broadband internet, will only worsen the situation. Therefore, different proposals have been put forward that improve or totally replace the current systems with more efficient and faster systems. Two examples of such proposals are the beyond 3G long term evolution (LTE) [3] and worldwide interoperability for microwave access (WiMAX) [4] wireless communication systems and their 4G enhancements, LTE-Advanced (LTE-A) [5] and WiMax-2 [2]. It is stipulated by the International Telecommunication Union (ITU) that 4G wireless communication systems should have peak data capacities of 1.5 Gbps and 500 Mbps in the downlink and uplink, respectively [6]. To provide those data rates, the 4G systems will have to use bandwidths in the order of 100 MHz.

To efficiently handle such large bandwidths, 4G systems employ multi-carrier trans-

mission systems such as orthogonal frequency division multiplexing (OFDM) [7], which divides the wideband channel into smaller orthogonal narrowband channels referred to as subcarriers. OFDM conveniently provides scalability with which multiple users can conveniently share the available resources using a multiple access scheme referred to as orthogonal frequency division multiple access (OFDMA) [8]. In addition, the OFDM system is also effective at using larger bandwidths because of its inherent ability to effectively combat severe frequency selective channels with simple equalisers, hence keeping the complexity of these new broadband wireless systems acceptable [9].

Another kind of multiple access technique used in modern high speed wireless communications is single carrier - frequency division multiple access (SC-FDMA) [8]. SC-FDMA is a special case of precoded OFDMA [10, 11], with the underlying difference being that the data is transmitted in the same domain (time) it was created, giving it a single carrier structure, nevertheless, the underlying multi-carrier nature of OFDMA is still present. Unlike OFDMA, where each data symbol occupies a single frequency band (subcarrier), the energy of each data symbol in SC-FDMA is spread over several subcarriers, which combats the situations where there are deep fades on certain subcarriers. At the receiver, equalisation of the SC-FDMA symbols is done in the frequency domain [12] which is similar to that of the OFDMA system. Therefore, SC-FDMA has a lower peak-to-average power ratio (PAPR) [3], higher frequency diversity than OFDMA [8], little or no frequency synchronisation issues and similar complexity to the OFDMA system. Therefore, SC-FDMA is to be used in the uplink of the LTE and LTE-A systems [3, 13].

The large bandwidths and multi-carrier techniques used in the 4G systems, allow for channel dependent allocation of resources to the users in the system. Multi-carrier systems can effectively use dynamic resource allocation (RA) algorithms for bandwidth allocation, by allocating resources according to different users' time and frequency selectivity. Therefore, 4G systems, when coupled with dynamic RA, benefits from in-

creased bandwidth efficiency, which is not the case for older wireless communication systems [3]. Resource allocation techniques have been explored in the literature for the OFDMA and SC-FDMA systems [14–25] and references therein. Most of the existing RA algorithms allocate subcarriers singly to different users, and perform bit and power allocation for each subcarrier. However, the large amount of subcarriers in the current wide band wireless communication systems renders the complexity of implementing these subcarrier by subcarrier RA algorithms intractable. Therefore, 4G systems allocate subcarriers in blocks referred to as physical resource blocks (PRBs) in the LTE-A system [3] and sub-channels [26] in the WiMAX-2 system. Users are allocated one or more blocks depending on their needs.

1.1 Motivation and Objectives

There are a few existing greedy algorithms that allocate PRBs to users [13, 27–29]. Greedy algorithms [27] are used to keep the complexity low, especially when there are many users in the system, as is proposed for the large cell sizes in the 4G systems [13,26]. However, due to the myopic nature of greedy algorithms, the performances achieved are not always acceptable, especially in terms of capacity, bit error rate (BER) and outage probability simultaneously.

The existing greedy algorithms such as the one dimensional (1-D) and two dimensional (2-D) greedy [27, 28] are too myopic in nature. The 1-D greedy algorithm allocates a PRB to each user independently, without considering the effect of the allocation on the performance of other users. The 2-D greedy algorithm allocates the best PRBs in the early iterations, at the price of allocating very poor PRBs to users allocated in the later iterations. The result of both these algorithms is poor average BER and bandwidth wastage, due to very high outage probability. The existing optimal Hungarian algorithm [30], is too complex to be used for real time wireless communica-

tion systems, while heuristic algorithms such as genetic algorithms (GA) [31] may not always meet the strict timing requirements of real time communications, due to long a convergence time. Therefore, novel high performance, low complexity efficient greedy PRB allocation algorithms are desired.

In this work, the main objective is the development of practical and computationally efficient PRB allocation algorithms that can be used in 4G wireless communication systems.

1.2 Summary of Contributions

The following are the main contributions of this thesis:

- Three enhanced ranking PRB allocation algorithms are proposed, which are referred to as the maximum greedy (MG), mean enhanced greedy (MEG) and single mean enhanced greedy (SMEG) algorithms. The enhanced ranking is used to determine the order with which the greedy algorithm optimises PRB allocation, since a greedy algorithm cannot simultaneously optimise PRB allocation across the users. Simulation results show that the proposed algorithms significantly outperform the existing 1-D and 2-D greedy algorithms in terms of BER and data rate fairness. In particular, the MEG algorithm is shown to achieve an SE performance close to that achieved by the Hungarian algorithm (optimal algorithm to maximise the required wireless utility), while requiring a much lower computational complexity. In addition, the effects of imperfect channel estimation, root mean square (RMS) delay, Doppler spread and channel estimate feedback delay on performance are investigated. Furthermore, the impact of different optimisation utilities (such as BER and SE) on performance of the allocation algorithms is investigated.

- The work in the first contribution is extended to utilise multi-criteria ranking

(MCR) for greedy PRB allocation, where different ranking criteria, such as the mean and standard deviation of users utility, are assigned different weights. Extensive numerical analysis is used to determine the best operating weights for the criteria. Simulation results show that the proposed MCR based greedy algorithms can provide near-optimal PRB allocation in terms of BER, SE and outage probability, irrespective of the optimisation utility employed. In particular, when MCR is coupled with the channel frequency response (CFR) utility, the BER and outage probability performance is comparable to case with the BER utility, while at a much lower complexity.

- A so-called selective greedy PRB allocation is proposed to reduce the complexity of the algorithms in the first two contributions, where the greedy PRB allocation is applied to a number of selected users with poor rankings, while the rest users with better rankings area allocated PRBs randomly (without optimisation). The random PRB allocations to better ranked users incurs negligible computational cost. Simulation results show that the selective mean enhanced greedy (SLMEG) and the selective MCR greedy (SLMCRG) algorithms outperform the 1-D and 2-D greedy algorithms in terms BER and outage probability, especially at high SNR.

1.3 List of Publications

The following publications have arisen as a direct result of the research carried out during the author's PhD study.

Journal Papers

1. O. Nwamadi, X. Zhu and A.K. Nandi, " Dynamic physical resource block allocation algorithms for uplink long term evolution", to appear in *IET communica-*

tions, 2011.

2. O. Nwamadi, X. Zhu and A.K. Nandi, "Multi-criteria physical resource block allocation for uplink LTE", submitted to *Signal Processing* for publication in 2011.

Conference Papers

1. O. Nwamadi, X. Zhu and A.K. Nandi, "Dynamic subcarrier allocation for single carrier - FDMA systems", in Proceedings, *Europen Signal Processing Conference (EUSIPCO)*, Lausanne, Switserland, August 2008.

2. O. Nwamadi, X. Zhu and A.K. Nandi, "Enhanced greedy algorithm based dynamic subcarrier allocation for single carrier - FDMA systems", in Proceedings *IEEE Wireless Communication and Networking Conference (WCNC)*, Budapest, Hungary, April 2009.

3. O. Nwamadi, X. Zhu and A.K. Nandi, "Comparison of optimisation criteria for dynamic subcarrier allocation in single carrier - FDMA systems", in Proceedings, *IEEE Computers and Devices for Communication conference*, Calcutta, India, December 2009.

4. O. Nwamadi, X. Zhu and A.K. Nandi, "Low complexity mean-greedy algorithms for dynamic subcarrier allocation in single carrier - FDMA systems", in Proceedings, *Europen Signal Processing Conference (EUSIPCO)*, Aalborg, Denmark, August 2010.

5. O. Nwamadi, X. Zhu and A.K. Nandi, "Multi-criteria ranking based greedy algorithm for physical resource block allocation in LTE systems", submitted to *Europen Signal Processing Conference (EUSIPCO)*, Barcelona, Spain, 2011.

Chapter 2

Wireless Communications

In this chapter, wireless communications is introduced. In Section 2.1, the wireless communication channel parameters and models are explained. An overview of wireless communication systems, with an emphasis on the 4G systems is presented in Section 2.2. Finally, the multi-carrier and multi-user wireless communication techniques used in the 4G systems are explained in section 2.3.

2.1 Wireless Communication Channels

2.1.1 Additive White Gaussian Noise Channel

The fundamental problem that affects all types of communications is noise. Noise are the unwanted signals that affect the fidelity of the desired signal. In wireless communications, there are numerous sources of noise: thermal noise that exists in all matter, artificial noise from other electrical machinery and impulse noise from radiation emitting devices [9]. Due to the central limit theorem, the composition of these different noise sources is white and Gaussian distributed. The effect of this composite noise on the transmitted data is additive, hence the name additive white Gaussian noise

(AWGN). The received data through an AWGN channel is given by

$$r(t) = x(t) + n(t) \tag{2.1}$$

where $r(t)$ and $x(t)$ are the received and transmitted data at time t, respectively, and $n(t)$ is the effect of AWGN at time t modelled by a complex Gaussian random variables with a noise power density of $N_0/2$ per dimension. The easiest way of combating AWGN is to make the power of the transmitted signal considerably greater than that of the noise.

2.1.2 Large Scale Fading

Path loss and shadowing are the main causes of large scale fading (experienced over hundreds/thousands of metres) in wireless communication systems. Path loss is the reduction in the average received power due to the distance between transmitter and receiver, while shadowing is the change in received power due to terrain and large obstacles in path of transmission. Unlike AWGN, the effects of large scale fading is multiplicative, not additive [32,33]. The received signal is expressed by

$$r(t) = \sqrt{P}x(t) + n(t) \tag{2.2}$$

where $r(t)$, $x(t)$ and $n(t)$ are the received, transmitted and noise signals, respectively. While P is the average large scale fading factor which includes the effects of both the path loss and shadowing. In general, P is to a large extent dependent on the distance between transmitter and receiver and time independent, however, in large coverage areas, P may exhibit a time dependence if the mobile is traveling quickly away from the base station (BS) [33]. P also has a random effect due to shadowing, because the effect of shadowing is not deterministic [34]. To compensate for the effect of path loss, the transmit power of the signal is increased, within acceptable bounds. Unfortunately,

this will not always solve the shadowing problem, because shadowing is random.

2.1.3 Small Scale Fading

Small scale fading is the general term for the rapid fluctuations of the amplitude, phase and delay of the transmitted signal while propagating through the channel. These amplitude and phase fluctuations are caused by the interference due to reflection and diffraction between multiple versions of the transmitted signal that arrive at the receiver at different times (delays). Unlike large scale fading, the effects of small scale fading are realised over very small distances (a few wavelengths) and are time dependent. The parameters that affect small scale fading are discussed below based on [9, 32, 33].

Power Delay Profile

The *Power Delay Profile* (PDP) is the average power of the lth path in the channel impulse response (CIR) $h(l)$, which is a function of the reflection and diffraction elements in the channel. The PDP is usually exponentially decreasing, which implies that the average power of $h(l)$ decreases exponentially with increase of the delay. This is because signals with large delay will most likely have travelled larger distances, which in turn cause them to have weaker signal power at the receiver (path loss). The PDP of the channel, $h(l)$ is expressed by

$$E|h_l| = b \exp\left(\frac{-\sigma_l}{\sigma}\right) \tag{2.3}$$

where the expectation operator E implies that the PDP is an ensemble average of a large number of channel realisations, b is the normalisation parameter, σ_l is the delay of the lth path and σ is the root mean square (RMS) delay spread. A normalised exponential PDP of a channel is shown in Figure 2.1

The PDP of a typical urban (TU) wireless channel with six delay bins is displayed

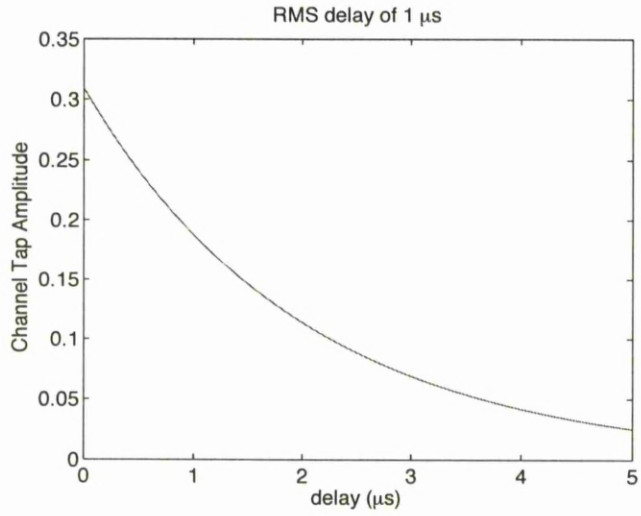

Figure 2.1: Normalised exponential power delay profile

Table 2.1: Power delay profile for the T.U. six channel [1].

Delay (μs)	0.0	0.2	0.6	1.6	2.4	5.0
Power (dB)	-3.0	0.0	-2.0	-0.6	-0.8	-10.0

in Table 2.1.

Root Mean Square Delay Spread

The RMS delay spread of the channel is the square root of the second central moment of the PDP, and is expressed by

$$\sigma = \sqrt{\frac{\sum_l P(\sigma_l)\sigma_l^2}{\sum_l P(\sigma_l)} - \left(\frac{\sum_l P(\sigma_l)\sigma_l}{\sum_l P(\sigma_l)}\right)^2} \tag{2.4}$$

where $P(\sigma_l) = |h(l,i)|^2$ is the power of the lth path of h in the ith time interval. According to (2.4), $\sigma = 0$ if $h(l,i) = 0\ \forall l \neq 0$ and $\sigma > 0$ otherwise. Therefore, for a channel with only one path $h(l,i)$ at $l = 0$, the RMS delay is equal to zero. The RMS delay spread is highly correlated to the amount of frequency dispersion channel has on

the transmitted signal. This frequency dispersion increases the frequency diversity of the channel.

Coherence Bandwidth

The *coherence bandwidth* B_c, is the group of frequencies over which the effects of the channel remain static or highly correlated. This implies that a signal with bandwidth B_s, passing through a channel with coherence bandwidth B_c, will experience minimal variations in its amplitude and phase, if $B_s < B_c$. When the frequency correlation function is above 0.5, the B_c is approximately related to the RMS delay spread by [33],

$$B_c \approx \frac{1}{5\sigma} \tag{2.5}$$

Therefore, a large RMS delay spread implies a small bandwidth over which the effect of the channel on signal remains static. A channel with a large RMS delay spread, is highly frequency dispersive. This frequency dispersiveness can be harnessed by sufficient coding or channel dependent scheduling.

Doppler Spread

The *Doppler spread* B_d is the amount of broadening a signal experiences as it propagates through the channel. This is affected by the relative speed and direction between the transmitter, receiver and other objects in the terrain. The Doppler shift f_d is given by

$$f_d = \frac{v}{\lambda} \cos\theta \tag{2.6}$$

where v is relative velocity between transmitter, receiver and other reflective and refractive objects in the terrain, λ is the wavelength of the carrier frequency and θ is the angle between the the direction of motion of receiver and transmitter. The Doppler spread is the maximum Doppler shift defined as $B_d = f_m = \frac{v}{\lambda}$.

Coherence Time

The *coherence time* T_c, is the period (time) over which the channel does not exhibit any significant changes in amplitude or phase. In other words, this is the period over which two samples of the channel have a high correlation. When the time correlation function is above 0.5, the T_c is is given by [33],

$$T_c = \frac{9}{16\pi f_m} \tag{2.7}$$

where f_m is the maximum Doppler shift (Doppler spread). This implies that a signal with symbol duration T_s passing through a channel with coherence time T_c, will experience minimal time variations of its amplitude and phase if $T_s < T_c$.

Types of small scale fading channels

Based on the parameters explained above, the small scale fading effects of the channel can be characterised into the following categories.

Flat fading channel: A channel is regarded as flat fading if the bandwidth of the signal B_s is much smaller than the coherence bandwidth of the channel B_c and the RMS delay spread of the channel σ is much smaller than the symbol duration of the signal T_s. Furthermore, from (2.5), when the RMS delay spread is zero, the coherence bandwidth is infinite, meaning the channel is frequency flat over all the frequencies concerned.

$$B_s << B_c \text{ and } T_s >> \sigma \tag{2.8}$$

Frequency selective fading channel: A channel is regarded as frequency selective, if the bandwidth of the signal B_s is greater than the coherence bandwidth of the channel B_c and the symbol period of the signal T_s is smaller than the RMS delay spread of the channel σ. In general, the higher the RMS delay spread, the more frequency selective

a channel. According to (2.5), as the RMS delay spread increases, the bandwidth over which the channel is frequency flat (B_c) reduces.

$$B_s > B_c \text{ and } T_s < \sigma \tag{2.9}$$

Slow fading channel: A channel is regarded as slow fading if the signal symbol period T_s is much smaller than the coherence time T_c of the channel and the bandwidth of the signal B_s is much greater than the Doppler spread of the channel B_d. According to (2.6) the slower a mobile moves, the smaller its Doppler spread becomes, hence increasing its probability (the symbol period of the signal T_s is also important) of encountering a slow fading channel.

$$T_s << T_c \text{ and } B_s >> B_d \tag{2.10}$$

Fast fading channel: A channel is regarded as fast fading if the signal symbol period T_s is larger than the coherence time of the channel T_c and the bandwidth of the signal B_s is smaller the Doppler spread of the channel B_d. This means that the signal passing through this kind of channel will experience time variations of its amplitude and phase. The probability of encountering a fast fading channel is increased when the speed of the mobile increases, because the coherence time decreases with an increase in Doppler spread according to (2.6) and (2.7).

$$T_s > T_c \text{ and } B_s < B_d \tag{2.11}$$

The first two types of channel (flat and frequency selective fading) determine the frequency diversity of the channel while the last two (slow and fast fading) determine the time diversity of the channel.

Nevertheless the combination of these effects create four types of channel: slow flat fading, fast flat fading, slow frequency selective and fast frequency selective fading.

Current 4G systems have large bandwidths, high data rates and a maximum specified centre frequency in the order of 11 GHz. Therefore, the most encountered channel is the slow frequency selective fading channel [33]. It is slow fading because at speeds of about 200 km/h (a practical upper-limit), B_d is about 2 kHz (using centre frequency of 11 GHz and (2.6)), which is less far less than the minimum 1.25 MHz bandwidth of the LTE system (the minimum bandwidth in WiMAX is 5 MHz), and at the same speed, T_c is about 89.52 μs (using (2.7)), which is greater than the 1/1.25 MHz = 800 ns symbol time T_s, hence satisfying (2.10). It is also frequency selective because the RMS delay spreads σ, of the wideband channels is in the order of 1 to 10 μs [3], which is greater than the maximum 800 ns signal period T_s and the signal bandwidth of 1.25 MHz is larger than the coherence bandwidth B_c which has values of about 200 kHz (calculated with (2.5) and minimum RMS delay of 1 μs), hence satisfying (2.9).

An effective way to include all the parameters of the wireless communications channel into the mathematical model $h(l, i)$, is the Clark's model which is explained in [33]. In the Clarke's model, the time autocorrelation, of the complex envelop of the channel, R_e is specified by

$$R_e(\tau) = P_{av} J_0(2\pi B_d \tau) \tag{2.12}$$

where P_{av} is the average received power in the channel, J_0 is the zeroth-order Bessel function of the first kind, B_d is the Doppler spread and τ is the time offset. The power spectrum of the wireless channel is determined by the Fourier transform of R_e, which is expressed by

$$S_e = \begin{cases} \frac{P_{av}}{\sqrt{1-(\frac{f}{B_d})^2}} & f < B_d \\ 0 & f > B_d \end{cases} \tag{2.13}$$

where f/B_d is the the normalised frequency of the channel. To generate the channel, two independent Gaussian noise sources are filtered by (2.13) above, before being passed through an IFFT to get the time domain characteristics as described in [33]. An

alternative process used to generate the channel is the autoregressive process, which is based on the Bessel function [35].

The signal detected at the receiver at discrete time instant i is the convolution of the CIR ($h(l,i)$) with the transmitted signal expressed by

$$r(i) = \sqrt{P}\sum_{l=0}^{L-1} h(l,i)s(i-l) + n(i) \tag{2.14}$$

where $h(l,i) \in \mathbb{C}$ is the lth path gain ($l = 0, 1, \cdots, L-1$), which combines the effects of the small scale fading and the transmit and receive pulse shaping filters at time i [34], P is the effect of large scale fading, while $n(i)$ is the complex AWGN with noise power spectral density of $N_0/2$ per dimension. L is the total number of resolvable multi-paths (taps) in the channel. $h(l,i)$ is a complex independent and identically distributed (*i.i.d.*) random variable which have a Rayleigh distributed magnitude according to

$$p(|h(l,i)|) = \frac{|h(l,i)|}{\eta^2}\exp(-\frac{|h(l,i)|^2}{2\eta^2}) \tag{2.15}$$

and uniformly distributed phase. The Rayleigh distribution is shown in Figure 2.2.

Figure 2.3 shows a typical snapshot of how the power in dB of a Rayleigh fading channel varies with time. It is clear to see the reoccurrence of deep fades - instances where the power of the channel is very low (less than -20 dB). The Rayleigh channel model is most relevant in non line of sight (NLOS) situations, where there is no direct path between transmitter and receiver, which is mostly the case in urban scenarios of wireless communication systems. Other distributions, such as the Rice distribution [34] is used to model the channel when there is a LOS, as well as other signal scatterers between transmitter and receiver.

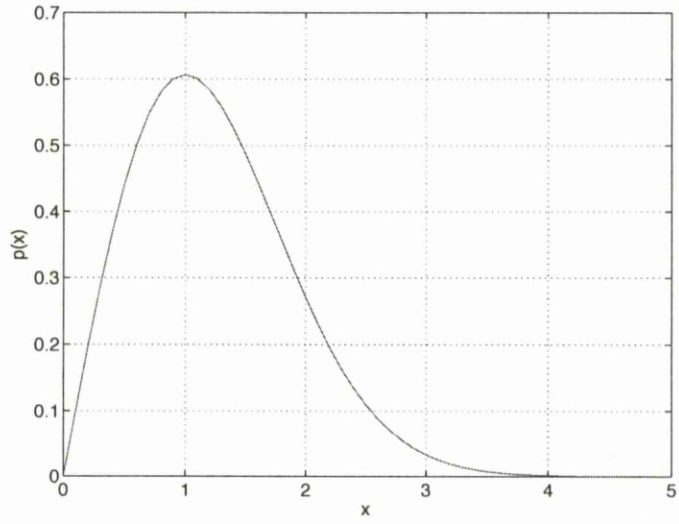

Figure 2.2: Rayleigh distribution of the magnitude of channel for $\eta = 1$.

2.2 Wireless Communication Systems

Wireless communications, as the name implies, is the ability to transfer information across two physically remote points without the need for a physical connection. The ability to send information in this manner has existed for a long time, for example, the smoke signals at the top of a mountain that relays information to observes in remote locations. However, the use of electromagnetic signals has made wireless communications more efficient and widespread. Wireless communications has predominantly been used to carry speech signals, either as messages between two points, for example, one way radio communications (walkie talkie), or as broadcast of a message between one point and many others, for example, news broadcast, where many people with receiving devices can tune to required frequency to receive the signals. First generation personal wireless communication systems such as AMPS and ETACS were used predominantly for speech communications [33].

In more recent times, wireless communications are not used to carry only voice

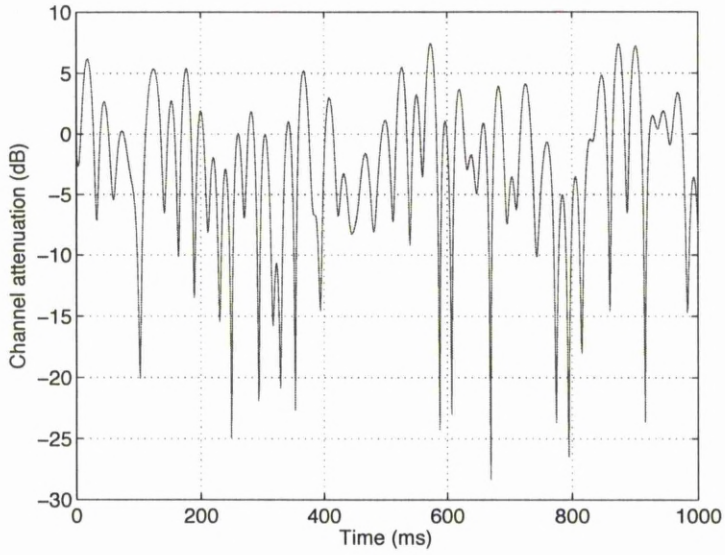

Figure 2.3: The power in dB of a typical Rayleigh fading channel at 2 GHz

signals but also various kinds of data, such as text and pictures and the development of digital communications has greatly benefited this new wave of data transfer. The first widespread digital communication systems are the GSM and the CDMA based IS-95A (cdmaOne), which are both regarded as 2nd generation (2G) wireless communication systems. Their data rates of about 10 Kbps was sufficient for voice communications, but too slow for data communications that is found on the internet. Hence, enhancements to the GSM system in the form of GPRS (171 kbps) and EDGE (384 kbps) and to the cdmaOne system IS-95B (64 kbps), were created. These enhancements commonly referred to as 2.5G allowed efficient IP based transmission of data. However, these 2.5G speeds were still unsuitable for real time video data. Hence, the 3G UMTS (2 Mbps) and CDMA2000 (2.4 Mbps) systems that employ the W-CDMA technique were invented [33] enhance video communications. However, with the explosion of smart handheld devices that frequently access the internet, it became clear that these systems will not be sufficient for all the internet traffic. Therefore, the UMTS system

has enhancements such as HSPA and HSPA+ [3] that improve the data transfer rate. However, all these systems, while supporting IP data transfer, still possess circuit switched connections for voice communications.

Proposals to create future high speed data communications then began and a move to all IP data transfer was chosen. Two such systems are the third generation partnership project - long term evolution (3GPP-LTE), commonly known as the LTE system and the WiMax system developed by the IEEE. To provide the required date rates, large transmission bandwidths of up to 20 MHz are employed. In addition, new radio techniques such as OFDMA and SC-FDMA that effectively use these large bandwidths are also used. These LTE and WiMax systems are not real 4G systems, because they do not meet with the ITU specifications. Hence, the LTE-Advanced (LTE-A) [5] and WiMax 2 are the 4G enhancements to the LTE and WiMax systems, respectively. To achieve the required data rates, these systems will use bandwidths up to 100 MHz bandwidth and will employ advanced techniques such as MIMO [36], carrier aggregation [37], relay [38], co-ordinated multi-point (CoMP) [39] and collaborative spatial multiplexing (CSM) [40] [41]. The LTE-A and WiMax 2 will be backward compatible with the current systems. Therefore, the core technologies such as OFDMA and SC-FDMA will be the same [42, 43].

Table 2.2 shows a comparison between the pre-4G (LTE and WiMax) and 4G systems (LTE-A and WiMax 2).

2.3 Wireless Communication Techniques

Time division duplex (TDD) [33] systems enables a user to transmit and receive data in two time slots on the same frequency spectrum. This allows full duplex communications, where a user can transmit as well as receive data. An advantage of TDD operation is that channel estimation is simpler, because estimating the channel in one

Table 2.2: Comparison between the common pre-4G and 4G systems.

	LTE	LTE-A	WiMax	WiMax 2
Radio Tech.	SC-FDMA (UL) OFDMA (DL) MIMO	SC-FDMA (UL) OFDMA (DL) MIMO CSM, CoMP Relay	OFDMA MIMO	OFDMA MIMO Relay
Peak Data Rate (Mbps)	300(DL) 75(UL)	1000 (DL) 500 (UL)	128 (DL) 66(UL)	300 (DL) 112 (UL)
Subcarrier Mapping	Localised	Localised	Interleaved Localised	Interleaved Localised
Bandwidth (MHz)	1.25 to 20	1.25 to 100	5, 7, 8.75, 10	5 to 20
Forward Error Correction	Turbo Convolutional	Turbo Conv.	Turbo Block Conv.	Turbo Block Conv. LDPC

direction (transmission), also gives the channel in the opposite direction (reception), due to channel reciprocity [44].

Frequency division duplex (FDD) [33] systems enables a user to transmit and receive data on two frequency spectrums simultaneously. This also allows full duplex communications. It is more complex to estimate the channel for FDD systems, because the two channels need to be estimated, hence there is wastage of spectrum due to excessive channel overhead for sounding/reference signals for both channels [3]. TDD and FDD are the fundamental techniques used to guarantee two-way communications. They are employed in both of the discussed 4G systems.

Examples of multiuser systems are time division multiple access (TDMA), frequency division multiple access (FDMA) and code division multiple access (CDMA) that share the time, frequency and code resources among all the users, respectively [9]. Space division multiple access (SDMA) [45] is a multiuser access scheme, where directional antennas are used to stir signals to different users in space. In modern high speed

wireless communication systems, two or more of these multiple access systems can be employed. For example, the GSM system uses TDMA overlaid on an FDMA system, while the CDMA2000 system uses CDMA overlaid on an FDMA system [9].

2.3.1 OFDMA Technique System Model

OFDMA is the multiple access technique based on OFDM. OFDM is a form of multi-carrier communications, where the available spectrum is divided into smaller orthogonal parts known as *subcarriers* [7] and each subcarrier is used to carry a symbol(s) of data, simultaneously. Due to the orthogonality of the subcarriers, the data transmitted on the subcarriers are free from intercarrier interference which is the usual problem with older non-orthogonal FDM systems [46]. Three orthogonal subcarriers are depicted in Figure 2.4.

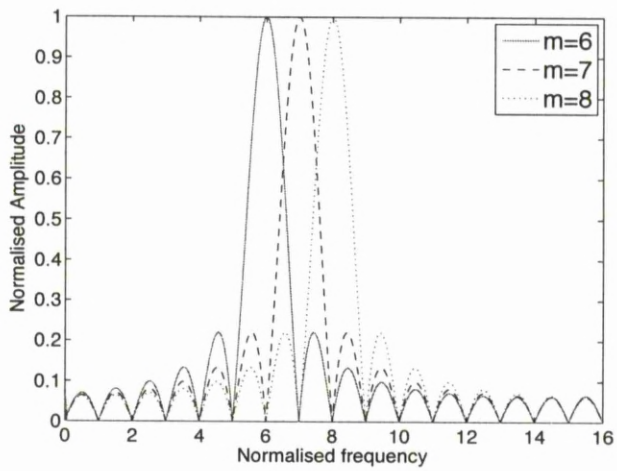

Figure 2.4: Three subcarriers in an OFDM system

Figure 2.5 depicts the block diagram for the OFDM system. Forward error correction (FEC) may or may not be applied to the data (depends on the system), then the data are parallelised. The fast Fourier transform (FFT) operations are used to modu-

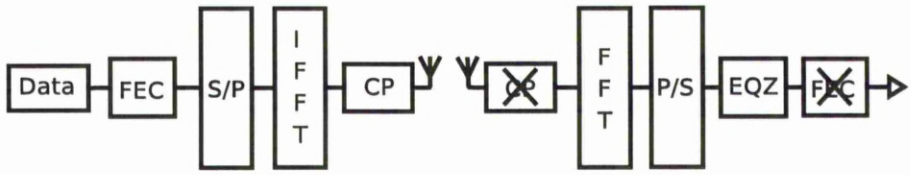

Figure 2.5: OFDM block diagram

late the signals onto the different orthogonal subcarriers [46, 47]. In the presence of a frequency selective channel, block data transmission techniques such as these are prone inter-block interference (IBI). To overcome the effects of IBI, a cyclic prefix (CP) - a copy of at least the last $(L-1)$ symbols - is appended to the front of the block of data, where L is the number of multipath in the frequency selective channel. In addition to tackling IBI, the CP makes the channel appear cyclic, so that the frequency selective channel appears as a flat fading channel [7]. The $(N \times N)$ time-domain circulant Toeplitz channel convolution matrix is given by $\mathbf{H}$, which includes CP insertion and removal, with the first column $\mathbf{H}^{(:,1)} = [h(0)\ h(1)\ \cdots\ h(L-1)\ 0\ \cdots\ 0]^T$ and first row $\mathbf{H}^{(1,:)} = [h(0)\ 0\ \cdots\ 0\ h(L-1)\ h(L-2)\ \cdots\ h(1)]$. The received signal is given by,

$$\mathbf{r} = \mathbf{H}\mathbf{F}_N^H\mathbf{d} + \mathbf{n} \tag{2.16}$$

where $\mathbf{d}$ is the data vector and $\mathbf{F}_N^H$ is the $(N \times N)$ inverse discrete Fourier transform (IDFT) matrix, $\mathbf{n}$ is the AWGN vector with complex-valued elements that have zero mean and variance N_0. At the BS, the received signals are demodulated by the N-point discrete Fourier transform (DFT), to get $\tilde{\mathbf{r}} = [\tilde{r}^0 \cdots \tilde{r}^{N-1}]$, where $\tilde{r}^n$ is the received data on the nth subcarrier $(n = 0, \cdots, N-1)$. $\tilde{\mathbf{r}}$ is expressed as

$$\tilde{\mathbf{r}} = \mathbf{F}_N\mathbf{H}\mathbf{F}_N^H\mathbf{d} + \mathbf{F}_N\mathbf{v} \tag{2.17}$$

Defining $\tilde{\mathbf{H}} = \mathbf{F}_N\mathbf{H}\mathbf{F}_N^H$, where $\mathbf{H}$ is diagonalised by pre- and post multiplication with

the DFT and IDFT matrices, respectively. Substituting $\tilde{\mathbf{H}}_\mathbf{u}$ into (2.17) gives

$$\tilde{\mathbf{r}} = \tilde{\mathbf{H}}\mathbf{d} + \tilde{\mathbf{v}} \tag{2.18}$$

where $\tilde{\mathbf{H}}$ is the $(N \times N)$ is the diagonal channel frequency response (CFR) matrix. This implies that the frequency selective channel is transformed into multiple frequency flat channels with the addition and removal of CP, hence linear one tap equalisers can be used to remove the effect of the channel instead of long finite impulse response (FIR) filters. This means that the complexity of an OFDM system is tractable even for systems with very large bandwidths, where the multipath of the channel can be very long.

In OFDMA, different users are allowed to transmit data on a portion of the available subcarriers. However, due to interference issues users cannot share subcarriers simultaneously, *i.e.*, users are orthogonal in the frequency domain [8]. The block diagram for OFDMA is shown in Figure 2.7 with U users and a total number of N data carrying subcarriers. The N subcarriers are divided into K physical resource blocks (PRBs) $(K \geq U)$, with M subcarriers in each block $(N = KM)$. Let d_u^m denote the mth $(m = 0, \cdots, M-1)$ data symbol of unit average symbol energy within a block $\mathbf{d}_u = [d_u^0 \ \cdots \ d_u^{M-1}]^T$ of M symbols transmitted by the user u $(u = 0, \cdots, U-1)$. Each user is allocated M subcarriers by the subcarrier mapping module, where each user's subcarrier mapping is unique. There are three types of subcarrier mapping: *localised mapping*, where each user is allocated a contiguous set of subcarriers, *interleaved mapping*, where the users subcarriers are alternated and *distributed mapping*, where users are allocated subcarriers in neither a perfectly localised or interleaved way [8]. The mapping can be viewed as a multiplication of a mapping matrix $\mathbf{M}_u$ of size $(N \times M)$

with the DFT of $\mathbf{d}_u$. Assuming $K = U$, the localised mapping matrix $\mathbf{M}_u$ is given by

$$\mathbf{M}_u = \begin{bmatrix} \mathbf{0}_{(k_u M)\times M} \\ \mathbf{I}_M \\ \mathbf{0}_{(N-k_u M-M)\times M} \end{bmatrix} \tag{2.19}$$

which indicates that $k_u M$ to $(k_u M + M - 1)$ subcarriers $(0 \leq k_u \leq K-1)$ are allocated to the uth user. Similarly the interleaved mapping is given by

$$\mathbf{M}_u = \begin{bmatrix} \mathbf{\Delta}_{k_u,0} \\ \mathbf{\Delta}_{k_u,1} \\ \vdots \\ \mathbf{\Delta}_{k_u,M-1} \end{bmatrix} \tag{2.20}$$

where $\mathbf{\Delta}_{a,b}$ represents an $(M \times M)$ matrix that has 1 in the ath row and the bth column and zero elsewhere. The distributed mapping matrix will have one in random positions as desired. A visual representation of the three mapping methods are shown in Figure 2.6 for $U = 3$ users, a total of $N = 9$ subcarriers and $M = 3$ subcarriers per user.

After subcarrier mapping, an N-point IDFT is used to transform the data into the time domain and a CP is appended before transmission, similar to the single user OFDM case.

At the receiver, the CP is removed and the received signal is the sum of all the users transmissions given by

$$\mathbf{r} = \sum_{u=0}^{U-1} \mathbf{H}_u \mathbf{F}_N^H \mathbf{M}_u \mathbf{d}_u + \mathbf{v} \tag{2.21}$$

where $\mathbf{H}_u$ is the circulant channel matrix which includes the effects of CP insertion and removal for the uth user, $\mathbf{M}_u$ is the subcarrier allocation matrix, $\mathbf{d}_u$ and $\mathbf{v}$ are the user's data and noise vectors, respectively. The DFT operation is used to the demodulate the

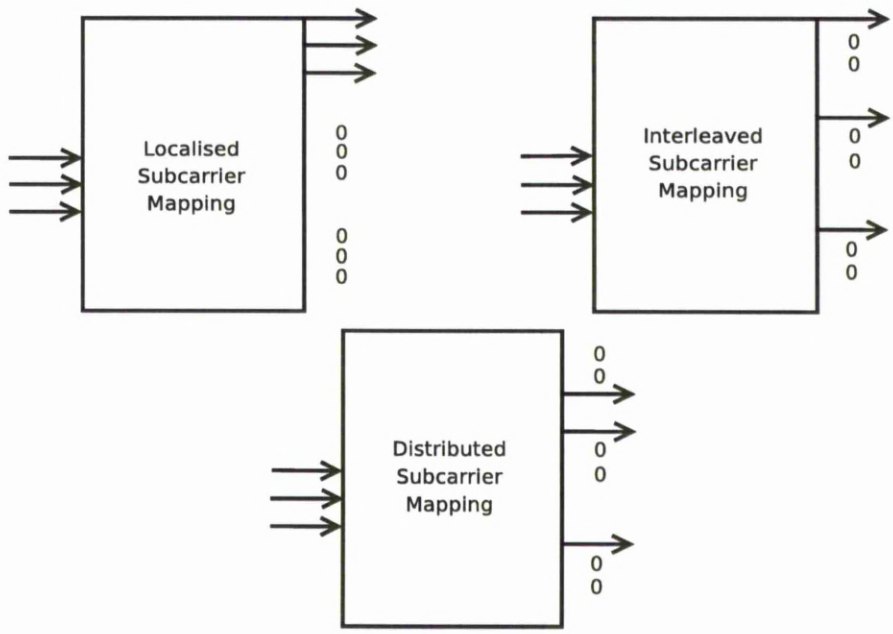

Figure 2.6: Different types of subcarrier mapping for $U = 3$ users, $N = 9$ subcarriers with $M = 3$ subcarriers per user.

data to obtain

$$\tilde{\mathbf{r}} = \sum_{u=0}^{U-1} \mathbf{F}_N \mathbf{H}_u \mathbf{F}_N^H \mathbf{M}_u \mathbf{d}_u + \mathbf{F}_N \mathbf{v} \tag{2.22}$$

Similar to the OFDM system, $\tilde{\mathbf{H}}_u = \mathbf{F}_N \mathbf{H}_u \mathbf{F}_N^H$, where $\mathbf{H}_u$ is diagonalised by pre- and post multiplication with the DFT and IDFT matrices, respectively. Substituting $\tilde{\mathbf{H}}_\mathbf{u}$ into (2.22) gives

$$\tilde{\mathbf{r}} = \sum_{u=0}^{U-1} \tilde{\mathbf{H}}_u \mathbf{M}_u \mathbf{d}_u + \tilde{\mathbf{v}} \tag{2.23}$$

where $\tilde{\mathbf{H}}_u = \text{diag}([\tilde{H}_u^0 \cdots \tilde{H}_u^{N-1}]^T)$ and $\tilde{H}_u^n = \sum_{l=0}^{L} h_u(l) \exp(-j2\pi nl/N)$, $(n = 0, \cdots, N-1)$ is the discrete frequency response of the channel for the uth user. $\tilde{\mathbf{v}} = \mathbf{F}_N \mathbf{v}$ is the frequency domain AWGN. Due to the orthogonality of the mapping, each subcarrier n can be associated with a unique user and each user's frequency domain data $\tilde{\mathbf{r}}_\mathbf{u} = [\tilde{r}_u^0 \cdots \tilde{r}_u^{M-1}]^T$ is de-mapped from $\tilde{\mathbf{r}}$ using $\mathbf{M}_u^T$, which is the transpose of the

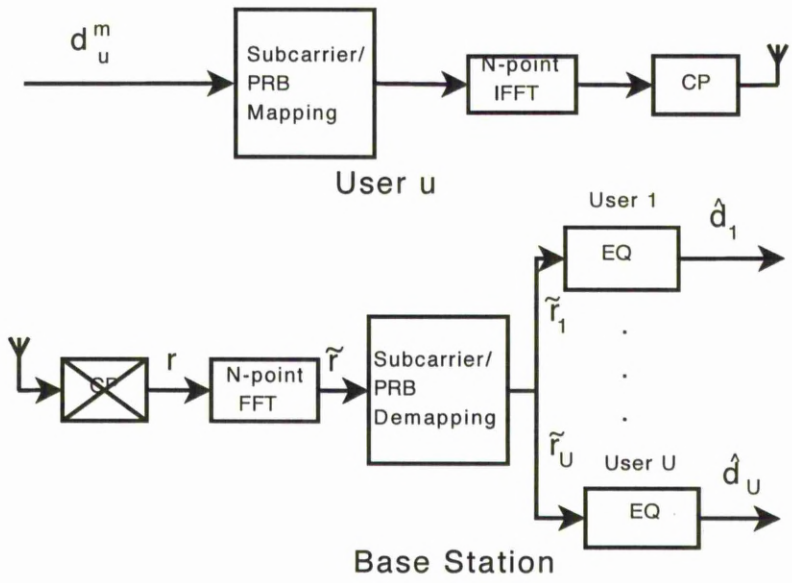

Figure 2.7: OFDMA block diagram

initial mapping matrix. Each user's received data is given by

$$\tilde{\mathbf{r}}_u = \mathbf{M}_u^T \tilde{\mathbf{r}} = \mathbf{M}_u^T \tilde{\mathbf{H}}_u \mathbf{M}_u \mathbf{d}_u + \tilde{\mathbf{v}}_u \tag{2.24}$$

where $\tilde{\mathbf{v}}_u = \mathbf{M}_u^T \tilde{\mathbf{v}}$ is a $(M \times 1)$ noise vector for the uth user. Since the users subcarriers are orthogonal to one another, channel equalisation can be done independently for each user as shown in Figure 2.7. OFDMA minimises the interference between users in the system and also allows the use of less complex channel equalisation. Hence, the OFDMA system keeps all the advantages of the single user OFDM system.

2.3.2 SC-FDMA Technique System Model

SC-FDMA is the multiple access technique based on single carrier - frequency domain equalisation (SC-FDE). SC-FDE, unlike OFDM, is a single carrier communication technique. However, the data is transmitted in blocks similar to OFDM. SC-FDE

also includes a CP to the blocks of data before transmission, in a similar fashion to OFDM, as seen in Figure 2.8. At the receiver, the CP is removed and the signal is transformed into the frequency domain before channel equalisation is performed [48]. After equalisation, the data is then transformed back into the time domain, after which FEC decoding takes place.

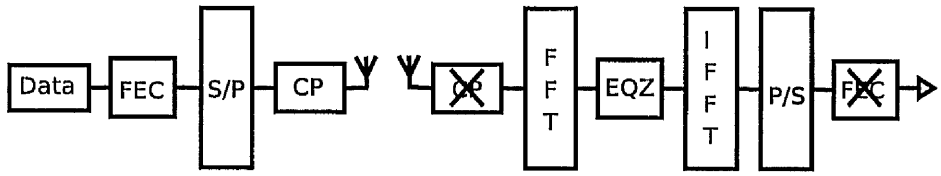

Figure 2.8: SC-FDE block diagram

At the receiver, the signal is given by

$$\mathbf{r} = \mathbf{H}\mathbf{d} + \mathbf{n} \tag{2.25}$$

where $\mathbf{H}$ is the time domain circulant channel matrix and $\mathbf{n}$ is the (AWGN) vector with complex-valued elements that have zero mean and variance N_0, similar to the OFDM case. This is then transferred into the frequency domain by N-point DFT, to get $\tilde{\mathbf{r}} = [\tilde{r}^0 \cdots \tilde{r}^{N-1}]$, where $\tilde{r}^n$ is the received data on the nth frequency bin ($n = 0, \cdots, N-1$). $\tilde{\mathbf{r}}$ is expressed as

$$\tilde{\mathbf{r}} = \mathbf{F}_N\mathbf{H}\mathbf{d} + \mathbf{F}_N\mathbf{n} \tag{2.26}$$

Defining $\tilde{\mathbf{d}} = \mathbf{F}_N\mathbf{d}$ and $\tilde{\mathbf{H}} = \mathbf{F}_N\mathbf{H}\mathbf{F}_N^H$, where $\mathbf{F}_N\mathbf{H}\mathbf{d} = \mathbf{F}_N\mathbf{H}\mathbf{F}_N^H\mathbf{F}_N\mathbf{d}$ and $\mathbf{H}$ is diagonalised just like in the OFDM system. Substituting $\tilde{\mathbf{d}}$ and $\tilde{\mathbf{H}}$ into (2.17) gives

$$\tilde{\mathbf{r}} = \tilde{\mathbf{H}}\tilde{\mathbf{d}} + \tilde{\mathbf{n}} \tag{2.27}$$

which is the frequency domain representation of the SC-FDE system. Simple one tap equalisation can now be performed in the frequency domain for each frequency bin.

SC-FDE keeps the same advantages of OFDM, and avoids the problems of subcarrier synchronisation [49]. Furthermore, in uncoded systems, SC-FDE provides more frequency diversity [11], because the symbol energy is spread across the whole bandwidth, unlike OFDM where symbol energies are restricted to single subcarrier which could be prone to severe fading. In addition, SC-FDE has a PAPR than the OFDM system, which is suitable for mobile applications where the mobile device power consumption is of great importance. Due to the non-linear amplifier design in transmission circuits, high PAPR causes more power wastage [50].

In SC-FDMA, the users' data is transmitted in the same domain it is created, unlike the OFDMA system. This is achieved by DFT precoding of the user's data, therefore, SC-FDMA is sometimes referred to as pre-coded OFDMA. Unlike OFDMA, where each data symbol occupies a single frequency band (subcarrier), the energy of each data symbol in SC-FDMA is spread over several subcarriers, which combats the situations where there are deep fades on certain subcarriers. Therefore, SC-FDMA has a lower PAPR, and higher frequency diversity than OFDMA [8], and it has been proposed to be used in the uplink LTE [3]. A single user SC-FDMA system, it is similar to an SC-FDE system. The SC-FDMA system is illustrated in Figure 2.9. The major difference between SC-FDMA and OFDMA system is the transferring/spreading of each user's data block $\mathbf{d}_u$ into the frequency domain by an M-point DFT in SC-FDMA, before being mapping symbols to subcarriers. The mapped data are transferred back into the time domain by N-point IDFT and each block of N symbols is prepended with a CP. The CP is discarded at the receiver to combat IBI and to make the channel appear to be circular, similar to the OFDMA system.

The received signal block $\mathbf{r} = [r^0 \ \cdots \ r^{N-1}]^T$ after CP removal at the BS is expressed as

$$\mathbf{r} = \sum_{u=0}^{U-1} \mathbf{H}_u \mathbf{F}_N^H \mathbf{M}_u \mathbf{F}_M \mathbf{d}_u + \mathbf{v} \tag{2.28}$$

where $\mathbf{v} = [v^0 \cdots v^{N-1}]^T$ is the AWGN vector with complex-valued elements that have zero mean and variance N_0. Similar to the OFDMA system, at the BS, the received signals are transferred into the frequency domain by N-point DFT,

$$\tilde{\mathbf{r}} = \sum_{u=0}^{U-1} \mathbf{F}_N \mathbf{H}_u \mathbf{F}_N^H \mathbf{M}_u \mathbf{F}_M \mathbf{d}_u + \mathbf{F}_N \mathbf{v} \tag{2.29}$$

Defining $\tilde{\mathbf{H}}_u = \mathbf{F}_N \mathbf{H}_u \mathbf{F}_N^H$, where $\mathbf{H}_u$ is diagonalised by pre and post multiplication with the DFT and IDFT matrices, respectively. Substituting $\tilde{\mathbf{H}}_\mathbf{u}$ into (2.17) gives

$$\tilde{\mathbf{r}} = \sum_{u=0}^{U-1} \tilde{\mathbf{H}}_u \mathbf{M}_u \mathbf{F}_M \mathbf{d}_u + \tilde{\mathbf{v}} \tag{2.30}$$

where $\tilde{\mathbf{H}}_u$ is the frequency response of the channel for the uth user, similar to OFDMA. $\tilde{\mathbf{v}} = \mathbf{F}_N \mathbf{v}$ is the frequency domain AWGN. The received data corresponding to each user $\tilde{\mathbf{r}}_\mathbf{u} = [\tilde{r}_u^0 \cdots \tilde{r}_u^{M-1}]^T$ is de-mapped from $\tilde{\mathbf{r}}$ using $\mathbf{M}_u^T$, which is the transpose of the initial mapping matrix,

$$\tilde{\mathbf{r}}_u = \mathbf{M}_u^T \tilde{\mathbf{r}} = \mathbf{M}_u^T \tilde{\mathbf{H}}_u \mathbf{M}_u \mathbf{F}_M \mathbf{d}_u + \tilde{\mathbf{v}}_u \tag{2.31}$$

where $\tilde{\mathbf{v}}_u = \mathbf{M}_u^T \tilde{\mathbf{v}}$ is an $(M \times 1)$ noise vector for the uth user.

2.3.3 Peak to Average Power Ratio

The PAPR of the transmitted signal $x(t)$ (signal after addition of CP), defined by

$$PAPR = \frac{\max_x |x(i)|^2}{E[|x(i)|^2]} \tag{2.32}$$

is the ratio of the peak power of transmitted signal to the average value of the signal [50]. A high PAPR is particularly detrimental to uplink transmission of mobile devices, where there is limited power due to current battery performances. PAPR

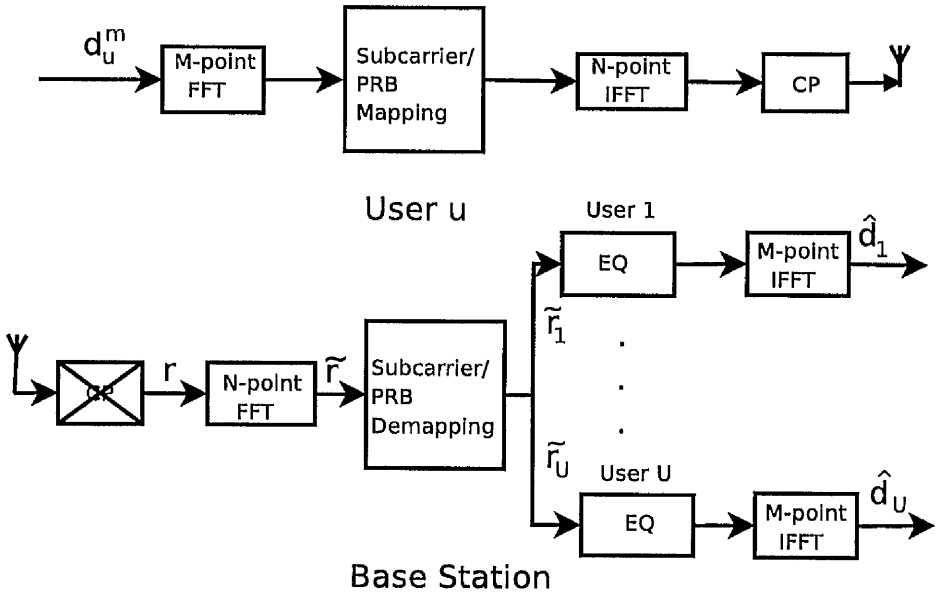

Figure 2.9: SC-FDMA block diagram

is also dependent on the type of subcarrier mapping used. In [8], it is shown that the interleaved mapping has the smallest PAPR when compared to the localised and distributed subcarrier mapping techniques.

2.3.4 Equalisation for OFDMA and SC-FDMA

As previously discussed, the wireless channel and noise create inter-symbol interference (ISI) which affects the quality of the received signal. These adverse effects can be removed by channel equalisation [34]. From (2.18) and (2.27), equalisation is performed independently on each subcarrier (OFDM) or frequency bin (SC-FDE), respectively [46]. The soft estimate of the data $\hat{\mathbf{d}}_u = [\hat{d}_u^0 \cdots \hat{d}_u^{M-1}]^T$ after equalisation is given by

$$\hat{\mathbf{d}}_u = \mathbf{F}_M^H \mathbf{W}_u \tilde{\mathbf{r}}_u \tag{2.33}$$

where $\mathbf{W}_u$ is the frequency domain channel equaliser matrix. There are many equalisation techniques in the literature that involve both linear and non-linear signal processing. In this work, the linear minimum mean square error (MMSE) technique is used because of its relative simplicity in terms of complexity, and its generally acceptable performance. Other methods such as the zero forcing (ZF) and maximum likelihood detection (MLD) are briefly discussed.

Minimum Mean Square Error (MMSE)

The $(M \times M)$ frequency domain MMSE equaliser weight matrix $\mathbf{W}_u$, is given by [51]

$$\mathbf{W}_u = \bar{\mathbf{H}}_u^H (\bar{\mathbf{H}}_u \bar{\mathbf{H}}_u^H + N_0 \mathbf{I}_M)^{-1} \tag{2.34}$$

where $\bar{\mathbf{H}}_u = \mathbf{M}_u^T \tilde{\mathbf{H}}_u \mathbf{M}_u$ is the diagonal $(M \times M)$ frequency domain channel response for the uth user, de-mapped by a pre- and post multiplication of $\tilde{\mathbf{H}}_u$ with the inverse mapping and mapping matrices, respectively. $\mathbf{W}_u$ is derived by minimising the block mean square error (MSE) J_u, expressed as

$$J_u = \frac{1}{M} \sum_{m=0}^{M-1} \mathrm{MSE}_u^m = \frac{1}{M} \mathrm{tr}(\mathbf{R}_{ee;u}) \tag{2.35}$$

where $\mathrm{MSE}_u^m = E|d_u^m - \hat{d}_u^m|^2$ is the MSE between d_u^m and its soft estimate $\hat{d}_u^m$. $\mathbf{e}_u = \hat{\mathbf{d}}_u - \mathbf{d}_u$ denotes the error vector between $\mathbf{d}_u$ and its soft estimate $\hat{\mathbf{d}}_u$ and $\mathbf{R}_{ee;u} = E[\mathbf{e}_u \mathbf{e}_u^H]$ is the error auto-correlation matrix for user u which is expressed as

$$\mathbf{R}_{ee;u} = \mathbf{I} - \bar{\mathbf{H}}_u^H (\bar{\mathbf{H}}_u \bar{\mathbf{H}}_u^H + N_0 \mathbf{I}_M)^{-1} \bar{\mathbf{H}}_u \tag{2.36}$$

The MSE for each subcarrier $0 \leq m \leq (M-1)$ allocated to the uth user is given by the mth diagonal element of $\mathbf{R}_{ee;u}$

$$\text{MSE}_u^m = \frac{1}{|\tilde{H}_u^{k_u M+m}|^2/N_0 + 1} \tag{2.37}$$

The output signal-interference-to noise ratio (OSINR) (received SNR after equalisation) of each subcarrier is given related to the MSE_u^m by $\gamma_u^m = \frac{1}{\text{MSE}_u^m} - 1$ which gives,

$$\gamma_u^m = \frac{|\tilde{H}_u^{k_u M+m}|^2}{N_0} \tag{2.38}$$

This is suitable for OFDMA, where each subcarrier is independent of each other and the OSINR for a PRB for the uth user is the average of each subcarrier output SINR, $\gamma_u = \frac{1}{M}\sum_{m=0}^{M-1}\gamma_u^m$.

In SC-FDMA, the MSE of the uth user is the average MSE of the subcarriers in the PRB allocated to that user, $\text{MSE}_u = (1/M)\sum_{m=0}^{M-1}\text{MSE}_u^m$. Similarly, the output SINR γ_u of the uth user is related to the MSE by $\gamma_u = \frac{1}{\text{MSE}_u} - 1$ [11, 51]. Therefore, the output SINR of the PRB allocated to the uth user is given by

$$\gamma_u = \frac{1}{\frac{1}{M}\sum_{m=0}^{M-1}\frac{1}{|\tilde{H}_u^{k_u M+m}|^2/N_0+1}} - 1 \tag{2.39}$$

Zero Forcing (ZF)

The ZF equaliser completely removes the ISI caused by the channel. The ZF equaliser weight matrix is the inverse of the diagonal frequency domain channel matrix [52], expressed as

$$\mathbf{W}_u = \bar{\mathbf{H}}_u^H(\bar{\mathbf{H}}_u\bar{\mathbf{H}}_u^H)^{-1} \tag{2.40}$$

where $\bar{\mathbf{H}}_u$ is the frequency domain channel for all the subcarriers or frequency bins, similar to the MMSE case (2.34). Notice that $\mathbf{W}_u\bar{\mathbf{H}}_u = 1$, which represents total removal

of the ISI. Since the received data $\tilde{\mathbf{r}}_u$ is a combination of frequency selective fading and AWGN, the AWGN will be amplified by a factor of $\mathbf{W}$ as shown mathematically below,

$$\mathbf{r}_u = \mathbf{W}_u(\bar{\mathbf{H}}_u\mathbf{d}_u + \bar{\mathbf{n}}) = \mathbf{d}_u + \mathbf{W}_u\bar{\mathbf{n}} \tag{2.41}$$

which is especially detrimental when the channel gain is very low (deep fades), hence giving $\mathbf{W}_u$ a very large noise amplification effect. In addition, when there are spectrum nulls (areas where the channel spectrum values are zero), the ZF equaliser cannot be estimated because of the issue of dividing by zero [34].

Maximum Likelihood Detection

MLD, as name implies, maximises the probability of detecting the data. For each received data bit or symbol, the ML equaliser searches through all the possible bit/symbol combinations to find the one which has the highest probability of being the transmitted bit [53]. The estimate of the nth received data $\hat{r}^n$ is expressed by,

$$\hat{d}_u^n = \min_s ||r_u^n - \bar{H}_u^n d_u(s)|| \; \forall \; d_u(s) \in D \tag{2.42}$$

where D is the set of all possible symbols of $d_u(s)$ and $s = 1, \cdots, S$, and S is the cardinality of D. Therefore, if the signal space D is large, then for every symbol on a subcarrier or frequency bin, a search has to be made over all the possible symbols. This is the optimal detector, however, it is complex to implement, especially when the number of subcarriers, the signal space and length of the channel are large [54].

Other Equalisers

Other equalisation schemes exist, such as decision feedback equaliser (DFE) and Blast [53] that help in reducing interference, by cancelling the interference of already detected symbols on yet to be detected symbols. Furthermore, iterative techniques such as

turbo equalisation [55] have been proposed that exchange information between the FEC decoder and the equaliser in order to improve the reliability of the detected symbol.

2.3.5 Simulation Results

In this section, some simulations results for the SC-FDMA and OFDMA systems are presented.

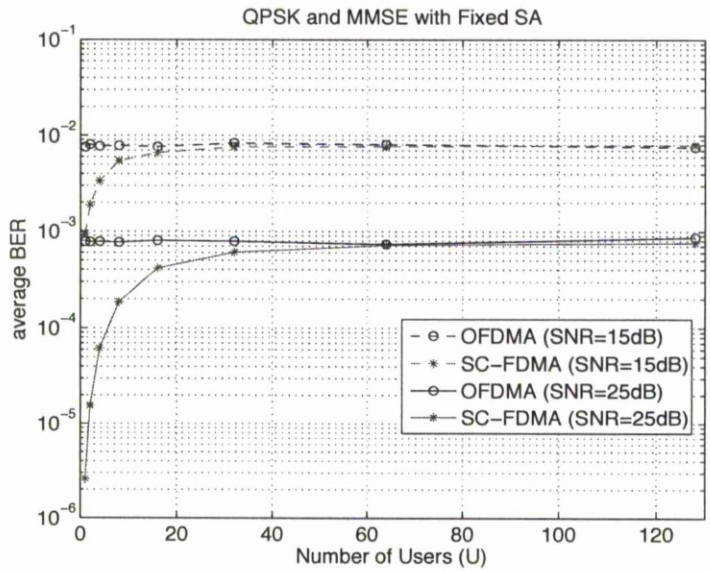

Figure 2.10: Uncoded performances of OFDMA and SC-FDMA at SNR = 15 dB and 25 dB with QPSK modulation.

Figure 2.10 shows the uncoded BER performance of the OFDMA and SC-FDMA system across a varying number of users for single BS (single cell) with fixed subcarrier allocation (SA) and quadrature phase shift keying (QPSK). Fixed SA is when the users are assigned subcarriers sequentially, without any optimisation. Notice that the OFDMA does not show any difference in performance irrespective of the number of users in the system, because its performance cannot get any worse due to independence

of the user subcarriers. In general, the OFDMA performance improves with increasing SNR. On the other hand, the SC-FDMA system has a decreasing performance with increasing number of users in the system. The single user case (SC-FDE) has the best performance, due to frequency diversity, however as the number of users increase the performance degrades, down to the OFDM performance. Therefore for the LTE system with a huge number of users, both systems will provide similar BER performances. Nevertheless, the SC-FDMA transmission technique is still beneficial due to its lower PAPR [8] is will be shown next.

Figure 2.11 uses the complementary cumulative distribution function (CCDF) to demonstrate the performance of the PAPR for both SC-FDMA and OFDMA using three modulation levels. Fifty thousand data transmissions are simulated and the probability that the PAPR is higher than a certain threshold is calculated. The QPSK SC-FDMA system has the best performance and is about 1 dB better than both the quadrature amplitude modulation 16 (QAM -16) an QAM-64 SC-FDMA systems. The OFDMA systems are about 3 dB worse than the QPSK SC-FDMA system in terms of PAPR, irrespective of modulation used.

Comparing Figure 2.12 to Figure 2.11 shows that the PAPR is affected by the amount of subcarriers are used to carry data. When $M = 120$ subcarriers carry data, the PAPR is higher than the situation when only $M = 12$ subcarriers are used to carry data. There is approximately a 1 dB performance degradation for all the SC-FDMA systems, while there is about a 2 dB performance degradation for all the OFDMA systems when the number of data carrying subcarriers increase ten fold.

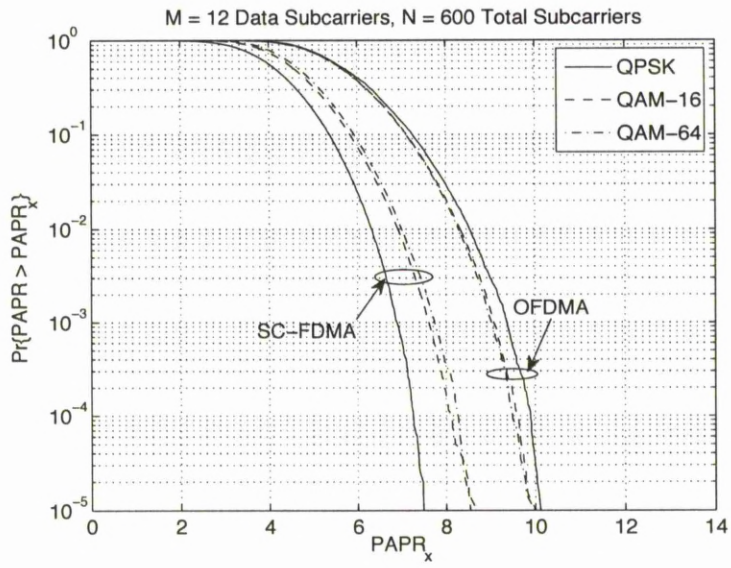

Figure 2.11: PAPR in dB of a block of $M = 12$ occupied subcarriers, with $N = 600$ total subcarriers in system.

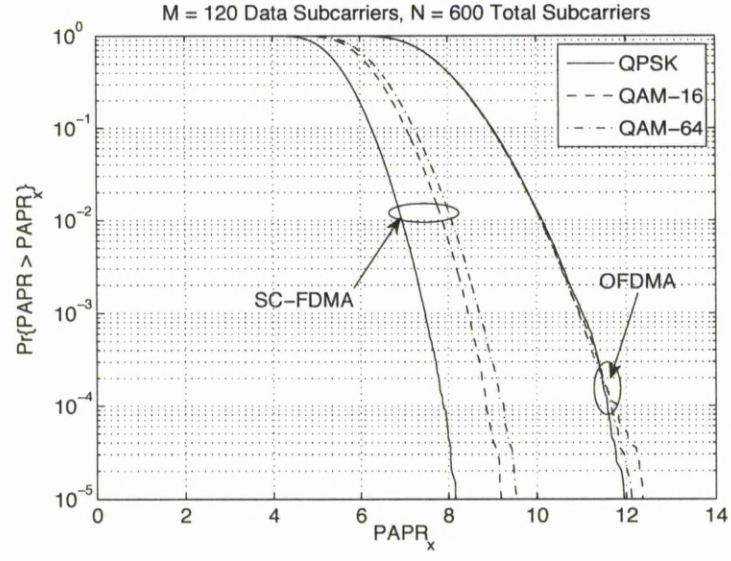

Figure 2.12: PAPR a block of $M = 120$ occupied subcarriers, with $N = 600$ total subcarriers in system.

Chapter 3

Resource Allocation

3.1 Introduction

The invention of discrete multi-tone (DMT) system - the wired version of OFDM - facilitated the invention of resource management based on the frequency domain characteristics of the channel [56]. In these single user systems, the frequency diversity of the channel is exploited by adapting the transmit power and the amount of bits transmitted on each frequency tone to the channel. The amount of transmitted bits was determined by changing the QAM modulation levels, while the transmission power was determined by a technique called water-filling (or pouring) [47,57–61]. Due to the time varying nature of wireless communications, dynamic bit and power allocation was extended to the single carrier time domain system in [62] and [63] for uncoded and trellis coded systems, respectively. The same water-filling power allocation technique was found to be optimal in the time domain, because of the duality of the time and frequency domain channels [64]. Hence, dynamic bit and power allocation is possible in the time and frequency domain for wideband multicarrier systems [44].

In multiuser systems where the available resources have to be shared amongst the active users, resource allocation plays an important role in the efficient utilisation of

the available resources. The most important (expensive) of these resources is the spectrum (transmission bandwidth), which has to be effectively utilised. Other resources such as the available transmission time, power and space can also be efficiently shared among the available users. This has spurred the development of many resource allocation techniques, whose implementations depend on the type of system. For example, the time slots [65,66], frequency subchannels [15,16], space and code resources have to be appropriately allocated in the TDMA, FDMA, SDMA and CDMA systems, respectively.

In multiuser multicarrier systems such as OFDMA, dynamic resource allocation to different users plays a crucial role in system performance in the presence of time varying frequency selective channels. Dynamic subcarrier allocation (SA) for OFDMA systems have been greatly explored, and many algorithms have been developed that allocate subcarriers, rate and power, to optimise the desired wireless communication *utility* . The most extensively used optimisation utility is the Shannon capacity, which is maximised in [14–18, 22, 24, 67, 68]. Other important optimisation utilities are the BER, transmit power, CFR, OSINR, etc. The transmit power utility is minimised [19,21,25], and the CFR is also maximised in [21,27]. Fairness is another important optimisation utility, and it can either be optimised in the time domain [15] or in frequency domain [65]. Due to the complexity of the optimal solution, especially when the number of users and subcarriers are large, the algorithms presented in above citations use greedy and iterative methods to find suitable but often sub-optimal solutions for the PRB allocation problem. Heuristic algorithms such as GA [31] and particle swarm optimisation [69] have also been used for resource allocation in OFDMA. However, their performances and computational complexities are variable and depend on many parameters, such as chromosomes length, generation size, number of generations and mutation factor for GA. Most of the aforementioned OFDMA resource allocation algorithms allocate a varying amount of individual subcarriers to users which can be

very computationally expensive, and is more suitable for downlink resource allocation, where the BS has the information for all the users and has enough processing power to perform all the optimisations. Nevertheless, this subcarrier by subcarrier allocation does not adhere to current 4G systems such as the LTE and WiMAX, where subcarriers are allocated in blocks. In [27], OFDMA subcarriers were allocated to users in blocks, similar to the LTE specification.

3.2 Dynamic Resource Allocation

In wireless communications, transmission of data from the BS to the mobile users is known as *downlink* transmission or forward link [3]. In this case, the BS acts as a common source for all users' data. Therefore, the BS can optimally allocate resources to different users so that the overall channel bandwidth can be utilised properly. To achieve this, the BS periodically gathers information about all the users' channel state information (CSI) using reference and channel sounding data.

On the other hand, the transmission of data from mobile devices to the BS is known as *uplink* or reverse link [3]. It is more difficult to design an optimal central resource allocator, because the BS does not have all the information about the users' transmissions. In current 4G systems, some information about the users' data are transmitted back to the BS, however, these contribute to the over-head data, which reduces the amount of resources left for relevant user data. The LTE and WiMAX-2 systems specify the transmission of a single bit to the BS, which indicates the priority of data about to be transmitted by a user [3,70]. The BS then specifies the the amount of resources to be allocated to the user. Nevertheless, the user independently determines which data (service) will currently utilise the allocated resources: a higher priority is given to real time services like voice, while email data can have more latency [70]. Furthermore, in a wireless communication link with rapidly changing channels (fast

fading), uplink resource allocation is harder to achieve, because the data reported to the BS might be out of date, hence making the resulting allocation irrelevant in the current time slot. Therefore, uplink resource allocation must be fast enough to match the speed at which the channel changes [71], which puts a huge restraint on the complexity of the algorithm used for resource allocation.

3.2.1 Bandwidth/PRB Allocation

In order to keep the complexity, overhead and PAPR low, especially in the uplink, the LTE system uses a PRB based allocation instead of the subcarrier by subcarrier allocation [3,72]. In Figure 3.1, the frequency domain channel with PRB resolution, for

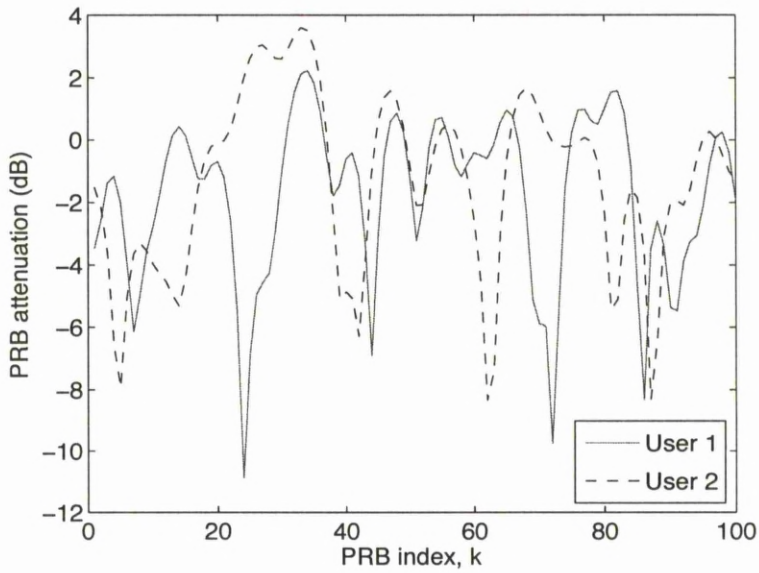

Figure 3.1: Frequency diversity: PRB frequency response for two users. 18 MHz bandwidth with 180 KHz per PRB

two users is shown. Observe that both users do not always simultaneously experience deep fades on all the PRBS. Therefore, when the PRBs are allocated to the users based on their channel performance, there will be a remarkable system performance

gain, because the deep fades that waste power and corrupt data would be avoided. This gain is known as the frequency diversity, which increases when there are more users in the system because the probability of allocating a PRB in deep fade is minimised. For example, in Figure 3.1, the deep fades around the 90th PRB cannot be avoided, irrespective of which user is allocated those PRBs, but as the number of users with independent fading increases, the probability of these PRBs being in deep fades for all the users reduces. In current wideband 4G systems, the bandwidth and hence the number of PRBs are considerably high. Therefore, many users can be allocated PRBs simultaneously making the cell size very large [3]. The large bandwidth and large number of users imply that the system performance can be considerably enhanced with dynamic PRB allocation.

Little work on the PRB based resource allocation has been reported in the literature, especially for SC-FDMA systems. In [28], a suboptimal two-dimensional (2-D) greedy PRB allocation algorithm was proposed to maximise the sum users' capacity in an SC-FDMA system, which is essentially the same as algorithm for OFDMA in [27]. However, the work in [28] ignores the fairness among users, and as a result, users with deeply faded channels, may get little or no PRBs. The algorithm in [29] uses the same algorithm in [28], but the fairness is improved by employing the logarithm capacity utility but this method of improving fairness lowers the peak data rates achievable. In addition, none of the aforementioned literature considered the effects of PRB allocation on the BER performance of uplink LTE systems. In [73] a greedy subcarrier allocation for SC-FDMA is proposed that strictly adheres to the subcarrier adjacency requirement of uplink LTE, however, it also allocates a random amount of subcarriers to users and not PRBs. Furthermore, the issues of adaptive transmission bandwidth and carrier aggregation are considered in [13] and [74] for uplink LTE systems.

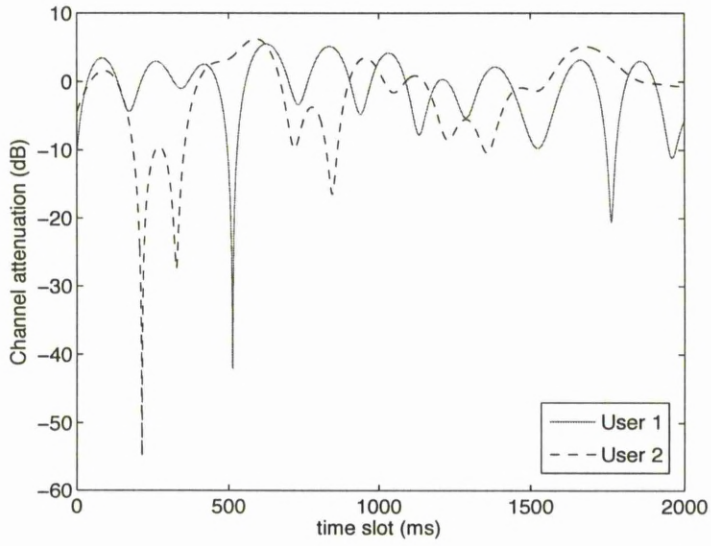

Figure 3.2: Time diversity: time varying channel for two users

3.2.2 Time Slot Scheduling/Allocation

Similarly, the time diversity of the fading channel is shown in Figure 3.2, and with the aid of proper time allocation techniques, the deep fades in the time domain can be avoided. As already mentioned, a TDMA system divides the available resources into time slots, and a user is allowed to transmit its data on a particular time slot. In older systems, for example, the GSM, time slot allocation is static, meaning the user is allocated a time slot at the beginning of the session and uses it for the whole duration needed. The allocation is carried out by a round robin scheduler, where the users take turns to use the available bandwidth, disregarding the channel information.

To improve the system capacity, time diversity can be also exploited. The *maximum rate* scheduler [3] is described by

$$u^* = \max_u(r_u^t) \tag{3.1}$$

where r_u^t is the instantaneous data rate of the uth user in transmission time interval (TTI) t. This scheduler allows the user with the highest instantaneous rate to transmit data in any TTI. It maximises the multi-user diversity and it is the theoretical optimal allocation strategy. However, the fairness between the users is lost and some users may not be allowed to transmit any data for long periods of time, because they consistently have a bad channel link. The bad channel link can come about when a user(s) is located at a large distance from the BS, *i.e.*, cell edge users or suffer severe shadowing due to terrain.

Another time domain allocation technique is the proportional fair scheduler [3,65], which is described by

$$u^* = \max_u \left(\frac{r_u}{\sum_{t=0}^{T-1} r_u^t} \right) \tag{3.2}$$

where T is a suitable interval over which the instantaneous data rate of the each user is averaged. This helps to maintain a certain fairness over the chosen interval. It ensures that the users take turns in using the channel based on their previous average rate. This strategy does not maximise the multi-user diversity, but guarantees that all users have the opportunity to transmit data, irrespective of their channel link quality.

3.2.3 Bit and Power Allocation

Power allocation involves sharing the available power resource among all the users in the system. Power allocation is more relevant in the downlink, because the BS has a common power source which can be effectively managed. However, in the uplink, the available power is distributed among the users. Therefore, it is more difficult to have a central power allocator.

CDMA has historically used power allocation to combat interference (the near far problem) [3]. However, it does not play a direct part in maximising the capacity of the user. In orthogonal multi-carrier systems, it is possible for each user to use the

water-filling algorithm on their allocated subcarriers to maximise capacity. However, this adds complexity to the system, increases the PAPR and provides very marginal gains, because it is well known that constant power allocation is near optimal when the subcarrier allocation is good, *i.e.*, when the subcarriers in deep fades have already been avoided [14, 44, 58, 59].

Bit allocation is the specification of the number of bits that a user is allowed to transmit in a subcarrier. This is the most common form of link adaptation, where higher QAM modulation levels are used when the subcarrier gain is high [56, 60]. Most current systems employ the BPSK, QPSK, QAM-16 and QAM-64 modulations, which provide spectral efficiencies of 1, 2, 4 and 6 bits/s/Hz, respectively [34]. It is also usual to vary the FEC coding rate, which determines the actual data throughput. The simultaneous adaptation of both the FEC coding rate and the modulation level, to the channel link performance is referred to as adaptive modulation and coding (AMC) [3]. Both the LTE and WiMAX systems specify the use of AMC to boost the user effective data rates.

In general, there is a link between all the resources to be allocated. For example, power allocation is affected by the time and frequency allocations, which in turn determines the bit allocation. However, jointly optimising allocation across all the resources involves multi-utility optimisation, which is highly complex, especially when there are more than two utilities or resources [75].

The following factors affect the mode and operation of the resource allocation algorithms:

- Power control is used to mitigate interference from other cells (beneficial to cell edge users) and used for path loss and shadowing compensation [13, 74]. This usually involves increasing the user transmit power by 1 dB or reducing it by 1 dB for subsequent TTI, depending on the received SINR in the current TTI. This implies that individual subcarriers are not power adjusted, and therefore

the water-filling optimum power allocation is somewhat irrelevant in the uplink LTE. Furthermore, in the literature [14, 59] and references therein, it is known that when the time slot and subcarrier allocation is properly carried out (very deeply faded time slots and or subcarriers are avoided), the water filling power allocation adds marginal gains to the system.

- In order to keep data overhead low, uplink LTE does not involve extensive time scheduling of data packets. Each data packet is assigned a priority, and only this parameter is transmitted to the BS. The BS uses the priority information to select the users that will be allowed to transmit in the next TTI and specifies the transport format (TF) based on PRB allocation to the chosen users. The TF contains all information required for a user transmission, which includes the number of PRBs and the modulation and coding scheme (MCS) allocated to the user. The user makes independent choice of which data service (data packets) is going to be transmitted on the current slot with the allocated transport format. Therefore, extensive packet scheduling is not very suitable for the uplink transmission [3, 70].

- AMC is employed for the uplink LTE. Information about the current code rate and modulation level is included in the TF information. However, the MCS level is the same irrespective of the amount of PRBs allocated to the user. If a large number of PRBs are allocated to a single user, the probability of being allocated the lowest MCS increases, because the adjacent PRBs in the TF are averaged to determine the composite MCS (LTE enforces adjacency). It is also shown in the literature that PRB allocation degrades as the PRB size increases, especially when it is much larger than the coherence bandwidth of the channel [44, 76]. Therefore, AMC works better with the TF that has a limited number of PRBs.

- PRB allocation is a very important aspect of resource allocation, especially for

the uplink LTE system where the benefits of the other adaptation schemes are somewhat limited. When PRB allocation is done efficiently, allocating PRBs in deep fades is minimised. This reduces power wastage, aids the application of efficient MCS levels on the allocated PRBs and prevents spectrum wastage by reducing data overhead. Furthermore, the computational cost reduction achieved with greedy PRB allocation improves the overall system efficiency.

- Finally, the WiMAX systems prefer interleaved subcarrier allocation, which exploits frequency diversity. However, WiMAX has a mode referred to as Band AMC [26], which groups subcarriers into subchannels or PRBs, similar to the LTE system. This allows the same PRB allocation algorithms to be applied to both the LTE and WiMAX systems in both uplink and downlink scenarios.

3.3 Problem Formulation

The objective of this research work is to allocate a PRB to each user so that the overall BER, SE and outage probability performance across all the users is optimised.

3.3.1 Objective Function

To achieve optimal PRB allocation, the following cost function must be maximised:

$$J = \sum_{u=0}^{U-1} \sum_{k=0}^{K-1} b_{uk} s_{uk} \tag{3.3}$$

subject to:

$$s_{uk} \in \{0, 1\} \tag{3.4}$$

$$\sum_{u=0}^{U-1} s_{uk} = 1 \tag{3.5}$$

$$\sum_{k=0}^{K-1} s_{uk} = 1 \tag{3.6}$$

where b_{uk} represents a certain wireless communication utility which is discussed in Subsection 3.3.2. When the kth PRB is allocated to the uth user, $s_{uk} = 1$, otherwise $s_{uk} = 0$. (3.4) - (3.6) ensure that only one PRB is allocated to one user. b_{uk} and s_{uk} can be put into square matrices, $\mathbf{B}$, the utility matrix, and $\mathbf{S}$, the allocation matrix, respectively, where the elements in each row belong to a unique user across all the PRBs and the elements in each column belong to a unique PRB across all the users. k and u are coupled into one notation k_u, which denotes the kth PRB allocated to the uth user.

3.3.2 Optimisation Utility

The various optimisation utilities, represented by b_{uk} in (3.3), provide information on the channel link quality. There are different optimisation utilities such as:

CFR

The channel frequency response (CFR) is the fundamental parameter used in describing the link quality between two transmission points. The CFR is the frequency domain equivalent of the CIR discussed in Chapter 2. The CFR is also essential for data equalisation, because all equalisation techniques discussed in Subsection 2.3.4, require an accurate channel estimate to calculate the required equalisation matrices. The CFR is estimated by transmitting data previously known at the receiver, referred to as reference and sounding data [3]. Across a PRB, the average channel gain is calculated by averaging each subcarrier CFR. Therefore, b_{uk} in (3.3) is the average gain of the M subcarriers in the kth PRB for the uth user, which is given by

$$b_{uk} = \frac{1}{M} \sum_{n=kM}^{kM+M-1} |\tilde{H}_u^n| \tag{3.7}$$

where, $\tilde{H}_u^n$ is the CFR for the nth subcarrier for the uth user, $k = 0, \cdots, (K-1)$ and $u = 0, \cdots, (U-1)$. b_{uk}, is maximised across all the users according to (3.3) - (3.6). The CFR utility is maximised in [21,27].

Output SINR

The OSINR is a useful utility, because it includes the effect of the transmitted power and the interference experienced by the user. It is also known as the received signal power after channel equalisation. The OSINR is dependent on what kind of equalisation is used, because different equalisers remove different amounts of interference. In SC-FDMA, the output SINR utility across all the users' PRBs using the MMSE equaliser is given by

$$b_{uk} = \frac{1}{\frac{1}{M}\sum_{n=kM}^{kM+M-1}(|\tilde{H}_u^n|^2/N_0+1)^{-1}} - 1 \tag{3.8}$$

where b_{uk} is the output SINR of the kth PRB for the uth user. Notice that this is similar to (2.39), while the OFDMA OSINR is given by

$$b_{uk} = \frac{1}{M}\sum_{n=kM}^{kM+M-1}\frac{|\tilde{H}_u^n|^2}{N_0} \tag{3.9}$$

which is related to (2.38). This utility is maximised, similar to the CFR utility. The maximum OSINR was used in [77], to allocate subcarriers to all the users. It was also employed in [25] to find the allocation that provides the minimum total transmit power in an OFDMA system.

SE

The Shannon channel capacity formula through an AWGN channel is given by [33]

$$C = \mathrm{B}\log_2(1+\mathrm{SNR}) \tag{3.10}$$

where B and SNR are the bandwidth and SNR, respectively. However, in the presence of Rayleigh fading channel and MMSE equalisation, the Shannon capacity utility of the kth PRB for the uth user is given by

$$b_{uk} = \mathrm{B}\log_2(1+\Gamma_{\mathrm{uk}}) \tag{3.11}$$

where Γ_{uk} is the OSINR is given by (3.8) for SC-FDMA. For OFDMA, the capacity of each subcarrier is found independently by substituting the output SINR for each subcarrier (2.38) into (3.10) and then the capacity of the PRB is the sum of all subcarrier capacities in the PRB. This utility is maximised in [28] and to improve fairness, the logarithm of this Shannon capacity is maximised in [29].

The disadvantage of the Shannon capacity utility is that it assumes that the BER is zero (perfect retrieval of transmitted data), which is not the always the case. To rectify this, the following utility is derived for QAM modulations in [62]

$$b_{uk} = \log_2\left(1+\frac{-1.5\Gamma_{\mathrm{uk}}}{\ln(5\Omega)}\right) \tag{3.12}$$

where b_{uk} is the spectral efficiency (SE) utility of the kth PRB for the uth user, Ω is the desired BER and Γ_{uk} is the output SINR of the kth PRB for the uth user given by (3.8) for SC-FDMA. For OFDMA, the capacity of each subcarrier is found independently by substituting the output SINR for each subcarrier (2.38) into (3.12). Then the SE of the PRB is the sum of all the subcarrier SEs in the PRB. Notice that a lower desired BER, reduces the peak SE. This utility is maximised in [14] for an OFDMA system.

BER

The BER is a very important measurement for wireless communications because the data throughput (actual amount of bits transmitted across the channel) is highly affected by the BER. The uncoded BER utility of the kth PRB for the uth user with

QAM modulation in an SC-FDMA system is estimated by [34]

$$b_{uk} \approx 2\left(1-\frac{1}{\sqrt{M}}\right) Q\left(\sqrt{\frac{3\Gamma_{uk}}{M-1}}\right) \tag{3.13}$$

where M is the the QAM level, Γ_{uk} is the output SINR (3.8)) and the Q-function of a value x is given by $Q(x) = \frac{1}{\sqrt{2\pi}} \int_x^\infty e^{-\frac{t^2}{2}} dt$. In OFDMA, the BER of each subcarrier is estimated by substituting (2.38) into (3.13) and then the BER of the PRB is determined by averaging the subcarrier BERs. This utility represents the uncoded BER, however, all modern broadband wireless communication systems employ FEC coding for error control, which is far more complex to estimate. A method used to estimate the coded BER for multi-carrier systems is discussed in subsection 3.3.2.

Effective Exponential SNR Mapping

FEC is the means by which the reliability of the received data can be improved by increasing the redundancy in the transmitted data. This has become the de-facto technique by which channel errors are tackled in modern wireless communication systems [78]. The advances in digital signal processing hardware and software have enabled the implementation of FEC in low power mobile devices. The most common and widely used error correcting codes in multiuser wireless communication systems are convolutional and turbo coding.

Effective exponential SNR mapping (EESM) [79, 80] is the technique by which the impact of FEC coding on data transmission is modelled. Unlike uncoded wireless communications, where the BER is a function of only the OSINR of the bit at the receiver as shown in (3.13), the BER of a coded signal is a function of many parameters such as the data block length, MCS, frequency and time diversity of the multi-carrier channel, etc. All these parameters make the a priori estimation of the BER more complicated. In fact, there is no closed form equation that provides an accurate estimate of the

coded BER in a multi-carrier system. The BER is determined by the EESM technique as expressed by

$$b_{uk} = BER_{AWGN}\{\gamma^e_{uk}\} \tag{3.14}$$

where b_{uk} is the estimated BER of the kth PRB for the uth user, which is mapped out from the database of BER performances under the AWGN channel and an identical FEC coding, represented by BER_{AWGN}. Due to the lack of closed form equations for the BER, even the BER_{AWGN} is found by simulation [79]. γ^e_{uk} is the effective OSINR of the kth PRB for the uth user, expressed as

$$\gamma^e_{uk} = -\beta \ln\left(\frac{1}{M}\sum_{n=kM}^{kM+M-1} e^{-\left(\frac{\gamma(n)_u}{\beta}\right)}\right), \tag{3.15}$$

where β is the correction factor and $\gamma_u(n)$ is the OSINR of the nth subcarrier for the uth user given by,

$$\gamma^n_u = \frac{|\tilde{H}^n_u|^2}{N_0}, \tag{3.16}$$

where $\tilde{H}^n_u$ is the CFR of the nth subcarrier for the uth user and N_0 is the single sided noise power spectral density. The correction factor β also needs to be determined for each MCS employed.

Throughput

The throughput is the actual amount of data transmitted over the communication link, unlike the system capacity which specifies the maximum achievable data rate. The throughput is highly dependent on the modulation and coding scheme (MCS) employed. The EESM derived BER, plays an important role in determining the PRB's throughput. The throughput of a PRB is given by

$$b_{uk} = \max_z\{\Lambda^0_{uk}, \cdots, \Lambda^{Z-1}_{uk}\} \tag{3.17}$$

where Λ_{uk}^{z} is the SE of the zth MCS. Λ_{uk}^{z} is expressed as

$$\Lambda_{uk}^{z} = \begin{cases} \lambda_m \lambda_c & \text{if } \Omega_{uk} \leq \Omega \\ 0 & \text{if } \Omega_{uk} > \Omega \end{cases} \tag{3.18}$$

where λ_m and λ_c are the SEs of the modulation level and FEC, respectively, Ω_{uk} is the EESM estimate of the PRB BER, and Ω is the BER threshold, below which error free data transfer is assumed. A sufficient values of Ω is 10^{-6}. In general, if the coding scheme is the same, the higher the modulation level, the larger the observed BER [9].

Table 3.1 summarises all the discussed optimisation utilities.

Table 3.1: Summary of optimisation utilites.

Utility	Synopsis
CFR	This is the channel frequency response of all the PRBs across all the users. This is the most readily available utility, gotten by pilot data transmission. All other utilities are functions of this particular utility.
OSINR	This is the observed SINR at the receiver after data equalisation for all the PRBs across all the users. It combines the effects of transmit power, channel and equalisation technique employed.
SE	This is the spectral efficiency of all the PRBs across all the users. It is theoretical data rate given by the Shannon formula.
BER	This is the BER of all PRBs across all the users. It depicts the reliability of a PRB to carry data through the communications link. In this work, EESM method is used to estimate the BER.
Throughput	This is the actual amount of data that can be transmitted though a PRB. In takes into account the MCS scheme used. It is the most suitable utility when AMC is employed in the system.

It is worth pointing out that all the output SINR, SE, BER and throughput utilities, all ultimately depend on the estimated CFR. Therefore, it can be stated that the CFR utility is the *fundamental* utility of a wireless communication link.

3.4 Existing PRB Allocation Algorithms

3.4.1 Hungarian Algorithm

The Hungarian algorithm [30, 81] was initially used to find the optimum result for the assignment problem. Similarly, in the graph theory, it is used to find the optimum matching of a weighted *bipartite graph* [82]. It optimises the sum minimum or maximum of the particular optimisation utility employed, hence if it is used with the CFR utility, it will find the maximum sum CFR across the users, but not necessarily provide the maximum sum capacity or minimum sum BER. It employs iterative row and column reductions to find the minimum cost of a complete matching given a certain utility matrix. The algorithm is briefly explained in Algorithm 1 below.

Algorithm 1 Hungarian Algorithm

1: Find minimum of each row in cost matrix $\mathbf{B}$ and subtract it from the corresponding row. Zeros should appear on each row.
2: If there are also zeros in each column, go to step 3, otherwise, perform step 1 on the columns. Now there should be zeros in all the row and columns.
3: Try to cover the zeros with the *minimum* number of lines (horizontal or vertical). If the minimum number of lines equals K (size of square cost matrix), then the final solution is reached. Otherwise go to Step 4.
4: Find the minimum cost in the uncovered part of the cost matrix, and subtract it from the uncovered rows, then add it to the covered columns.
5: Repeat steps 3 and 4 until the minimum number of lines covering the zeros in matrix is at least the size of one edge of the matrix.

If finding the maximum is required, apply the algorithm to $-\mathbf{B}$. An example is given below. Notice that the matrix is already negated, because the cost matrix is to be maximised.

$$\begin{bmatrix} -0.7 & -4.8 & -2.1 & -8.2 \\ -8.1 & -2.6 & -6.2 & -0.5 \\ -7.8 & -7.5 & -4.4 & -1.1 \\ -3.2 & -0.2 & -1.1 & -7.6 \end{bmatrix} \rightarrow \begin{bmatrix} 7.5 & 3.4 & 6.1 & 0 \\ 0 & 5.5 & 1.9 & 7.6 \\ 0 & 0.3 & 3.4 & 6.7 \\ 4.4 & 7.4 & 6.5 & 0 \end{bmatrix}$$

$$\rightarrow \begin{bmatrix} 7.5 & 3.1 & 4.2 & 0 \\ 0 & 5.2 & 0 & 7.6 \\ 0 & 0 & 1.5 & 6.7 \\ 4.4 & 7.4 & 4.6 & 0 \end{bmatrix} \rightarrow \begin{bmatrix} 4.4 & 0 & 1.1 & -3.1 \\ 0 & 5.2 & 0 & 7.6 \\ 0 & 0 & 1.5 & 6.7 \\ 1.3 & 4.3 & 1.5 & -3.1 \end{bmatrix}$$

$$\rightarrow \begin{bmatrix} 4.4 & \mathbf{0} & 1.1 & 0 \\ 0 & 5.2 & \mathbf{0} & 10.7 \\ \mathbf{0} & 0 & 1.5 & 9.8 \\ 1.3 & 4.3 & 1.5 & \mathbf{0} \end{bmatrix} \qquad \mathbf{S}_H = \begin{bmatrix} 0 & 1 & 0 & 0 \\ 0 & 0 & 1 & 0 \\ 1 & 0 & 0 & 0 \\ 0 & 0 & 0 & 1 \end{bmatrix}$$

Observe that after step 1, there are 2 columns that do not have any zero on them. Perform step 2. Two more zeros are added to the system, but all the zeros can be covered by 3 lines (the 2 middle rows and the 4th column) which is less than 4. The minimum cost, 3.1, is subtracted from the top and bottom rows (uncovered rows). This introduces negative numbers on the covered column. Adding 3.1 to the covered column (4th column) removes the negative numbers and adds more zeros to the system. For each iteration of steps 3 and 4, more zeros will be added to the system, with the last set of zeros guaranteed to be still in place [30].

It is worth noting that from the example above, there might be more than K zeros in

the final matrix, but only the important zeros are considered - a single zero in a row or a column or in both a row and column. After selecting this zero, the next zero is found from the cofactor matrix (matrix remaining after the row and column corresponding to the first zero are removed), this is iterated until the last zero is assigned. Finally $\mathbf{S_H}$ in the example above, has 1's in the positions of chosen zeros which represent the PRB allocation pattern. The solution is $4.8 + 6.2 + 7.8 + 7.6 = 25.3$.

In [83], a summary of other algorithms such as Edmonds and Karp's algorithm and Gabow's algorithm, that find the optimum solution, similar to the Hungarian problem, are provided.

3.4.2 1-D Greedy Algorithm

A greedy algorithm has a myopic view of the solution space. It analyses only a local part of the solution space (subspace or subgraph) at a time [84]. In this scenario the greedy method emulates a situation, where a user chooses the best part of the spectrum (PRB) based on only his/her channel information, rendering the chosen PRB in-accessible to subsequent users [27]. Since the users cannot be optimised simultaneously, a so-called *user-order* is necessary, which informs the 1-D greedy algorithm of the order in which the users should be optimised. A user-order is a permutation of row (user) indexes varying from 0 to $(U-1)$ of matrix $\mathbf{B}$, according to which the independent iterative PRB allocation is performed. In this work, a user-order is represented by a row vector $\mathbf{s}_a = [s_a^0 \ \cdots \ s_a^{U-1}]$, where s_a^v denotes the vth element of the ath $(a = 0, \cdots, A-1)$ user-order. For example, $\mathbf{s}_0 = [2\ 3\ 0\ 1]$ is the 0th user-order that tells the algorithm to maximise user (row) 2 first, followed by user 3, then user 0 and finally user 1. This algorithm is described sequentially in Algorithm 2.

The example above with performs PRB allocation with the user-order $\mathbf{s} = [3\ 1\ 2\ 0]$, with solution $7.6 + 8.1 + 7.5 + 2.1 = 25.3$, which is less than the optimum Hungarian result. $\mathbf{S}_{1D}$ is the final solution matrix. Note that from the example, there is an inherent

Algorithm 2 1-D Greedy Algorithm

1: Specify the user-order $\mathbf{s} = [s^0 \ \cdots \ s^{U-1}]$.
2: **for** Each element $v = 0, \cdots, (U-1)$ in the user-order **s do**
3: Allocate the best PRB, i.e., $k^* = \arg\max_k b_{s^v k}$, to the user indexed by s^v;
4: Set $b_{s^v k} = 0$ $(k = 0, \cdots, K-1)$ and $b_{s^v k^*} = 0$ $(v = 0, \cdots, U-1)$, so that users do not share subcarriers according to (3.5) - (3.6).
5: **end for**

bias in the 1-D greedy algorithm, where the available PRBs reduce by one after each iteration, leaving fewer and fewer choices to the remaining users, in fact the last user does not have any choice. This is one of the major problems with greedy algorithms. Nevertheless, in terms of complexity, this reduction in optimisation size is an advantage. Therefore, greedy PRB allocation algorithms that have high performance, irrespective of the reducing search space, are very beneficial.

$$\begin{bmatrix} 0.7 & 4.8 & 2.1 & 8.2 \\ 8.1 & 2.6 & 6.2 & 0.5 \\ 7.8 & 7.5 & 4.4 & 1.1 \\ 3.2 & 0.2 & 1.1 & \mathbf{7.6} \end{bmatrix} \rightarrow \begin{bmatrix} 0.7 & 4.8 & 2.1 & 0 \\ \mathbf{8.1} & 2.6 & 6.2 & 0 \\ 7.8 & 7.5 & 4.4 & 0 \\ 0 & 0 & 0 & 0 \end{bmatrix}$$

$$\rightarrow \begin{bmatrix} 0 & 4.8 & 2.1 & 0 \\ 0 & 0 & 0 & 0 \\ 0 & \mathbf{7.5} & 4.4 & 0 \\ 0 & 0 & 0 & 0 \end{bmatrix} \rightarrow \begin{bmatrix} 0 & 0 & \mathbf{2.1} & 0 \\ 0 & 0 & 0 & 0 \\ 0 & 0 & 0 & 0 \\ 0 & 0 & 0 & 0 \end{bmatrix}$$

$$\mathbf{S}_{1D} = \begin{bmatrix} 0 & 0 & 1 & 0 \\ 1 & 0 & 0 & 0 \\ 0 & 1 & 0 & 0 \\ 0 & 0 & 0 & 1 \end{bmatrix}$$

3.4.3 2-D Greedy Algorithm

The 2-D greedy algorithm [27, 28] is a sub-optimal algorithm used for solving the formulated combinational assignment problem. This algorithm iteratively searches for the best available PRB amongst all the users, *i.e.*, it searches through all the PRBs in matrix $\mathbf{B}$, finds the optimal PRB, and allocates it to the row (user) in which that PRB is found. This algorithm allocates very good PRBs to users in early iterations, at the cost of allocating the poorest PRBs to the users that are allocated in the later iterations. Algorithm 3 describes this algorithm. Steps 1 and 2, imply that the best PRB across all

Algorithm 3 2-D Greedy Algorithm

1: Find the best PRB for each user, *i.e.*, $b_{uk^*} = \arg\max_k b_{uk}$.
2: Find and allocate the best PRB to the user on which it exists, *i.e.*, $b_{u^*k^*} = \arg\max_u b_{uk^*}$
3: Set $b_{u^*k} = 0$ $(k = 0, \cdots, K-1)$ and $b_{uk^*} = 0$ $(u = 0, \cdots, U-1)$, so that users do not share subcarriers according to (3.5) - (3.6).

users and PRBs is found and allocated to the user on which the particular PRB is found. This means that the users' interactions are not taken into account, which implies that PRB allocation is made strictly from the view of the PRBs. This is analogous to the time domain maximum rate scheduler. Step 3, just ensures that the required constraints that one user gets only one PRB is upheld. The example for the 1-D greedy algorithm gives the same result for the 2-D greedy algorithm. Notice that, it is not always the

case, because a different user-order for the 1-D greedy algorithm will produce a different result. The final solution for the 2-D greedy example is $8.2 + 8.1 + 7.5 + 1.1 = 24.9$, which is less than both the Hungarian and 1-D greedy solution. However, note that the 2-D greedy solution is one of the possible solutions that the 1-D greedy can find, because the 1-D greedy is dependent on the user-order. For example, the user-order $\mathbf{s} = [0\ 1\ 2\ 3]$ with the 1-D greedy algorithm, will produce the same result as the 2-D greedy algorithm.

$$\begin{bmatrix} 0.7 & 4.8 & 2.1 & \mathbf{8.2} \\ 8.1 & 2.6 & 6.2 & 0.5 \\ 7.8 & 7.5 & 4.4 & 1.1 \\ 3.2 & 0.2 & 1.1 & 7.6 \end{bmatrix} \rightarrow \begin{bmatrix} 0 & 0 & 0 & 0 \\ \mathbf{8.1} & 2.6 & 6.2 & 0 \\ 7.8 & 7.5 & 4.4 & 0 \\ 3.2 & 0.2 & 1.1 & 0 \end{bmatrix}$$

$$\rightarrow \begin{bmatrix} 0 & 0 & 0 & 0 \\ 0 & 0 & 0 & 0 \\ 0 & \mathbf{7.5} & 4.4 & 0 \\ 0 & 0.2 & 1.1 & 0 \end{bmatrix} \rightarrow \begin{bmatrix} 0 & 0 & 0 & 0 \\ 0 & 0 & 0 & 0 \\ 0 & 0 & 0 & 0 \\ 0 & 0 & 1.1 & 0 \end{bmatrix}$$

$$\mathbf{S}_{2D} = \begin{bmatrix} 0 & 0 & 0 & 1 \\ 1 & 0 & 0 & 0 \\ 0 & 1 & 0 & 0 \\ 0 & 0 & 1 & 0 \end{bmatrix}$$

Notice that the Hungarian algorithm has a better spread of PRB allocations, with its minimum allocated value being 4.8. However, it does not choose the largest PRB

values. The 1-D and 2-D greedy algorithms prefer choosing the largest PRB values immediately. This increases the probability of poor PRB allocations such as the 1.1 and 2.1 values in the 2-D and 1-D greedy algorithms, respectively.

Chapter 4

Enhanced Ranking based Greedy PRB Allocation

4.1 Introduction

As discussed in Chapter 3, the 1-D and 2-D greedy algorithms are too myopic in nature. The 1-D greedy algorithm employes either a fixed user-order or randomly chooses a user-order for PRB allocation. The 2-D greedy algorithm does not consider user interaction, and performs allocation from the viewpoint of the PRBs. Both these methods increase the probability that some users are allocated poorly performing PRBs.

In this Chapter, three enhanced ranking based greedy PRB allocation algorithms, referred to as the maximum greedy (MG), mean enhanced greedy (MEG) and single mean enhanced greedy (SMEG) algorithms, are proposed. The MG algorithm finds the best greedy PRB allocation out of multiple evaluations of different user-orders, while the MEG algorithm uses the iterative calculation of the mean (average) of different users' PRB performances to determine the user-order with which the iterative greedy allocation is implemented. The SMEG algorithm is a reduced complexity version of the MEG, by replacing the MEG algorithm's iterative mean estimation of users' PRBs

with a single mean calculation. The proposed greedy algorithms are different from existing greedy algorithms (*e.g.* the 2-D greedy algorithm [27]), in that they provide an appropriate ranking of the users, so that the users with relatively poor channel qualities (low ranking) are given a higher priority during PRB allocation. Furthermore, unlike heuristic algorithms such as GA and particle swarm optimisation that have variable computational complexities, the proposed algorithms are deterministic, have fixed complexities and are relatively fast, which make them suitable for real time wireless communication systems.

The BER performance of the PRB allocation algorithms is crucial in wireless communications and was hardly considered in other relevant work. In addition, the proposed algorithms are applicable to both PRB based SC-FDMA and OFDMA systems. It is shown with simulations, that the SE performances of the proposed algorithms are close to the performance given by the Hungarian algorithm [30] (optimal searching algorithm to maximise the SE), while offering a huge computational advantage. The superior BER performances of the proposed algorithms allow them to have a more positive impact on the actual data throughput of the system when compared to the 1-D and 2-D greedy algorithms. In addition to the computational complexity and fairness analysis, the effects of imperfect channel estimation, root mean square (RMS) delay and Doppler spread on performance of the proposed algorithms are investigated.

Furthermore, a so called selective greedy (SG) algorithm is proposed to reduce the complexity of the greedy algorithms by by selecting only a fraction of the total number of users for optimisation. This SG algorithm is coupled with the mean enhanced ranking technique so that only very worst users (low ranking) optimise their PRB allocation, while the remaining highly ranked users are randomly allocated PRBs (without optimisation). The random allocations do not incur any computational cost. This combination of the SG and the mean enhanced ranking is referred to as the selective mean enhanced greedy (SLMEG) algorithm. It is shown with simulation, that the

SLMEG algorithm provides superior performance over the 1-D and 2-D greedy algorithms, when it is used to minimise the sum BER across the users, especially at fairly high SNRs.

4.2 Enhanced Ranking based Greedy Algorithms

4.2.1 Maximum Greedy Algorithm

As previously discussed, the 1-D greedy algorithm allocates PRBs to users by sequentially finding the maximum PRB in each row (user) of $\mathbf{B}$, while upholding constraints (3.4) - (3.6), which ensure that once a PRB is allocated to a user, no other users can subsequently find it. The proposed MG algorithm performs this sequential allocation multiple times according to pre-determined user-orders and selects the PRB allocation provided by the best user-order (the user-order is explained in the context of the 1-D greedy algorithm described in Chapter 3). Each user-order has a corresponding solution $T_a = \sum b_{\mathbf{s}_a k^*}$, which is the sum of all the k^* chosen PRBs values for the ath user-order. In this work, the A user-orders out of $A!$ user-orders are selected by taking the initial vector $\mathbf{s}_0 = [0\ 1\ \cdots\ (U-1)]$ and cyclically shifting it $(U-1)$ times. Therefore, the selected user-orders are given by $\{\mathbf{s}_0 = [0\ 1\ \cdots\ (U-1)]\ ,\ \mathbf{s}_1 = [1\ 2\ \cdots\ (U-1)\ 0]$, $\cdots$, $\mathbf{s}_{A-1} = [(U-1)\ 0\ 1\ \cdots\ (U-2)]\}$. This method of selecting user-orders ensures that each user-order's solution T_a definitely includes at least one user's best result, because a different user is always optimised first for each user-order chosen in this fashion. However, the user-order with the best overall solution is chosen, as described in Algorithm 4 below.

The selection of A user-orders in step 1 can be appropriately chosen based on the details of the system at hand, or can be randomly initialised. However, the method of initialisation in this work ensures that each users' optimum allocation is compared against each other. The maximisation in step 5, would become a minimisation if the

utility considered is to be minimised, for example the BER utility. The MG algorithm's computational complexity can be scaled by adjusting the value of A based on the desired performance. Nonetheless, analysing a relatively small number of user-orders will produce good results, as shown in Section 4.5. The MG algorithm will definitily provide the optimal performance of the particular utility if all the possible $A!$ user-orders' solutions are found and compared. This approach is highly computationally complex and requires lots of memory because over a million user-orders' solutions need to be evaluated and stored when there are more than 9 users in the system.

Algorithm 4 Maximum Greedy Algorithm

1: Select A user-orders.
2: **for** Each user-order $a = 0, \cdots, (A-1)$ **do**
3: Initialise the user-order's solution: $T_a = 0$
4: **for** each element $v = 0, \cdots, U-1$ in the user-order a, **do**
5: allocate the best PRB, i.e., $k^* = \arg\max_k b_{s_a^v k}$, to the user indexed by s_a^v;
6: accumulate allocated PRBs into the current user-order solution: $T_a = T_a + b_{s_a^v k^*}$;
7: set $b_{s_a^v k} = 0$ $(k = 0, \cdots, K-1)$ and $b_{s_a^v k^*} = 0$ $(v = 0, \cdots, U-1)$, so that users do not share subcarriers according to (3.5) - (3.6).
8: **end for**
9: **end for**
10: Select the user-order with the best solution in terms of sum PRB values i.e., $a^* = \arg\max_a T_a$, as the user-order with which PRB allocation is carried out.

An example of the MG algorithm is provided below, with only two user-orders evaluated.

1st instance of 1-D Greedy with user-order [0 1 2 3]

$$\begin{bmatrix} 0.7 & 4.8 & 2.1 & \mathbf{8.2} \\ 8.1 & 2.6 & 6.2 & 0.5 \\ 7.8 & 7.5 & 4.4 & 1.1 \\ 3.2 & 1.1 & 0.2 & 7.6 \end{bmatrix}$$

2nd instance of 1-D Greedy with user-order [3 2 1 0]

$$\begin{bmatrix} 0.7 & 4.8 & 2.1 & 8.2 \\ 8.1 & 2.6 & 6.2 & 0.5 \\ 7.8 & 7.5 & 4.4 & 1.1 \\ 3.2 & 1.1 & 0.2 & \mathbf{7.6} \end{bmatrix}$$

$$\begin{bmatrix} \mathbf{8.1} & 2.6 & 6.2 \\ 7.8 & 7.5 & 4.4 \\ 3.2 & 1.1 & 0.2 \end{bmatrix} \qquad \begin{bmatrix} 0.7 & 4.8 & 2.1 \\ 8.1 & 2.6 & 6.2 \\ \mathbf{7.8} & 7.5 & 4.4 \end{bmatrix}$$

$$\begin{bmatrix} \mathbf{7.5} & 4.4 \\ 1.1 & 0.2 \end{bmatrix} \qquad \begin{bmatrix} 4.8 & 2.1 \\ 2.6 & \mathbf{6.2} \end{bmatrix}$$

$$\begin{bmatrix} \mathbf{0.2} \end{bmatrix} \qquad \begin{bmatrix} \mathbf{4.8} \end{bmatrix}$$

Notice that the two user-orders provide different results. The [0 1 2 3] user-order provides a total of 24, while the [3 2 1 0] user-order provides a total of 26.4. Therefore the MG algorithm will choose the solution provided by the [3 2 1 0] user-order.

4.2.2 Mean Enhanced Greedy

The MEG algorithm utilises the users' PRB mean (average) performance for determining the dynamic user-order with which the users are optimised. Therefore, unlike the MG algorithm where multiple user-orders are evaluated, the MEG algorithm uses only one user-order, which is not initialised at the start of optimisation, but is constantly adjusted after each allocation of a PRB to a user.

The mean of the PRBs in each row of matrix **B** are calculated and the user with the least mean value is permitted to search for its best PRB, after which (3.4) - (3.6) are upheld. The mean of the remaining users PRBs are re-calculated after subsequent allocations, because the users' mean performances change due to parts of the spectrum

rendered unobtainable. The algorithm is described in Algorithm 5 below.

Algorithm 5 Mean Enhanced Greedy Algorithm

1: Calculate the mean PRB performances $T_u = \frac{1}{K}\sum_{k=0}^{K-1} b_{uk}$ for all available users.
2: Find user $u^* = \arg\min_u T_u$ with the worst mean PRB.
3: Allocate the best PRB, i.e., $k^* = \arg\max_k b_{u^*k}$, to user u^*.
4: Set $b_{u^*k} = 0$ $(k = 0, \cdots, K-1)$ and $b_{uk^*} = 0$ $(u = 0, \cdots, U-1)$, so that users do not share subcarriers according to (3.5) - (3.6).
5: Repeat steps 1-4 until all the users have been allocated PRBs.

An example of the MEG algorithm is given below, where the mean (average) of each iteration is in the vector on the right.

Utility Values	Average
$\begin{bmatrix} 0.7 & 4.8 & 2.1 & 8.2 \\ 8.1 & 2.6 & 6.2 & 0.5 \\ 7.8 & 7.5 & 4.4 & 1.1 \\ 3.2 & 0.2 & 1.1 & \mathbf{7.6} \end{bmatrix}$	$\begin{bmatrix} 3.95 \\ 4.35 \\ 5.20 \\ \mathbf{3.02} \end{bmatrix}$
$\begin{bmatrix} 0.7 & \mathbf{4.8} & 2.1 \\ 8.1 & 2.6 & 6.2 \\ 7.8 & 7.5 & 4.4 \end{bmatrix}$	$\begin{bmatrix} \mathbf{2.53} \\ 5.63 \\ 6.56 \end{bmatrix}$
$\begin{bmatrix} 8.1 & 6.2 \\ \mathbf{7.8} & 4.4 \end{bmatrix}$	$\begin{bmatrix} 7.15 \\ \mathbf{6.10} \end{bmatrix}$
$\begin{bmatrix} \mathbf{6.2} \end{bmatrix}$	$\begin{bmatrix} \mathbf{6.2} \end{bmatrix}$

The solution provided is the 26.4. Note that all the PRBs with low values have been avoided. Furthermore, notice that in the MEG algorithm, no explicit user-order is initialised at the start. However, the algorithm constantly determines the most appropriate user for optimisation in any particular iteration, by recalculating the mean and choosing the user with worst average PRB value, *i.e.*, steps 1 and 2 are repeated before any allocation of a PRB to a user. The standard parts of the greedy algorithm that allocate the PRB and uphold the required constraints are performed in steps 3 and 4, respectively. The minimisation and maximisation in steps 2 and 3, would become a maximisation and minimisation, respectively, if the BER utility were considered.

The MEG algorithm gives users that have a poor channel link quality, a higher priority, which allows them to search for PRBs first. This aims to maximise these poor users' probabilities of obtaining fairly good PRBs. While the users that on average, have good PRB values, will most likely be allocated good PRBs irrespective of their priority.

4.2.3 Single Mean Enhanced Greedy Algorithm

The SMEG algorithm reduces the complexity of the MEG algorithm by calculating the mean of the users' PRBs (b_{uk}) only once and followed by a sorting of the calculated mean values. Unlike the MG algorithm that evaluates the performance of multiple user-orders, the SMEG algorithm evaluates only $A = 1$ user-order. The only user-order is determined by ascending or descending (for BER) order of users' mean PRB performance $T_u = \frac{1}{K}\sum_{k=0}^{K-1} b_{uk}$. The SMEG algorithm is described in Algorithm 6 below.

An example of the SMEG algorithm is shown below. The mean of the users' utility values are in the vector on the right. Notice that the mean values do not change after every iteration, which is unlike the MEG algorithm.

Algorithm 6 Single Mean Enhanced Greedy Algorithm

1: Calculate the mean PRB performances $T_u = \frac{1}{K}\sum_{k=0}^{K-1} b_{uk}$ for all users $u = 0, \cdots, U-1$.
2: Determine $\mathbf{s} = [s^0 \ \cdots \ s^{U-1}]$ by ascending order of T_u's.
3: **for** For each element $v = 0, \cdots, U-1$ in the user-order $\mathbf{s}$, **do**
4: Allocate the best PRB, i.e., $k^* = \arg\max_k b_{s^v k}$, to the user indexed by s^v;
5: set $b_{s^v k} = 0$ $(k = 0, \cdots, K-1)$ and $b_{s^v k^*} = 0$ $(v = 0, \cdots, U-1)$, so that users do not share subcarriers according to (3.5) - (3.6).
6: **end for**

Utility Values

$$\begin{bmatrix} 0.7 & 4.8 & 2.1 & 8.2 \\ 8.1 & 2.6 & 6.2 & 0.5 \\ 7.8 & 7.5 & 4.4 & 1.1 \\ 3.2 & 0.2 & 1.1 & \mathbf{7.6} \end{bmatrix}$$

Average

$$\begin{bmatrix} 3.95 \\ 4.35 \\ 5.20 \\ \mathbf{3.02} \end{bmatrix}$$

$$\begin{bmatrix} 0.7 & \mathbf{4.8} & 2.1 \\ 8.1 & 2.6 & 6.2 \\ 7.8 & 7.5 & 4.4 \end{bmatrix} \qquad \begin{bmatrix} \mathbf{3.95} \\ 4.35 \\ 5.20 \end{bmatrix}$$

$$\begin{bmatrix} \mathbf{8.1} & 6.2 \\ 7.8 & 4.4 \end{bmatrix} \qquad \begin{bmatrix} \mathbf{4.35} \\ 5.20 \end{bmatrix}$$

$$\begin{bmatrix} 4.4 \end{bmatrix} \qquad \begin{bmatrix} \mathbf{5.20} \end{bmatrix}$$

The SMEG algorithm provides a solution of 24.9, which is slightly better than the 2-D greedy algorithm and worse than the MEG algorithm. However, the poor PRBs

have been avoided also. Steps 1 and 2 of the MEG algorithm, determine the enhanced ranking (user-order), with which the greedy algorithm (steps 3 - 6) uses to allocate PRBs. If minimisation of the utility is required, for example the BER utility, the user-order in step 2 would be determined by descending order of T_u's and the maximisation in step 4, would become a minimisation.

4.3 Selective Enhanced Ranking based Greedy Algorithms

In this section, a so-called selective greedy (SG) algorithm is proposed. It reduces the complexity of the greedy algorithm, by reducing the number of users that optimise PRB allocation. It is based on the hypothesis; if the PRB allocation for the fraction of users that have poor PRBs on average is optimised, then the remaining users, can be randomly allocated PRBs without the risk of allocating bad PRBs to them. Therefore, the greedy optimisation is *selectively* performed for a fixed number of users U_1, and after these fixed number of users have iteratively searched for PRBs, the remaining $(U - U_1)$ users are randomly allocated the remaining PRBs. For example, in a $U = 100$ user system, $U_1 = 50$ poorly ranked users are allowed to search for PRBs based on the performance of their b_{uk}'s, while the remaining 50 users are allocated PRBs randomly, without any consideration of their b_{uk} performance. The complexity of the system is reduced because only U_1 greedy search iterations are carried out, while the random allocation incurs negligible computational costs (similar to the fixed allocation/round-robin system). The proportion of selectiveness is given by $r = (\frac{U_1}{U})$. For example, in a $U = 100$, user system, if $U_1 = 75$ the proportion of selectiveness is $r = \frac{75}{100}$. This algorithm is described in Algorithm 7.

In step 1 of the SG algorithm, the user-order is determined in any appropriate fashion. On its own, similar to the 1-D greedy algorithm, the SG algorithm does not provide suitable results, however, its performance can be enhanced by using the mean

Algorithm 7 Selective Greedy Algorithm

1: Specify the user-order $\mathbf{s} = [s^0 \ \cdots \ s^{U-1}]$.
2: Initialise the desired amount of randomness, $r\%$.
3: Define the new reduced-size user order $\mathbf{s}_1 = [s^0 \ \cdots \ s^{rU-1}]$.
4: **for** Each element $v = 0, \cdots, rU-1$ in the new user-order $\mathbf{s}_1$ **do**
5: Allocate the best PRB, i.e., $k^* = \arg\max_k b_{s_1^v k}$, to the user indexed by s^v;
6: Set $b_{s^v k} = 0$ $(k = 0, \cdots, K-1)$ and $b_{s^v k^*} = 0$ $(v = 0, \cdots, U-1)$, so that users do not share subcarriers according to (3.5) - (3.6).
7: **end for**
8: Randomly allocate PRBs to the remaining $(1-r)U$ users.

enhanced ranking discussed earlier. For example, the algorithm that combines the SG algorithm and the SMEG algorithm is referred to as the selective mean enhanced greedy (SLMEG) algorithm. In addition, the SG algorithm can be combined with the MEG, where the mean is re-calculated after every iteration. However, this would increase the complexity. An example of the SLMEG algorithm is presented below:

Utility Values

$$\begin{bmatrix} 0.7 & 4.8 & 2.1 & 8.2 \\ 8.1 & 2.6 & 6.2 & 0.5 \\ 7.8 & 7.5 & 4.4 & 1.1 \\ 3.2 & 0.2 & 1.1 & \mathbf{7.6} \end{bmatrix}$$

Average

$$\begin{bmatrix} 3.95 \\ 4.35 \\ 5.20 \\ \mathbf{3.02} \end{bmatrix}$$

$$\begin{bmatrix} 0.7 & \mathbf{4.8} & 2.1 \\ 8.1 & 2.6 & 6.2 \\ 7.8 & 7.5 & 4.4 \end{bmatrix} \qquad \begin{bmatrix} \mathbf{3.95} \\ 4.35 \\ 5.20 \end{bmatrix}$$

$$\begin{bmatrix} 8.1 & 6.2 \\ 7.8 & 4.4 \end{bmatrix} \qquad \begin{bmatrix} 4.35 \\ 5.20 \end{bmatrix}$$

Notice that the algorithm stops after the first two allocations. The poor PRBs have been avoided and random PRB allocation can now take place, either one of the 8.1 and 4.4 or the 6.2 and 7.8 permutations can be used.

4.4 Complexity and Memory Analysis

4.4.1 Computational Complexity

The complexities of the proposed algorithms are derived and compared to those of the Hungarian algorithm [25, 30] and the sub-optimal 1-D and 2-D greedy algorithms [27,28], in terms of the number of comparisons needed to allocate PRBs to all the users in the system. In this work, since the number of users is equal to the number of PRBs, *i.e.*, $(U = K)$, the complexity of the algorithms will be written in terms of the the number of users U alone. A computation, such as addition, subtraction, multiplication or division is assumed to have the same complexity as one comparison. This might not be totally realistic, but it does serve as a benchmark for counting all the operations (comparisons and computations).

The computational complexity of the Hungarian algorithm is given by $\Upsilon_H = \frac{1}{6}(11U^3 + 12U^2 + 31U)$ [30]. The iterative nature of the algorithm means lots of comparisons are needed for the optimal solution.

The 1-D greedy algorithm needs $(U - 1)$ to find the best PRB for the first user. Nevertheless, the number of searches reduce by one, after each iteration, because fewer and fewer users need optimisation. Therefore, the total number of comparisons needed for the whole allocation procedure is $\Upsilon_{1D} = \sum_{u=1}^{U}(u - 1) = \frac{1}{2}(U^2 - U)$.

In a similar manner, the total number of comparisons needed by the 2-D greedy algorithm to find the best PRB in the first iteration, out of the initial U^2 PRBs in matrix $\mathbf{B}$ is $(U^2 - 1)$. However, after each iteration, the size of the matrix reduces by one until there is just one element remaining. Therefore, the total number of comparisons needed

for the whole allocation procedure is $\Upsilon_{2D} = \sum_{u=1}^{U}(u^2 - 1) = \frac{1}{3}U^3 + \frac{1}{2}U^2 - \frac{5}{6}U$.

The number of comparisons for the MG algorithm is given by $\Upsilon_{MG} = A\sum_{u=1}^{U}(u - 1) + (A - 1) = \frac{A}{2}(U^2 - U) + (A - 1)$, where the first term is the number of comparisons needed for the total iterative allocation of one user-order multiplied by the total number of user-orders A, and the second term is the number of comparisons used for finding the best out of A user-orders.

The following assumptions are used to derive the number of comparisons for the MEG algorithm:

1. Addition is taken as one computation for two numbers.
2. Division is also taken as one computation for two numbers.
3. Calculating the mean of U numbers needs $(U - 1)$ additions and one division. Which gives credence to assumption 2, because the complexity of one division is negligible when compared to all the additions, especially in a system with large number of users.

Based on the above assumptions, to calculate the mean of U PRBs, $U - 1 + 1 = U$ computations are required. Therefore, the number of computations for all the U users is U^2. The total number of computations needed for a complete allocation using the MEG algorithm is given by $\Upsilon_{MEG} = \sum_{u=1}^{U}(u^2+u-1) = \frac{1}{6}(U^2+U)(2U+1)+\frac{1}{2}(U^2-U)$, where the first term is the total number of computations needed for calculating the mean of all the users PRBs and the second term is the total number of computations needed for the iterative allocation of PRBs for one user-order (1-D greedy). After simplification, the total number of computations is given by $\Upsilon_{MEG} = \frac{1}{3}U^3 + U^2 - \frac{1}{3}U$.

The number of comparisons for the SMEG algorithm is given by $\Upsilon_{SMEG} = \sum_{u=1}^{U}(u - 1) + U^2 = \frac{1}{2}(3U^2 - U)$, where the first term is the number of comparisons needed for the iterative allocation of one user-order added to the total number of computations (U^2) needed for calculating the mean of the U users mean PRB values.

Table 4.1: Number of operations for each algorithm and normalised complexity, $A = U = 100$ for the maximum greedy algorithm

Algorithm	Number of computations	Normalised complexity	Memory Requirements
2-D Greedy [27] [28]	$\frac{1}{3}U^3 + \frac{1}{2}U^2 - \frac{5}{6}U$	68.30	2
Hungarian [25]	$(11U^3 + 12U^2 + 31U)/6$	374.52	Variable
1-D Greedy [27]	$\frac{1}{2}(U^2 - U)$	1	2
SG	$1/2(U_1^2 - U_1)$	0.56 (r = 75%) 0.25 (r = 50%)	2
MG	$A\frac{1}{2}(U^2 - U) + A - 1$	100	$U^2 + U + 4$
MEG	$\frac{1}{3}U^3 + U^2 - \frac{1}{3}U$	69.4	2
SMEG	$\frac{1}{2}(3U^2 - U)$	3.02	$\log U + U + 2$
SLMEG	$1/2(U_1^2 - U_1) + U^2$	2.58 (r=75%) 2.27 (r=50%)	$\log U + U + 2$

The SG algorithm has a lower complexity than the 1-D greedy algorithm because only a fraction of the users PRBs are allocated through optimisation. The SLMEG algorithm's computational complexity benefits from the computational saving of the SG algorithm. The SLMEG algorithm has an additional U^2 computations which is due to the estimation of the all the users' mean PRB values. Therefore, the total number of computations for a complete PRB allocation by the SLMEG algorithm is given by $1/2(U_1^2 - U_1) + U^2$, where $U_1 = rU$.

The complexities of the discussed algorithms are summarised in Table 4.1. Column 2 of Table 4.1 presents the computational complexity in terms of the number of users U. Column 3, presents the 1-D greedy normalised numerical complexity of the algorithms for $U = 100$ users.

4.4.2 Memory Requirements

In terms of memory, all the algorithms require U^2 memory slots to store the matrix of users' utility values. In addition, comparisons that find the minimum or maximum of a PRB value for a user can be efficiently done with two memory slots, using a compare

and discard scheme (where only two elements are compared in each instant, and the minimum in each comparison is saved while the other value is replaced by the new value to be compared). In all the greedy algorithms, except the MG algorithm, the required memory reduces after every iteration, therefore, to estimate the required memory, the largest memory required at the start of the algorithm is estimated. Furthermore, all the algorithms will need either U memory locations to store the final allocation result, nevertheless, extra memory is not needed because after the first iteration $2U$ memory slots are freed, which can then be used to store the solutions after each iteration.

The 1-D and 2-D greedy algorithms only require the two extra memory slots at the beginning of the algorithms to carry out the required comparisons.

The MEG algorithm is similar, because only two memory slots are required to store and compare the users' mean utility values, two users at a time. When the user with the smallest mean utility value is found, the same two memory slots can be used for that user's specific comparisons to find the best PRB.

The SMEG algorithm requires U memory slots to store all the users' mean PRB values because the users' mean utility values have to be ranked (sorted). This is unlike the MEG that just needs to find the poorest user. In addition, the MEG algorithm will need extra memory to perform the sorting; if the in place quicksort algorithm is employed, the extra memory requirement will be $\log(U)$. Finally, two memory slots are required for the comparisons required to find each user's best PRB, similar to the other greedy algorithms. Therefore, the SMEG algorithm needs a total of $U+2+\log U$ memory slots. The SLMEG algorithm required the same amount of memory as the SMEG algorithm.

The MG algorithm requires another U^2 memory slots to keep a copy of the users' utility matrix, which prevents the destruction of the utility matrix after an evaluation of the 1-D greedy algorithm. Furthermore, U memory slots are required to keep the user-order of the current 1-D greedy evaluation. In addition, it needs 2 memory slots

for the comparisons needed to find the best PRB. Finally, two slots are required to store and compare the final solutions of two subsequent user-orders. Therefore the largest memory required for the MG algorithm is $U^2 + U + 4$

The Hungarian algorithm is quite heuristic and there is no definite amount of memory requirement. Two slots are also needed for the comparisons needed to find minimum on each row and each column. A varying amount of memory is needed to specify the location of the zeros in the utility matrix after the first two iterations, the worst case here is U^2, where all the elements are equal. However, the algorithm stops in this instance. A varying amount of memory is also needed to find the lines needed to cover all the zeros.

4.5 Simulations

4.5.1 Setup

Monte Carlo simulations are used to determine the performance of the proposed algorithms, in comparison to the Hungarian algorithm [30], 2-D algorithm [27] and fixed subcarrier allocation (SA) method, a fixed pattern of allocating PRBs to users, which is analogous to the time domain round robin allocation method [3]. The average performances of BER, capacity and throughput provided, are averages across all the users in the system.

A centre frequency of 2 GHz is assumed, with six different transmission bandwidths, ranging from 1.25 MHz (6 PRBs which supports 6 users in this work) to 20 MHz bandwidth (100 PRBs which supports 100 users) $K = U$. Each PRB is made up of 12 subcarriers, with a subcarrier spacing of 15 KHz, therefore, each PRB occupies 180 KHz. Perfect CSI is assumed for all the simulations, except in Figure 4.6. The wireless channel is Clarke's NLOS Rayleigh fading with the typical urban (T.U.) area, 6 tap PDP (Table 2.1), which is generated by the process described in [33]. It has an

Table 4.2: Correction value β for EESM derived BER estimation.

	QPSK	QAM-16	QAM-64
OFDMA	1.3	3.0	8.0
SC-FDMA	1.3	4.5	15.0

approximate RMS delay spread of 1 μs [1], except in Figure 4.7 where and exponential channel is used so that the RMS delay spread can be varied according to (2.3). A Doppler spread of 370 Hz with channel coherence time of about 1.14 ms (calculated with $0.423/B_d$ as in [33]) is used except in Figure 4.8 where the speed of the mobile is varied to change the Doppler spread according to (2.6). The desired BER $\Omega = 10^{-5}$ and the QPSK modulation is used for all simulations except for the investigations into throughput and outage probability performances in Sub-section 4.5.5. The noise is modelled by AWGN described in Section 2.1.1, with noise power density of $N_0/2$ per dimension. The EESM technique is used to model an un-punctured 1/2 rate convolutional code with the correction values β, which are given in the Table 4.2 for all the modulation levels, therefore all BER performances are under this coding rate. The SNR is defined as the average ratio of the received signal power to noise power.

The β values in Table 4.2 are derived using the same technique in [79]. This calibration has to be performed before hand and the values stored in memory, in addition to the AWGN BER performance of a system with the same parameters described in the preceding paragraph.

4.5.2 BER and SE Performance Comparisons

In this Sub-section, the SE utility is used for PRB allocation. A 10 MHz bandwidth is used, which supports $K = 50$ PRBs and in this work $U = K$.

Figure 4.1 demonstrates the SE performance for all the discussed algorithms. With the exception of the fixed SA algorithm, there are negligible SE differences between all

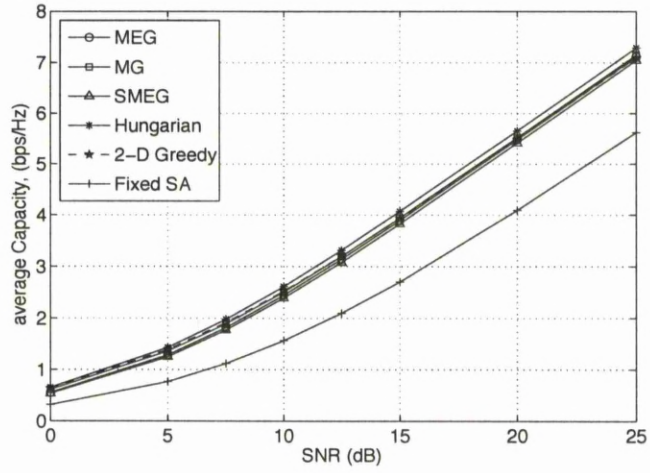

Figure 4.1: Average SE performance of the discussed dynamic PRB allocation algorithms for $U = 50$ users.

the algorithms, and they all have a gain of about 5 dB over the fixed SA at an average SE of 5 bps/Hz.

The real system performance such as throughput is highly dependent on actual BER. Hence, in Figure 4.2, the MEG provides the best BER performance, with a gain of approximately 5 dB and 8 dB at a BER of 10^{-5} over the Hungarian, and both the MG and SMEG algorithms, respectively. The MEG algorithm also has a gain of 13 dB over the 2-D greedy algorithm at a BER of 10^{-3}. Remember that the MEG achieves this with a comparable complexity to the 2-D greedy algorithm and a far lower complexity than the Hungarian algorithm, as presented in Table 4.1. Furthermore, both the SMEG and MG algorithms outperform the 2-D greedy algorithm by 10 dB and 8 dB, at a BER of 10^{-3}, respectively. The MG and SMEG algorithms performances come within 1 dB of the Hungarian algorithm at low SNR and have only about a 3 dB loss at high SNR, while having a huge computational complexity gain.

Figure 4.3 shows the impact of the number of users on the average SE performance of different algorithms at a fixed SNR of 15 dB. The SE improves with the increase

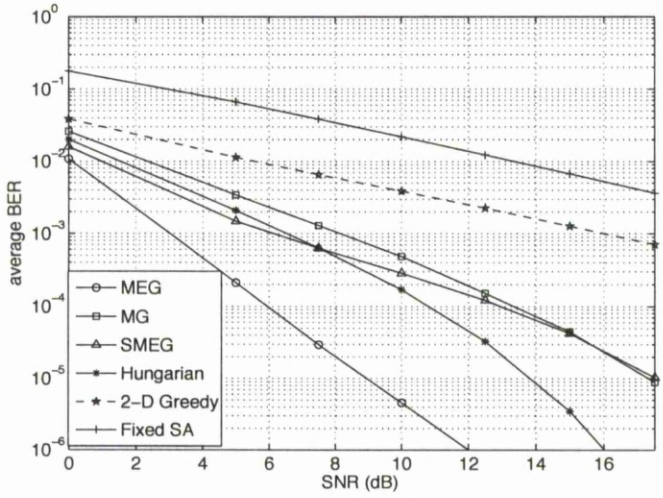

Figure 4.2: Average BER performance of discussed algorithms for $U = 50$ users.

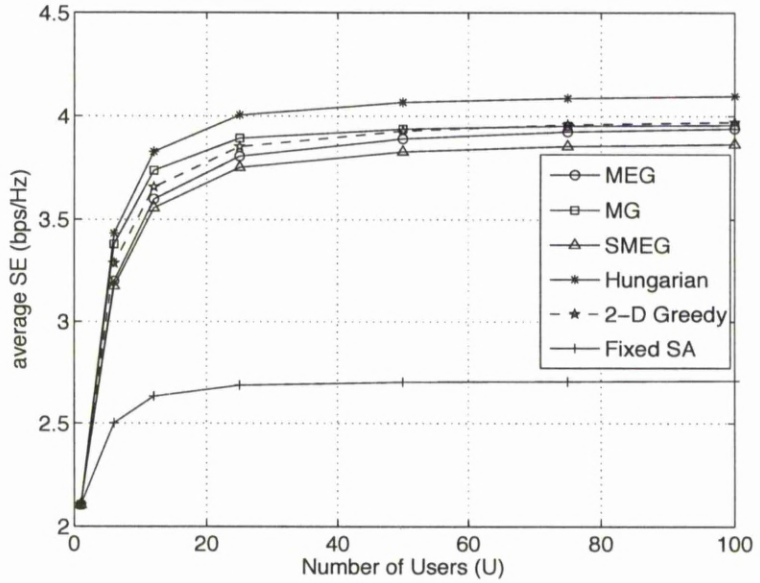

Figure 4.3: Impact of the number of users on the SE performance of the PRB allocation algorithms at SNR = 15 dB.

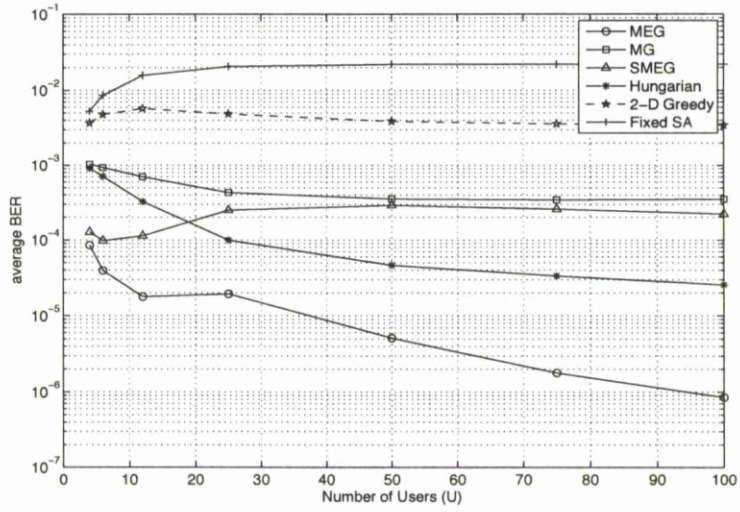

Figure 4.4: Impact of the number of users on the BER performance for the PRB allocation algorithms at SNR = 10 dB

of the number of users, due to multiuser diversity. The MEG, MG and 2-D greedy algorithms have negligible performance differences, and they come within 0.1 bps/Hz of the Hungarian algorithm, while the SMEG algorithm comes within 0.2 bps/Hz of the Hungarian algorithm.

Figure 4.4 shows the impact of the number of users on average BER performance of different algorithms at a fixed SNR of 10 dB. The MEG algorithm takes huge advantage of the multiuser diversity gain that comes about by an increase in number of users, achieving 10^{-6} for $U = 100$ users. The MG, SMEG and Hungarian algorithms have their minimum BER around 10^{-4} for $U = 100$ users. In particular, the SMEG algorithm, has a worse performance as the number of users in the system increases. This phenomenon could be attributed to the in-efficient ranking (user-order) of the SMEG algorithm which only performs well (very similar to the MEG) when there are about 6 users in the system. As the number of users increase, the ranking loses its ability to properly differentiate between users' performances. The 2-D greedy and fixed SA

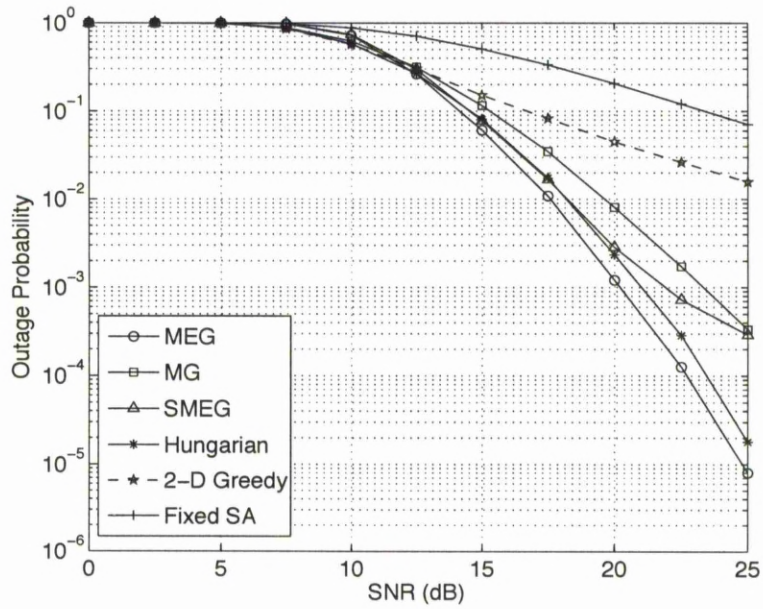

Figure 4.5: Outage probability performance of the PRB allocation algorithms for $U = 50$ users; minimum required user data rate is 0.5 Mbps.

algorithms extract no multiuser diversity gain from the system.

The actual data throughput performance of the proposed algorithms are superior to the 2-D greedy algorithm, because in Figure 4.2, the proposed algorithms achieve the desired BER at much lower SNR levels than the 2-D greedy algorithm. Therefore, extra processing (performance penalties in form of re-transmissions, stronger coding, etc.) would be needed by the 2-D greedy algorithm to practically achieve the desired BER, which in turn affects the actual data throughput.

The outage probability is a measure used to judge the fairness of a system, where all the users require the same quality of service (QoS). The probability that users do not meet the minimum required SE of 2.78 bps/Hz is demonstrated in Figure 4.5 . An SE of 2.78 bps/Hz is equivalent to 0.5 Mbps for one 180 KHz wide PRB. The MEG algorithm has a performance gain of about 1 dB, 2 dB and 3 dB at an outage probability of 10^{-3} over the Hungarian, SMEG and MG algorithms, respectively. The

MEG also has about 8 dB gain over the 2-D greedy algorithm at an outage probability of 10^{-2}. The 2-D greedy algorithm is the worst performing PRB allocation algorithm in terms of outage probability, with more than 10^{-2} at 25 dB, which is over three orders worse than the MEG algorithm. In addition, AMC will improve the outage probability of the proposed algorithms, because they give more users the opportunity to avoid bad (deeply faded) PRBs. AMC will not benefit the all the users which suffer outage under the 2-D greedy algorithm, because those users are not even allocated PRBs that can carry the minimum amount of data.

4.5.3 Effects of Channel Parameters

Effect of channel estimation error: The impact of pilot symbol assisted modulation (PSAM) [85] channel estimation, on the PRB allocation algorithms is investigated using,

$$\mathbf{h}_u = \mathbf{z}_u + \epsilon_u \tag{4.1}$$

where $\mathbf{h}_u = [h_u(0)\ h_u(1) \cdots h_u(L)]^T$ is a vector of the $(L+1)$ non-zero elements on the first column of the $(N \times N)$ time domain circular CIR matrix $\mathbf{H}_u$ and $\mathbf{z}_u$ is the estimate of $\mathbf{h}_u$. The error vector ϵ_u has $(L+1)$ *i.i.d.* elements, each being Gaussian with zero mean and variance $(1 - |\rho_{hz}|^2)$, where ρ_{hz} is the correlation co-efficient between $\mathbf{h}_u$ and $\mathbf{z}_u$. Note, $\rho_{hz} = 1$ corresponds to perfect channel estimation. In the simulations, $\mathbf{z}_u$ is used for dynamic PRB allocation, while perfect CSI is used for equalisation to isolate the impact of imperfect CSI on PRB allocation performance. In Figure 4.6, ρ_{hz} varies between 0.8 and 1, corresponding to 20 % and 0% channel estimation error, respectively. The MEG algorithm has the best performance compared to the other algorithms, while the SMEG, MG and Hungarian algorithms have similar performances. The 2-D and fixed SA algorithms do not show any performance gain, regardless of the quality of channel estimates.

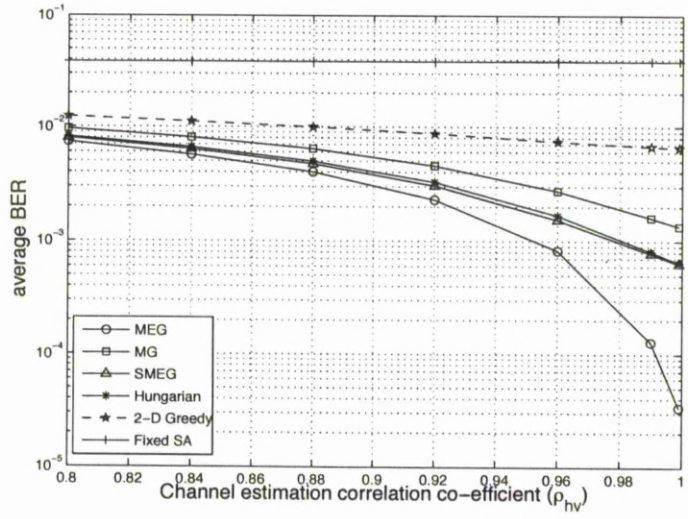

Figure 4.6: Effect of imperfect channel estimation on the BER performance of the PRB allocation algorithms. SNR = 7.5 dB and $U = 50$ users.

Effect of RMS delay spread: The effect of the RMS delay spread [33] of a wireless channel has hardly been investigated in the literature for a SC-FDMA system employing dynamic PRB allocation. An exponentially decaying 20-tap channel with the RMS delay spread varying between 0 μs and 4.5 μs is used in Figure 4.7 to illustrate this point. At 0 μs (flat fading channel), there is no difference between the algorithms due to lack of frequency diversity. However, as the RMS delay increases, the frequency diversity increases which the MEG algorithm fully exploits. Nevertheless, at very high RMS delay, the SMEG and MEG algorithms lack the information to provide good allocation due to the rapid changes in the frequency domain channel, hence they are outperformed by the Hungarian algorithm. Especially, the MEG algorithm has its best performance between 1 and 1.5 mus RMS delay, but when the frequency diversity in the channel increases, the mean criterion cannot fully describe the different performances of the users in the system. The fixed SA technique, extracts no frequency diversity gain from the system.

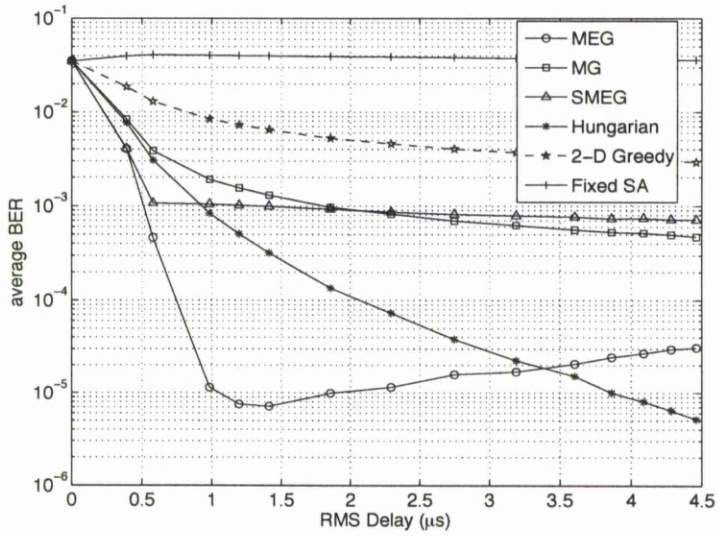

Figure 4.7: Effect of RMS delay spread on the BER performance of the PRB allocation algorithms, SNR = 7.5 dB and $U = 50$ users.

Effect of Doppler Spread: To investigate the effects of Doppler spread on the algorithms, the Doppler spread is varied between 10 Hz and 370 Hz (5 km/h and 200 km/h) and dynamic PRB allocation is performed every 10 ms, 10 times less than as specified in the uplink LTE standard. Figure 4.8 shows that at high Doppler spread, the performance of all the algorithms are similar because the channel is changing too fast, and the specified user allocation is outdated. The advantage of the MEG algorithm is in the low Doppler spread region, where the performance constantly improves as the Doppler spread reduces, while the other algorithms have an almost constant performance between values of 10 Hz and 100 Hz. Therefore, when the users have low mobility, the MEG would be beneficial, while for high mobility systems, the SMEG would be suitable due to its lower complexity and comparable performance.

Furthermore, Figure 4.8 also sheds light on the feedback delay of CSI. The one millisecond (ms) LTE TTI, is suitable for speeds of up to 200 km/h, this can be verified with equation 5.40c in [33], where a 200 km/h user would have a channel coherence

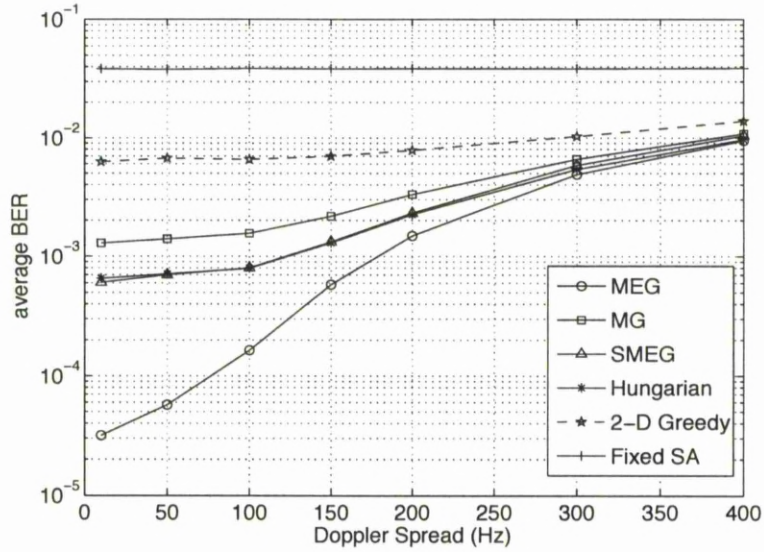

Figure 4.8: Effect of Doppler spread on performance with SNR = 7.5 dB and allocation performed once every 10 ms.

time of about 1.1 ms for a centre frequency of 2 GHz. However, feedback of the CSI every 1 ms would be computationally intensive. Therefore, in Figure 4.8, allocation is performed once every 10 ms, which reduces the computational burden on the system. It also shows that a CSI feedback delay of at most 10 ms still provides good performance at reasonable user speeds.

4.5.4 Effects of Optimisation Utilities

Figure 4.9 shows the average BER performance of the discussed algorithms, with the same setup as Figure 4.2. This BER utility based MEG and SMEG algorithms have identical performance to the optimal Hungarian algorithm, while requiring much lower computational complexities, according to Table 4.1. The BER utility based MG is marginally worse than the optimum Hungarian algorithm. All the proposed algorithms outperform the 2-D greedy algorithm by approximately 10 dB at a BER of 10^{-3}. At a SNR of 10 dB, the 2-D greedy algorithm achieves a BER of 8×10^{-3} which is not

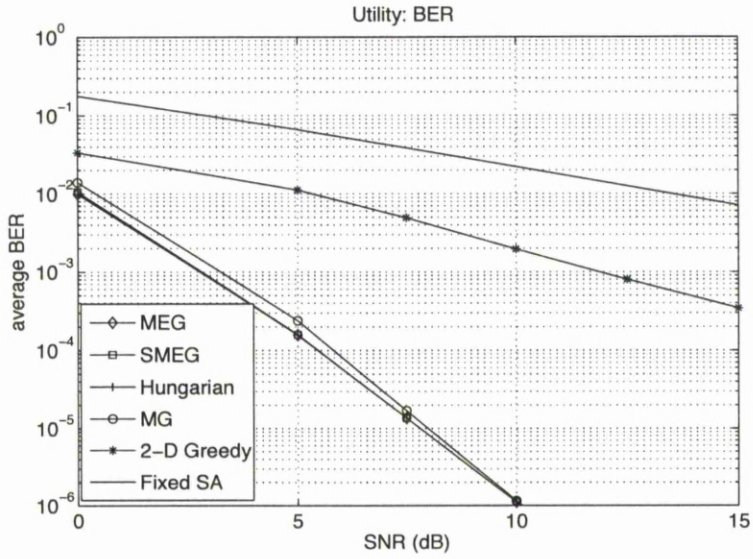

Figure 4.9: Average BER performance of the algorithms with $U = 100$ users, with the EESM derived BER utility.

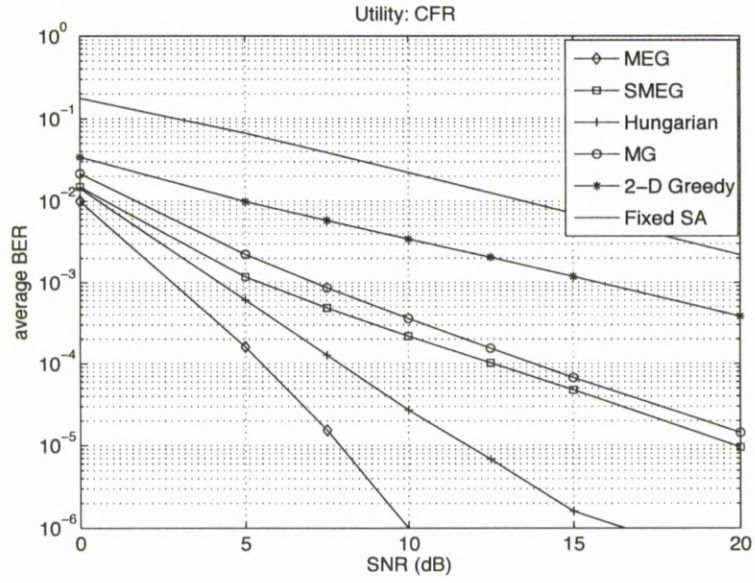

Figure 4.10: Average BER performance of the algorithms with $U = 100$ users and CFR utility.

even suitable for speech communications. Comparing figures 4.2 and 4.9, it is easy to see that the 2-D greedy algorithm does not perform any better under the BER utility. This could be attributed to the inherent unfairness of the 2-D greedy algorithm.

In Figure 4.10, the performances of the algorithms using under the CFR utility are illustrated. Observe that the BER performances of all the algorithms are worse than their corresponding counterparts in Figure 4.9. Maximising the CFR utility would definitely provide the optimal BER performance in a single user case. However, for the complete problem formulation in this work, directly using the Hungarian algorithm to maximise the CFR does not provide the optimal BER performance. The impact of the CFR utility on BER performance is even more obvious when used with the greedy algorithms. The greedy algorithms, except the MEG, do not achieve a BER of 10^{-5}, even at a SNR of 15 dB. The only algorithm that employs CFR as utility and still has a very similar performance under the BER utility, is the MEG algorithm.

In Figure 4.11, the performances of the algorithms using under the OSINR utility are shown. Observe that the BER performances of all the algorithms are worse than their corresponding counterparts in Figure 4.9. This is similar to the CFR utility based optimisation. However, Hungarian algorithm is particularly adversely affected by this OSINR utility, because even the OSINR based SMEG algorithm outperforms both the Hungarian and MG algorithms. The MEG algorithm still has the best performance, achieving 10^{-5}, at an SNR of 12.5 dB. However, comparing Figure 4.11 with Figures 4.9, 4.10 and 4.2, this OSINR utility gives the worst MEG performance.

Figure 4.12 shows the BER performances of the SLMEG algorithm under two utilities (BER and CFR) and two amount of randomness ($r = 75\%$ and $r = 50\%$) for $U = 100$ users. The BER utility based SMEG algorithm, which has very near optimal performance as seen in Figure 4.9 is included for comparison. From Figure 4.12, it is easy to see that the BER utility based SLMEG algorithm with both $r = 75\%$ and $r = 50\%$ is about 2 dB and 8 dB worse than the SMEG algorithm at a BER of 10^{-5},

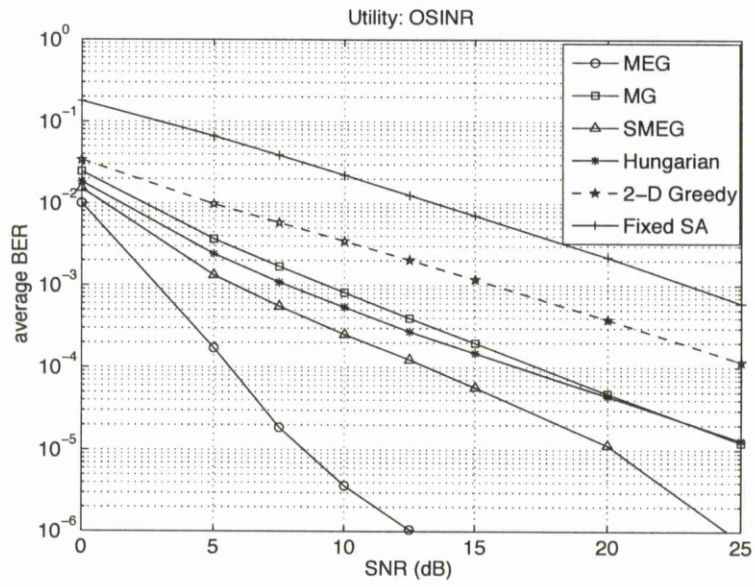

Figure 4.11: Average BER performance of the algorithms with $U = 100$ users under the OSINR utility.

respectively. The CFR utility based SLMEG algorithms perform very poorly and at SNR = 25 dB, do not still achieve a BER of 10^{-5}. This implies that the SLMEG algorithm provides a suitable performance only when the user-order is efficient. In this case, the user-order produced by ranking the users' BER is superior to the user-order produced by ranking the users' CFR. Comparing Figures 4.9 and 4.12, the BER utility based SLMEG algorithm also outperforms the 2-D greedy, 1-D greedy and fixed SA algorithms, which need above 25 dB to achieve a BER of 10^{-5}.

4.5.5 Effect of Adaptive Modulation

In this Section, the throughput utility is used to investigate the impact of AM on the PRB allocation algorithms. A single FEC coding scheme and three modulation schemes, QPSK, QAM-16 and QAM-64 are used. The outage probability in this case, is the probability of a user not being able to use any of the modulation schemes, thereby

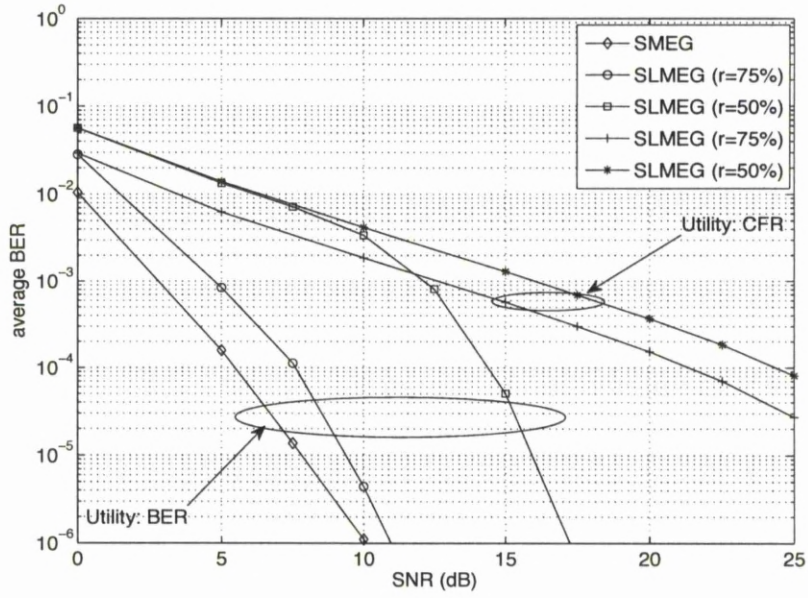

Figure 4.12: Average BER performance of the SMEG and SLMEG algorithms for $U = 100$ users under the BER utility.

having a throughput of zero (no transmission).

Comparing Figures 4.13 and 4.14, there is a marginal difference between maximising the CFR utility and maximising the throughput utility. The throughput is far more complex to estimate, because the EESM has to be carried for as many AMC levels that are employed. In this work, three EESM calculations are performed for each of the three modulation levels. The correction factor β for all the modulation levels is given in Table 4.2. Therefore, in order to keep the complexity low, it is better to maximise CFR and then select the appropriate MCS for each PRB. This implies that the EESM BER is calculated only once.

Comparing Figures 4.15 and 4.16, it is easy to see that maximising CFR degrades the outage probability performance of the low complexity greedy algorithms. Although the greedy algorithms have near optimal throughput performance under the CFR util-

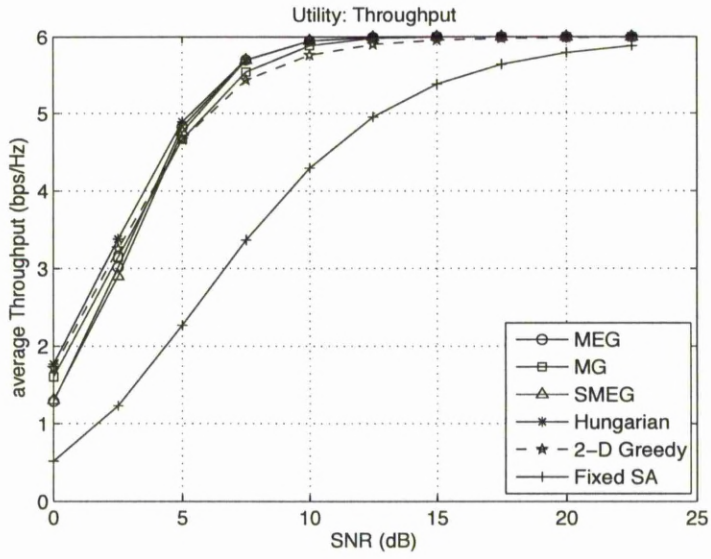

Figure 4.13: Average throughput performance of the algorithms for $U = 100$ users under the throughput utility.

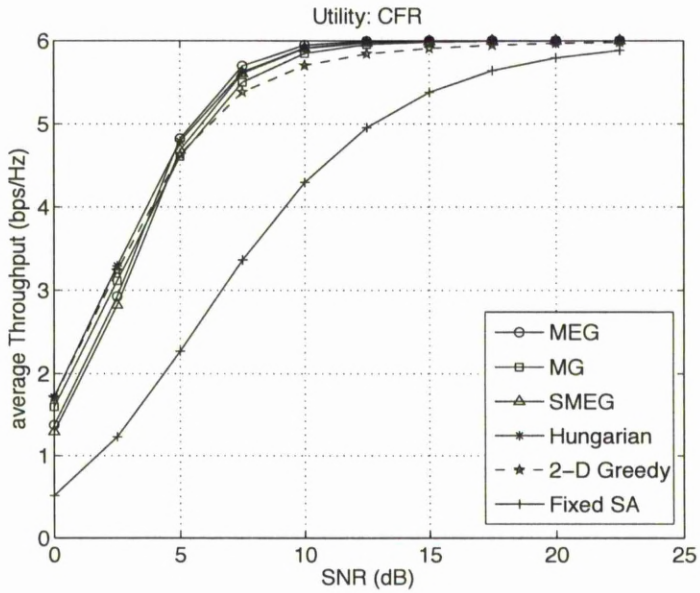

Figure 4.14: Average throughput performance of the algorithms for $U = 100$ users under the CFR utility.

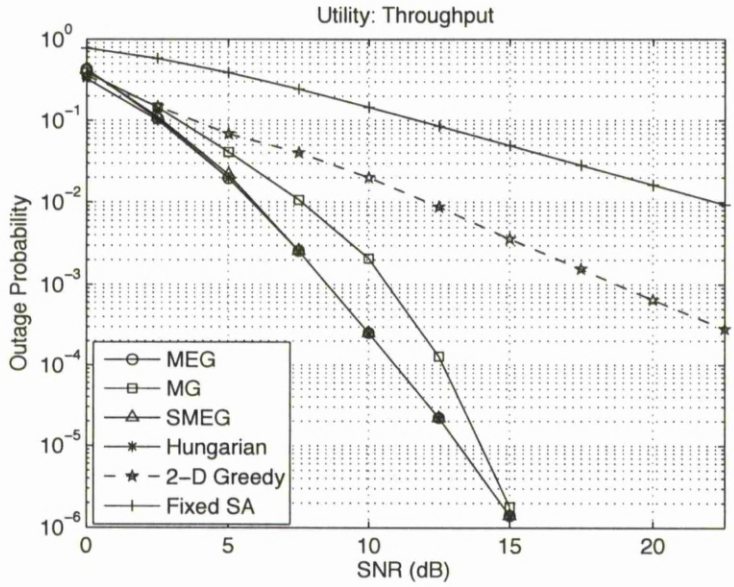

Figure 4.15: Outage probability performance of the algorithms for $U = 100$ users and the throughput utility.

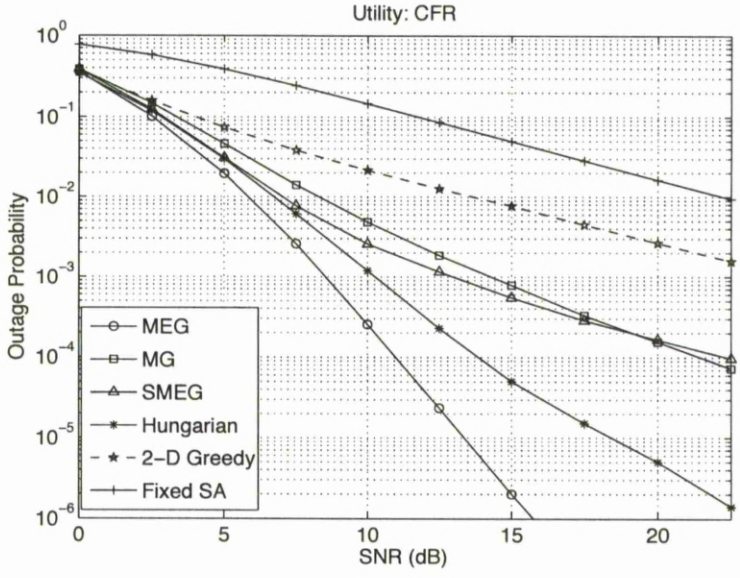

Figure 4.16: Outage probability performance of the algorithms for $U = 100$ users and the CFR utility.

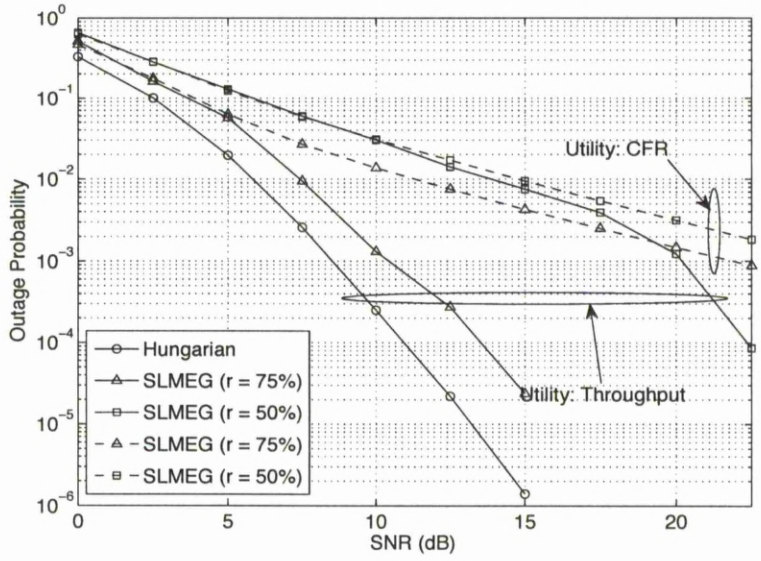

Figure 4.17: Outage probability performance of the SLMEG algorithms for $U = 100$ users and the CFR and throughput utility.

ity, some of the users cannot transmit any data, while others utilise the highest rate MCS, thereby increase the unfairness between the users.

The outage probability of the SLMEG algorithms are shown in Figure 4.17. Maximising the CFR does not provide appropriate results, while maximising the throughput definitely provides a good outage probability performance for SLMEG algorithm with only 75% of the users selected for optimisation. The SLMEG algorithm with only 50% of the users selected for optimisation also has a suitable outage probability performance at high SNR.

4.5.6 WiMAX Performances under the AMC Profile

The WiMAX system supports a Band AMC profile, which provides blocks of subcarriers similar to the PRB in LTE. These blocks are referred to as subchannels in the WiMAX system. Each subcarrier is 10.94 kHz and there are nine subcarriers in a subchannel,

Table 4.3: Power delay profile for the Pedestrian B WiMAX channel [2].

Delay (μs)	0.0	0.2	0.8	1.2	2.3	3.7
Power (dB)	0	-0.9	-4.9	-8.0	-7.8	-23.9

therefore, each subchannel is 98.46 kHz wide. This is far less than the 180 kHz PRB in LTE, therefore the WiMAX AMC profile has the ability to group two or three subchannels together, for allocation to a single user. To make a fair comparison between both systems, two subchannels are grouped together in this work to form a 196.92 kHz wide block, allocated to a user, once every 1 ms, similar to the LTE simulations. With this setting, the 10 MHz WiMAX channel will support only 48 users, instead of the 50 supported in LTE, however, the 48 users will have slightly higher capacity, due to a slightly higher subchannel bandwidth. In addition to this, the WiMAX system uses the pedestrian and vehicular channels defined in [2]. For the simulations, the pedestrian B (Ped. B) channel is employed, which has a PDP described in Table 4.3. This channel has a delay spread of about 0.25 μs. All other simulation parameters are similar to the LTE simulations.

Figures 4.18 and 4.19 show the BER performance of the algorithms under the SE utility and WiMAX settings, for the T.U 6 and the Ped. B channels, respectively. The algorithms performances are similar to Figure 4.2 for the LTE system. However, in the Ped. B channel, the SMEG has a better performance than the Hungarian and MG algorithms, because of the lower delay spread in the channel. This is similar to the performance trends shown in Figure 4.7, where the delay spread in the channel was varied. In Figure 4.20, the BER utility is used with the T.U 6 channel, and the performance is similar to the Figure 4.9, where all the algorithms have similar near optimal BER performances, with the exception of the 2-D greedy algorithm.

Figure 4.21 shows the throughput performance of the algorithms under the throughput utility. The same performance trends as shown in the LTE system are observed,

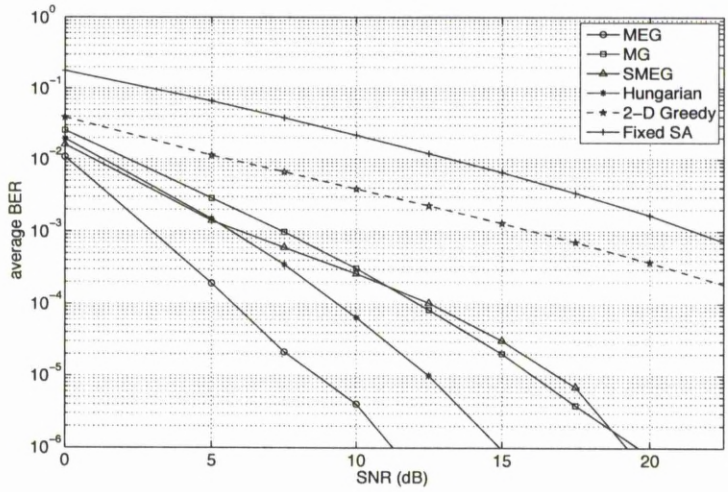

Figure 4.18: Average BER performance of the algorithms under the WiMAX Band AMC profile using the T.U. 6 channel and SE utility for $U = 48$ users.

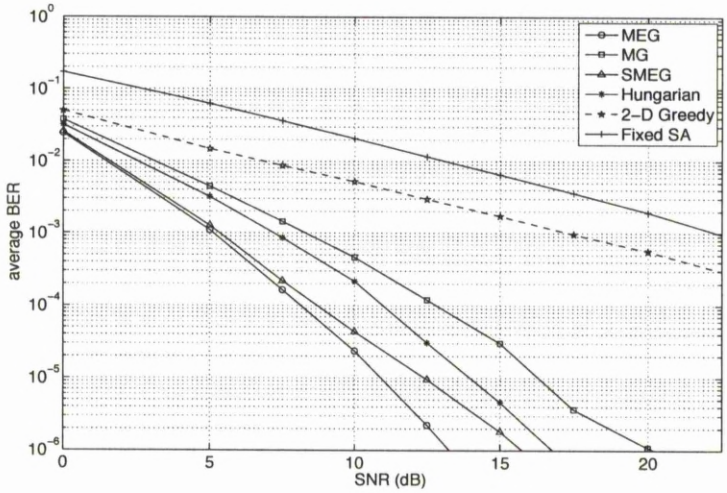

Figure 4.19: Average BER performance of the algorithms under the WiMAX Band AMC profile using the Ped. B channel and SE utility for $U = 48$ users.

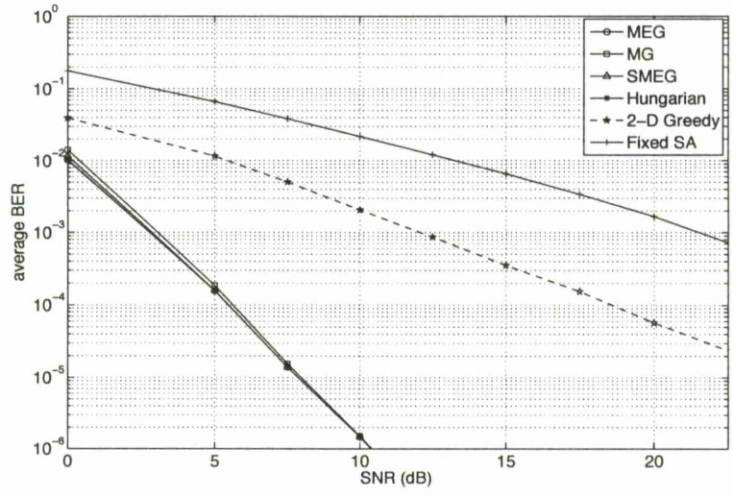

Figure 4.20: Average BER performance of the algorithms under the WiMAX Band AMC profile using the T.U. 6 channel and BER utility for $U = 48$ users.

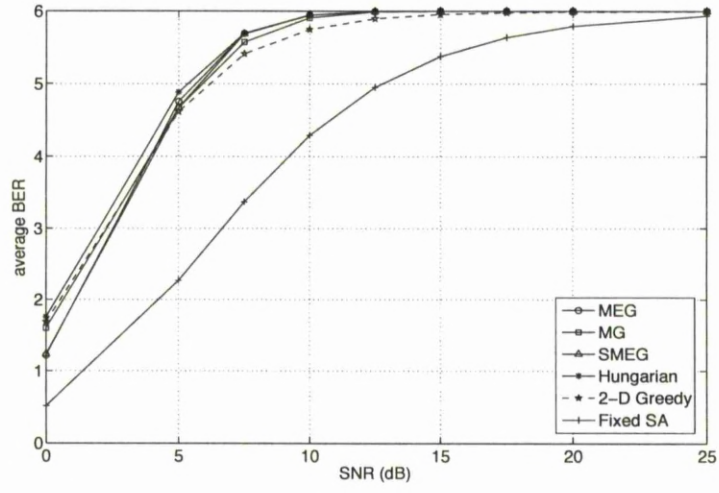

Figure 4.21: Average throughput performance of the algorithms under the WiMAX Band AMC profile using the T.U. 6 channel and Throughput utility for $U = 48$ users.

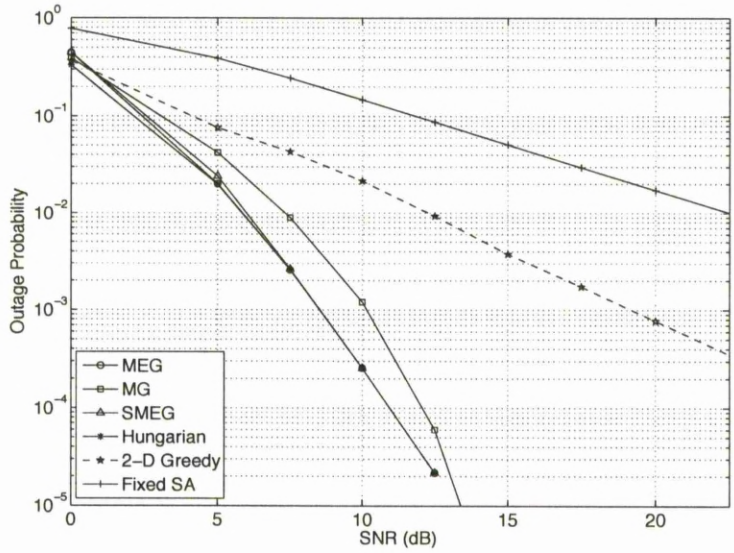

Figure 4.22: Outage Probability performance of the algorithms under the WiMAX Band AMC profile using the T.U. 6 channel and Throughput utility for $U = 48$ users.

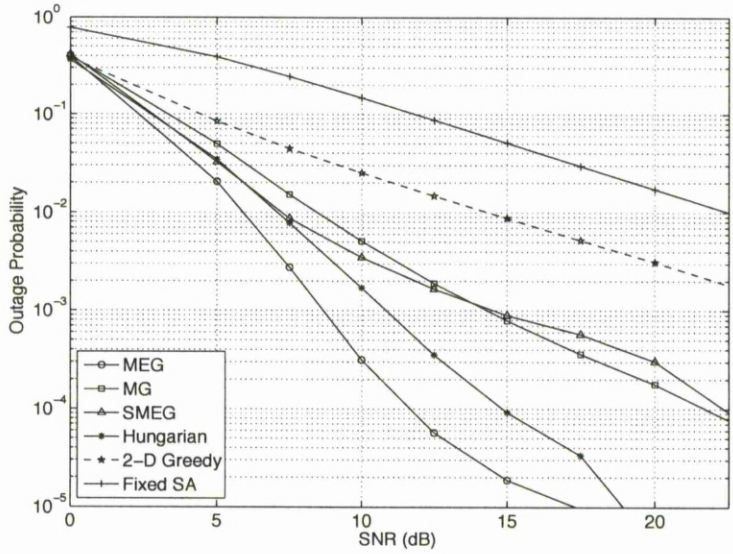

Figure 4.23: Outage Probability performance of the algorithms under the WiMAX Band AMC profile using the T.U. 6 channel and CFR utility for $U = 48$ users.

where all the algorithms have near optimal performance, with the 2-D greedy having the second best performance at very low SNR, but having the worst performance at SNRs over 5 dB. At very low SNR, there are very few PRBs that can reliably transmit data, therefore making fairness priority in the proposed algorithms detrimental at very low SNR, while the 2-D greedy and Hungarian algorithms will allocate the best PRBs to the users that have them. Irrespective of this trend in throughput performances, Figures 4.22 and 4.23 show that the outage probability of the proposed algorithms are better than the 2-D greedy algorithm from SNR of 2 dB and above. Comparing both outage probability figures, it can be observed that the CFR utility has a worse performance than the BER utility for every algorithm, as was shown for the LTE system also.

4.6 Summary

In this chapter, three PRB allocation algorithms for the LTE system are proposed. They significantly outperform the 1-D and 2-D greedy algorithms in terms of BER and data rate fairness especially with high RMS delay spreads, while maintaining a similar system SE. The proposed MEG algorithm provides the best BER performance, near optimal SE performance and best level of fairness among all users, with a much lower computational complexity than the Hungarian algorithm (optimal searching algorithm to maximise the SE). The SMEG algorithm achieves a significant complexity reduction over the MEG algorithm with little performance degradation especially in the presence of high Doppler spread and low channel estimation accuracy. The MG algorithm has the advantage of a scalable complexity which depends on the performance trade-off required.

The impact of the optimisation utility on the proposed enhanced greedy algorithms is investigated, and it is shown that the BER utility is the best optimisation utility

for the proposed greedy algorithms. The BER utility based versions of the algorithms achieve very near optimal BER and outage probability performances, simultaneously. The BER utility also achieves the best SE and BER performance trade-off, because the loss in SE is marginal under the BER utility is employed, while achieving huge BER performance gains over the SE utility.

The WiMAX system, with band AMC settings, provides similar performances to the LTE system. The effect of the optimisation utilities can also be observed under the WiMAX settings. The only difference is when a different channel model is used, in this case the Ped. B channel, where poorer performances are observed due to the lower RMS delay spread in the Ped. B channel.

A lower complexity selective greedy (SG) algorithm is also proposed. It reduces the complexity of the 1-D greedy algorithm by eliminating a fraction of the number of user optimisations (minimisation or maximisation). It selectively optimises PRB allocation for only the poorly ranked users, while it randomly allocates PRBs to the remaining well ranked users. Nevertheless, the SG algorithm is very inefficient when used by itself for PRB allocation. Based on this, a composite SLMEG algorithm is formed, which couples the BER utility and the mean enhanced ranking technique with the SG algorithm. The BER utility based SLMEG algorithm is shown to provide superior BER and outage probability performances to the existing 1-D and 2-D greedy algorithms, especially at high SNR.

Chapter 5

Multi-Criteria Ranking based Greedy PRB Allocation

5.1 Introduction

In Chapter 4, the greedy PRB allocation algorithm is enhanced by ranking the mean numerical values of each user's PRB utilities. As shown by simulation results, the BER utility has the best trade-offs between the BER, outage probability and SE performances for all the greedy algorithms. The CFR, SE and OSINR utility based MG and SMEG algorithms do not provide very good results. In this Chapter, a so called multi-criteria ranking based greedy (MCRG) algorithm is proposed, which provides near optimal BER, outage probability and SE performances irrespective of the optimisation utility.

The MCRG algorithm is based on the multi-criteria decision aid (MCDA) technique [86, 87]. MCDA techniques are used to rank projects or items according to multiple ranking criteria, simultaneously. In this work, a multi-criteria ranking (MCR) technique, which is a combination of the Electre I [88] and Promethee II [89] MCDA techniques, is used to rank the numerical values of users' PRBs according to multiple

ranking criteria (RC), simultaneously. The MCR is exploited in a similar manner to the SMEG algorithm in Chapter 4, to provide a near optimal user-orders, that achieve near optimal performance. Yet, this approach is particularly beneficial when the CFR utility is employed because the computational complexity of the overall PRB allocation process is lowered, while the BER, SE and outage probability performances can be maintained. In contrast to the BER, SE and output SINR utilities, determining the numerical values of the CFR utility is readily available after channel estimation.

In addition, the SG algorithm, presented in Chapter 4, is also combined with the proposed MCR technique to reduce the overall complexity of PRB allocation. The proposed algorithm is referred to as the SLMCRG algorithm, and it has a similar performance to the BER utility based SLMEG algorithm proposed in Chapter 4, and outperforms the 1-D and 2-D greedy algorithms in terms of BER and outage probability, especially at high SNR, but with a far lower computational complexity.

5.2 Overview of Multi-Criteria Optimisation

In the literature, the term *multi-criteria optimisation* means finding the solution to (3.3) and its constraints with multiple utilities simultaneously [75]. These utility functions are also known as objectives, attributes or criteria, and a simultaneous optimisation is referred to as multi-utility, multi-objective, multi-attribute or multi-criteria optimisation. There are many techniques used in solving such problems [86]. A summary of the techniques used in solving multi-utility optimisation problems is given below.

- The algorithm described in [75] is used for finding the solution to a multi-utility assignment problem. However, it is very complex, involving multiple evaluations of the optimum single utility based Hungarian algorithm. Therefore, for real time systems such as wireless communications, this solution is not suitable.

- A composite utility function could be formed by adding or multiplying the respective functions together [86, 87]. The resulting composite utility function is then solved by a suitable single utility optimisation technique. However, the resulting composite function may not accurately represent the initial problem, hence the resulting solution may not be of the right quality.

- The multi-criteria problem is transformed into a single criteria one by changing all but one of its utilities into constraints, and then solving the remaining single utility optimisation problem with classical techniques such as linear programming [90]. Using this technique may result in cases where no acceptable solution is found, because the constraints are strict values (goals) [91].

- The problem could also be transformed into a weighted single utility problem, where the weights are determined by the other utilities [90]. The proportional fair scheduling [3] can be viewed as an example of this, where the average capacity of the users' over period T is used to scale the instantaneous capacity before optimisation is carried out. Nevertheless, selecting weights is often a difficult task, and an in-depth knowledge of the system and requirements is needed by the decision maker, which is not always possible.

- Multi-criteria evolutionary techniques, such as simulated annealing, particle swarm optimisation, GAs, etc, are also used to solve multi-criteria problems. However, they normally have many parameters that have to be properly tuned. They also have an unbounded iterative nature, which is not very suitable for real time wireless communications [86, 91].

A major issue with most multi-utility optimisation problems is the existence of multiple efficient solutions known as the Pareto set [92]. Often the selection of the "best" solution from the Pareto set, is another complex optimisation problem.

In this Chapter, a novel approach is used for PRB allocation, where the MCR techniques are used to provide an efficient user-order first, and then the PRB allocation is performed by the greedy algorithm. This approach keeps the overall computational complexity low which is suitable for real wireless communications.

The discussed optimisation utilities, the SE, BER and output SINR are monotonically increasing (for SE and output SINR) or decreasing (for BER) functions of the CFR for a single user case. Therefore, maximising only one utility, the CFR, would be sufficient. However, due to the interactions between multiple users in the system, the maximum sum CFR across all the users, does not always provide the minimum sum BER or maximum sum SE. This interaction is also true between SE and BER (the maximum sum SE does not always provide the minimum sum BER). Therefore, the MCR technique proposed here does not involve optimising across the multiple utilities simultaneously, but involves achieving the best trade-off between the BER, SE and outage probability performance, irrespective of the single optimisation utility available.

5.3 MCR based Greedy Algorithm

A novel combination of two MCDA techniques, known as the Electre I [88] and Promethee II [89] are used to determine the user-order with which greedy PRB allocation is performed. These MCDA techniques provides a framework by which users can be systematically sorted, based on all the desired RC, simultaneously.

Figure 5.1 shows a general representation of an enhanced greedy PRB allocation process. At the first stage, the users' numerical values of one chosen utility out of the BER, CFR, SE, OSINR or throughput are calculated. At the second stage, the estimated utilities are passed onto one or more of the C RC, $RC_0, \cdots, RC_{C-1}$, which converts all of each users' PRB utility values into a single numerical value. If there is only one RC (the mean), then this stage is just the calculation of the mean PRB values

across all the users, similar to the SMEG algorithm in Chapter 4. At the third stage, these RC values are passed to the MCR module that produces the required user-order. If there is one RC, then the MCR module is just a normal sorting operation. Finally, the user-order is passed to the greedy algorithm module, where either one of the 1-D greedy or the SG algorithm is used to complete PRB allocation process to the available users.

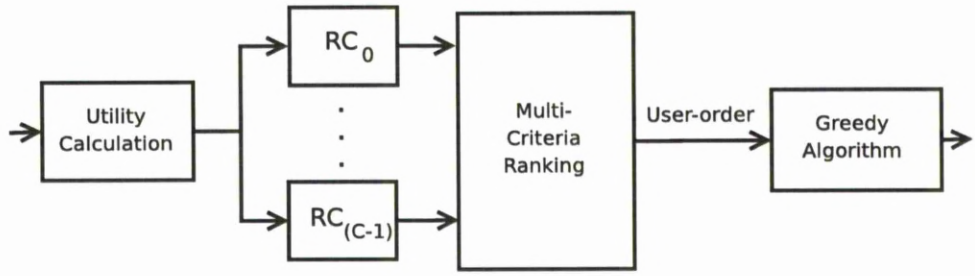

Figure 5.1: Block diagram for the PRB allocation process using different utility, ranking criteria and greedy algorithms.

In this chapter, when more than one RC is used, the unique part of the process described by Figure 5.1 is the MCR module. The MCR module is described below:

Firstly, C RC functions $f_c(u)$ $(c = 0, \cdots, C-1)$ are built up, where user u $(u = 0, \cdots, U-1)$ is an arbitrary user. $f_c(u)$ is a RC function of the uth user b_{uk} values. For each of the C criteria, a weighed w_c $(0 \leq w_c \leq 1)$ is assigned, and the relationship between all the w_c is

$$\sum_{c=0}^{C-1} w_c = 1. \tag{5.1}$$

Between any two users u and v $(u, v = 0, \cdots, U-1,\ u \neq v)$, each criterion function f_c is evaluated. If $f_c(u) \geq f_c(v)$, it means user u outranks user v with respect to criterion

f_c. Accordingly, an outranking relationship indicator $d_{c,uv}$ is defined by

$$d_{c,uv} = \begin{cases} 1 & \text{if } f_c(u) \geq f_c(v) \\ 0 & \text{if } f_c(u) < f_c(v) \end{cases} \tag{5.2}$$

where $d_{c,uv}$ specifies the relationship between users u and v on criterion c. The total effect of this outranking relation across all the C criteria is calculated by the expression

$$p_{uv} = \sum_{c=0}^{C-1} d_{c,uv} w_c \tag{5.3}$$

These are known as the *concordance* values which have to be calculated between any two users in the system. It is easy to know that $p_{vu} = 1 - p_{uv}$, according to (5.2) and (5.1). (5.1), (5.2) and (5.3) are parts of the Electre I algorithm.

Next, each user u's total concordance value is calculated by summing up p_{uv} across all users v ($v = 0, \cdots, U-1,\ v \neq u$):

$$P_u = \sum_{v=0,\, v \neq u}^{U-1} p_{uv}. \tag{5.4}$$

These total concordance values P_u, also known as the *outward flow* and is a concept derived from the Promethee II [89] algorithm. This outward flow parameter specifies the relationship between a user u and all the other users. A high valued P_u implies that overall in terms of the C criteria, user u is better than many users, while a low valued P_u indicates that user u is worse, in those criteria, than other users. This parameter is easier to calculate than the discordance, and it does not need to be tuned. It is more efficient in providing a complete ranking of all the users in the system.

Therefore, to determine the user-order for PRB allocation, the resulting P_u values are sorted in ascending order, and the users with the lower P_u values are allocated PRBs first. The MCR algorithm is described in Algorithm 8.

Algorithm 8 MCR Algorithm

1: Set up criteria weights w_c $(c = 0, \cdots, C-1)$.
2: Initialise the users' total concordance values $P_u = 0$.
3: **for** each pair of users $u, v = 0, \cdots, U-1$, $u \neq v$ **do**
4: Initialise each pair of users' concordance value $p_{uv} = 0$;
5: **for** each criterion $c = 0, \cdots, C-1$ **do**
6: Calculate $d_{c,uv}$ based on (5.2);
7: Update each user pair concordance value, $p_{uv} = p_{uv} + d_{c,uv} w_c$.
8: **end for**
9: Update each user's total concordance value, $P_u = P_u + p_{uv}$.
10: **end for**
11: Determine the user-order $[\mathbf{s}^0 \cdots \mathbf{s}^{U-1}]$ by ascending order of P_u.

A combination of the 1-D algorithm and the MCR module described above, produces the so called MCRG PRB allocation algorithm. The user-order determined in Step 11 of the MCR algorithm is used in the 1-D greedy algorithm to complete the PRB allocation.

Other MCDA outranking methods such as the Electre II, III, IV, IS, TRI, [87], Analytic Hierarchy Process (AHP) [93] and Technique For Order preference BY Similarity to Ideal Situation (TOPSIS) [94] exist. Some of them use fuzzy logic techniques to enhance the decision making algorithms. To the best of my knowledge, these outranking methods have never been applied to resource allocation for a wireless communication system. However, they have been applied to the problem of selecting the best network for a mobile device in the presence of different available networks such as 2G, 3G, 4G, WiMAX and WiFi etc [93, 95, 96].

In this work, three RC are considered:

$$f_0(u) = \frac{1}{K} \sum_{k=0}^{K-1} b_{uk} \tag{5.5}$$

where $f_0(u)$ is the mean of the users b_{uk} performance, and

$$f_1(u) = -\sqrt{\frac{1}{K}\sum_{k=0}^{K-1}\left(b_{uk} - \frac{1}{K}\sum_{i=0}^{K-1} b_{ui}\right)^2} \tag{5.6}$$

where $f_1(u)$ is related to the standard deviation (STD) of the users' b_{uk} performance, and

$$f_2(u) = \begin{cases} 1 & \text{if } \min_u b_{uk} \geq \alpha \\ 0 & \text{otherwise} \end{cases} \tag{5.7}$$

where $f_2(u)$ is a binary indicator, that specifies whether a user has all of its PRBs greater than a minimum value threshold (MVT) represented by α. Even if only one PRB belonging to a user has a minimum (or maximum for BER) PRB value below than the threshold, that user's f_2 value is zero. Table 5.1 presents a summary of the RC's.

Table 5.1: Summary of ranking criteria.

Ranking Criterion	Synopsis
Mean (f_0)	This is the mean (average) of the users PRB utility values.
STD (f_1)	This is related to standard deviation of the users PRB utility values.
MVT (f_2)	The probability of allocating a PRB with CFR value below this threshold should be minimised.

These RC's are used in pairs (f_0, f_1) and (f_0, f_2). In terms of (f_0, f_1), the best users should have high mean (f_0) and a low STD (f_1) - which depicts an overall high channel link quality user. These high quality users should be allocated last because they will still have a high probability of obtaining good PRBs. While the worst users have a very low mean with a low STD (generally far away from the BS) or very low mean and high standard deviation (presence of many deep fades) - these users should search for

PRBs first to maximise their probability of obtaining suitable PRBs. Furthermore, in terms of (f_0, f_2), the best users should have a high mean and ideally should not have any PRBs below the α, while the worst users should have a low mean with at least one PRB below α.

Notice that the RC are not specifically related to wireless communications, but are general statistical functions that provide information on the general performance of the users. This implies that the weights of these RC are not directly related to the designer's requirements in terms of SE, BER or outage probability performances. Therefore, extensive *robustness* and *sensitivity* [87] analysis are required to determine the appropriate weights for the RC. In order to keep the analysis tractable, the RC are used in pairs, because it is easy to determine the interaction between the weights of two RC, rather than among three or more RC simultaneously.

5.4 Selective MCR based Greedy Algorithm

Similar to Chapter 4, the selective reduced complexity SG algorithm (Algorithm 7) described in Section 4.3, can be coupled with the MCR technique to lower the overall complexity of PRB allocation. Therefore, in terms of Figure 5.1 the user-order provided by the MCR module will be directly used in the SG algorithm instead of the 1-D greedy algorithm. In this work, this selective MCR based greedy algorithm is referred to as the selective multi-criteria ranking greedy (SLMCRG) algorithm.

Table 5.2, shows a summary of both the algorithms and their efficient operating parameters. These parameters are found numerically as will be shown in Section 5.6.

5.5 Complexity and Memory Analysis

In this section, the complexities of the proposed MCRG and SLMCRG algorithms are derived, in terms of the number of operations required for complete PRB allocation

Table 5.2: MCR greedy algorithms and descriptions.

Algorithm	Synopsis	Suitable Operating Parameters
MCRG	Multi-criteria ranking greedy algorithm: uses the 1-D greedy algorithm and gets its user-order from the MCR of the users' utilities with respect to two or more ranking criteria.	CFR utility based has parameters ($w_0 = 0.1$, $w_2 = 0.9$, $\alpha = 0.4$) and ($w_0 = 0.6$, $w_1 = 0.4$)
SLMCRG (r)	Selective multi-criteria ranking greedy algorithm: uses the random greedy algorithm and gets its user-order from the ranking of the users' CFR with respect to two or more ranking criteria. It optimises PRB allocation for r percent of users, hence saving computational cost.	(For $r = 75\%$; $w_0 = 0.1$, $w_2 = 0.9$ and $\alpha = 0.2$) and (for $r = 50\%$; $w_0 = 0.1$, $w_2 = 0.9$, and α is variable, suitable values for each SNR is given in Table 5.9)

to all the users. In Chapter 4, the 1-D greedy and SG algorithms are already shown to have complexities of $1/2(U^2 - U)$ and $1/2(U_1^2 - U_1)$, respectively. Therefore, this section focuses on the number of computations needed to implement the MCR module is derived.

The number of operations needed for calculating $f_0(u)$ given by (5.5) for each user with $K = U$ PRBs is U, which includes $(U - 1)$ additions and one division. While the number of operations for calculating $f_1(u)$ given by (5.6) for each user is $(3U + 1)$, which includes $(U - 1)$ additions, U subtractions, U multiplications (for square), one division and one square-root. In addition, the number of operations for calculating $f_2(u)$ given by (5.7) for each user is U, which includes $(U - 1)$ comparisons to find the minimum and one comparison of the minimum with α.

The number of operations needed for estimating P_u (5.4) for each user is $(U - 1)$ additions. Therefore, combining the complexity of estimating the RC's with the complexity of P_u, the total number of operations needed for the (f_0, f_1) option over U users is $U(U + 3U + 1 + U - 1) = 5U^2$, while the (f_0, f_2) option has a total number of

operations over U users given by $U(U+U+U-1) = 3U^2 - U$.

The number of comparisons needed to calculate all the $d_{c,uv}$ is $2C\binom{U}{2} = C(U^2-U)$. However, only half of the $d_{c,uv}$'s need to be calculated, since $d_{c,vu} = 1 - d_{c,uv}$ according to (5.2). Thus, the complexity required for calculating $d_{c,uv}$ is only $(U^2 - U)$ when $C = 2$. The complexity of calculating the remaining concordance values in (5.3) is negligible compared to the complexity of calculating $d_{c,uv}$ because of the symmetry. Therefore, the overall complexity required to calculate the all the concordance values is $(U^2 - U)$.

The total complexity of the proposed MCRG (w_0, w_1) algorithm is $5U^2+(U^2-U)+1/2(U^2 - U) = 13/2U^2 - 3/2U$ and the complexity of the MCRG (w_0, w_2) algorithm is $(3U^2 - U) + (U^2 - U) + 1/2(U^2 - U) = 9/2U^2 - 5/2U$. Table 5.3 presents a symbolic complexity comparison of the proposed MCRG algorithm with the optimal Hungarian algorithm [30] and the 1-D and 2-D greedy [27] algorithms. It can be seen that the MCRG algorithm is around U times less complex than the optimal Hungarian algorithm. This lower complexity is highly beneficial in current and future broadband wireless systems such as LTE, where each single cell needs to accommodate over $U = 100$ users.

The CFR utility is readily available after channel estimation and is directly used for PRB allocation. Therefore, there is no added complexity when using the CFR as an optimisation utility. This is highly advantageous, because the other utilities are functions of the CFR utility and many computations are needed to estimate the BER, SE, OSINR or throughput utilities.

To estimate the complexity of the EESM BER, the following assumption is made: all the operations for the natural log and exponential can be implemented easily by using look-up tables and are approximated as one computation (this is a very generous assumption, and the cost of memory is not included). The OSINR (3.16) for each of the UM subcarriers per user are first calculated, with complexity of $3MU^2$, which includes

Table 5.3: Number of operations for each algorithm. $A = U = 100$ for the MG algorithm

Algorithm	Number of Computations
2-D Greedy	$1/3U^3 + 1/2U^2 - 5/6U$
Hungarian	$(11U^3 + 12U^2 + 31U)/6$
1-D Greedy	$1/2(U^2 - U)$
MG	$A1/2(U^2 - U) + A - 1$
MEG	$1/3U^3 + U^2 - 1/3U$
SMEG	$3/2U^2 - 1/2U$
SLMEG	$1/2U_1^2 - 1/2U_1 + U^2$
MCRG (w_0, w_1)	$13/2U^2 - 3/2U$
MCRG (w_0, w_2)	$9/2U^2 - 5/2U$
SLMCRG (w_0, w_2)	$4U^2 - 2U + 1/2U_1^2 - 1/2U_1^2$

UM operations for absolute value, UM operations for squaring and UM operations for dividing by noise spectral density. The number of operations for calculating the effective SNR (3.15), is $(3M + 2)U^2$, which includes UM operations for dividing by β, UM operations for look-up of the exponential value, UM operations for the averaging, U operations for look-up of the natural logarithm value and U operations for the final multiplication with β. Finally, the values of the effective SNR are mapped to the corresponding AWGN BER values stored in memory, which requires another U look-up operations. Therefore, the absolute lower-bound complexity for finding the EESM BER is $3MU^2 + (3M + 2)U^2 + U^2 = U^2(6M + 3)$ (this is the absolute lower bound achieved only when the operations are done as efficiently as possible).

In a similar manner, the complexity of the OSINR utility is calculated by counting the number of operations in (3.8), which gives $62U^2$. The complexity of the SE utility is found by counting all the operations needed to estimate (3.12), which gives $65U^2$ operations. The complexity of the throughput is approximately z times more than the complexity of the EESM BER, where z is the number of MCS levels. The BER of each MCS needs to be calculated using the EESM method.

Table 5.3 shows the number of computations needed for total PRB allocation to

Table 5.4: Number of operations required for each utility. z is the number of MCS schemes available.

Algorithm	Number of Computations for Utility
CFR	N/A
OSINR	$62U^2$
SE	$65U^2$
BER	$75U^2(BER)$
Throughput	$z75U^2$

all the users. The MCRG algorithms have U^2 complexities similar to the previously discussed 1-D greedy and SMEG algorithms, which is unlike the U^3 complexities of the MEG, MG, Hungarian and 2-D greedy algorithms. Particularly, the MCRG(w_0, w_2) version is less complex than the MCRG (w_0, w_1) counterpart, due to the cheaper f_2 criterion. Table 5.4 presents the number of computations needed to calculate the utilities. The OSINR, SE, BER and throughput utilities have large number of computations that will overshadow the complexity of the low complexity greedy algorithms. The CFR utility has no added computational complexity for the reasons already discussed.

Table 5.5 shows the numerical complexities of all the algorithms normalised to the complexity of the 1-D greedy algorithm with $U = K = 100$. In terms of the CFR utility, which is purely the complexity of the algorithm (CFR adds no computations), the SG algorithm has the lowest complexity, which is a fraction of the complexity needed for the 1-D greedy algorithm, while the SMEG, SLMEG and SLMCRG algorithms are about 2, 3 and 8 times more complex than the 1-D greedy algorithm. The two versions of the MCRG algorithm is approximately 9 and 13 times more complex than the 1-D greedy algorithm for the (w_0, w_2) and (w_0,w_1) versions, respectively. The 2-D greedy, MG and MEG are about 68, 69 and 100 times more complex than the 1-D greedy algorithm, while the Hungarian algorithm is about 375 times more complex than the 1-D greedy algorithm. Notice that the other utilities add a large amount of computations to the PRB allocation, which overshadows the complexities of the algorithms alone.

Table 5.5: Normalised complexity, including the effects of EESM BER and CFR averaging. $A = U = 100$ for the maximum greedy algorithm

Algorithm	CFR	OSINR	SE	BER
2-D Greedy	68.30	193.58	199.65	219.85
Hungarian	374.52	499.76	505.83	526.03
1-D Greedy	1	126.25	132.31	152.52
MG	100	225.25	231.31	251.52
MEG	69.4	194.60	200.67	220.87
SMEG	3.02	127.27	134.33	154.54
MCRG (w_0, w_1)	13.1	138.35	144.41	164.62
MCRG (w_0, w_2, α)	9.04	134.29	140.35	160.56
SG($r = 75\%$)	0.56	125.81	131.87	152.08
SG($r = 50\%$)	0.25	125.50	131.56	151.76
SLMEG ($r = 75\%$)	2.58	127.833	133.89	154.10
SLMEG ($r = 50\%$)	2.27	127.52	133.58	153.78
SLMCRG (w_0, w_2,r=75%)	8.60	133.85	139.91	160.12
SLMCRG (w_0, w_2,r=50%)	8.29	133.54	139.60	159.80

Therefore, it is beneficial to have algorithms that will provide near-optimal BER, SE and outage probability performances under the CFR utility. The weights of the RC are numerically found offline based on the system parameters, therefore, the estimation of the weights do not affect the real time complexity of the allocation algorithms.

If the number of available computations is fixed, as is the case with fixed hardware computer systems, then it would be worthwhile to estimate the number of users that each algorithm will be able to support. For example, a computer that can at most provide 100 000 computations per μs, then different algorithms will support different amount of users in the systems as shown in Table 5.6. Notice that both versions of the MCRG algorithm do not have a BER utility equivalent because they operate on the CFR utility. The BER utility drastically reduces the amount of users that the system will be able to support, irrespective of the algorithm. The CFR utility allows more users, however, the 1-D and SMEG algorithms that support a high number of users under the CFR utility have poor performance and do not provide much multiuser

Table 5.6: Number of users supported each algorithm using a 100 000 computation per μs computer, under both the CFR and BER utilities. $A = U = 100$ for the maximum greedy algorithm

Algorithm	CFR	BER
2-D Greedy	66	33
Hungarian	37	27
1-D Greedy	447	36
MG	58	33
MEG	65	33
SMEG	258	36
MCRG (w_0, w_1)	124	
MCRG (w_0, w_2, α)	149	

diversity gains as shown in Figure 4.4. Figure 5.3 shows that the MCRG algorithms provide high multiuser diversity gain under the CFR utility, especially at high number of users, which the CFR utility supports.

The memory requirements for the MCRG and SLMCRG algorithms are derived similar to the other algorithms in Chapter 4. The MCRG algorithm requires two memory slots to store the weights, two memory slots in each iteration to store the $d_{c,uv}$ and p_{uv} values, two memory slots to store the evaluations for the both RC, U memory slots to store all the users P_u values and $\log(U)$ memory slots for in-place sorting the P_u values. The two memory slots used for the greedy comparisons to allocate PRBs can be re-used when the MCR is finished, because both parts of the algorithm are independent. Therefore, the total memory required for the MCRG algorithm is $2 + 2 + 2 + U + \log U = U + \log U + 6$. The SLMCRG algorithm requires the same amount of memory as the MCRG algorithm.

5.6 Simulations

5.6.1 Setup

Monte Carlo simulations is used to demonstrate the performance of the proposed MCR based greedy algorithms. Similar set up is used in Section 4.5. The uplink SC-FDMA model for the LTE system is employed, with a bandwidth of 18 MHz. This bandwidth is divided into $N = 1200$ subcarriers which are grouped into $K = 100$ PRBs with $M = 12$ subcarriers in each PRB. Each PRB is 180 KHz wide. The channel model used for all simulations is the standard typical urban (T.U.) area channel with 6 taps as shown in Table 2.1, which has an approximate RMS delay spread of 1 μs [3]. Perfect channel state information (CSI) is assumed. All data are QPSK modulated and normalised to unit energy. The SNR is defined as the average ratio of the received signal power to noise power.

5.6.2 Results

Figure 5.2 depicts the performance of the MCRG algorithm under different ranking criteria pairs with the suitable parameters which are carefully chosen by simulations. The MCRG (w_0, w_2, α) algorithm with $\alpha = 0.4$, $w_0 = 0.1$ and $w_2 = 0.9$ provides a near optimal (BER utility based Hungarian algorithm) BER performance, while the MCRG (w_0, w_1) algorithm with $w_0 = 0.6$ and $w_1 = 0.4$ is about 2 dB worse than the optimal performance at BER of 10^{-5}. However, its performance gets worse at high SNR, approximately 15 dB for BER of 10^{-6} compared to 10 dB for the MCRG (w_0, w_2, α). This implies that the RC combination of (f_0, f_2) is preferred over the (f_0, f_1) combination.

Notice that the MCRG algorithms in Figure 5.2 outperform the Hungarian and all the greedy algorithms in Figure 4.10, even though both figures are CFR utility based. This implies that the MCR algorithm efficiently ranks the users' CFRs, whose

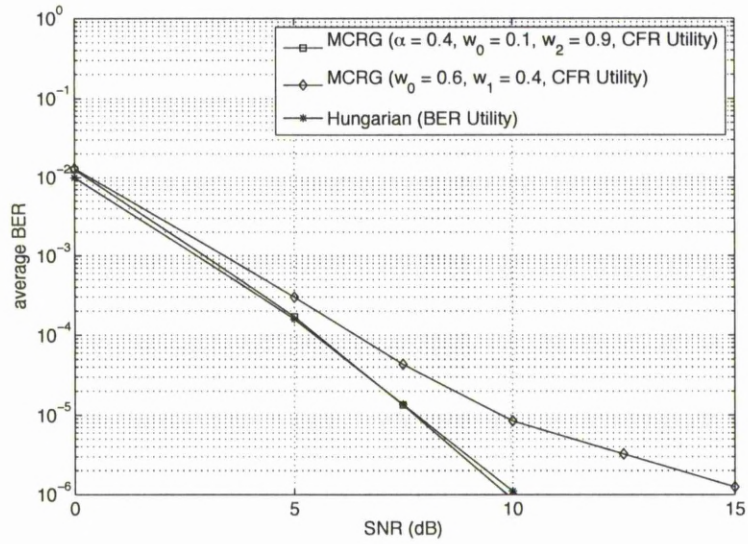

Figure 5.2: Average BER performance of the algorithms with $U = 100$ users, for both configurations of the MCRG algorithm.

ranking result is exploited by the 1-D greedy algorithm to provide near-optimal BER performances.

Figure 5.3 presents the effect of increasing number of users on the average BER performance. The MCRG (w_0, w_2, α) achieves a near optimal BER performance, especially with a large number of users in the system. Both MCRG algorithms extract a higher multiuser diversity gain when compared to the existing 2-D greedy algorithm. The 2-D greedy algorithm does not provide satisfactory BER performances, irrespective of the utility or number of users in the system. The fixed SA degrades in performance as the number of users in the system increases, due to the lack of optimisation for PRB allocation.

Figure 5.4 shows the cumulative distribution function (CDF) of the minimum allocated PRB CFR values for the optimal algorithm (BER utility based Hungarian algorithm) at different SNRs. The plotted CFR values are obtained by selecting the minimum PRB CFR value across all allocated users in every TTI. The CDFs, exhibits

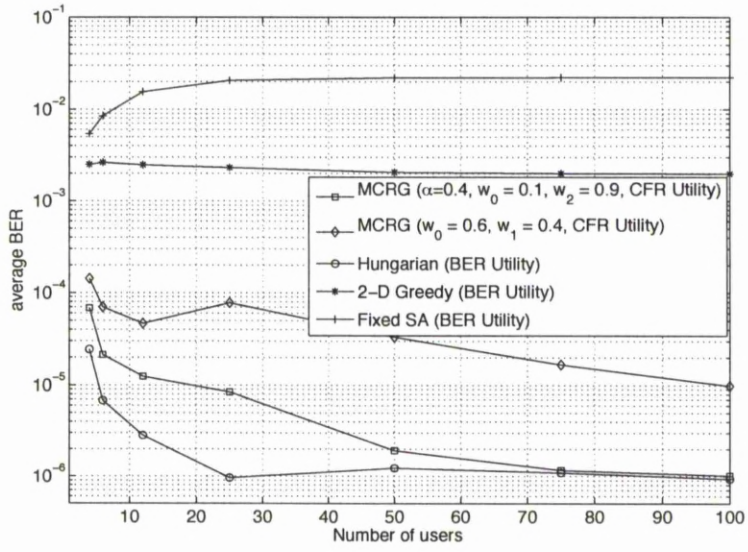

Figure 5.3: Effect of multiuser diversity on the average BER performance of the algorithms at SNR = 10 dB.

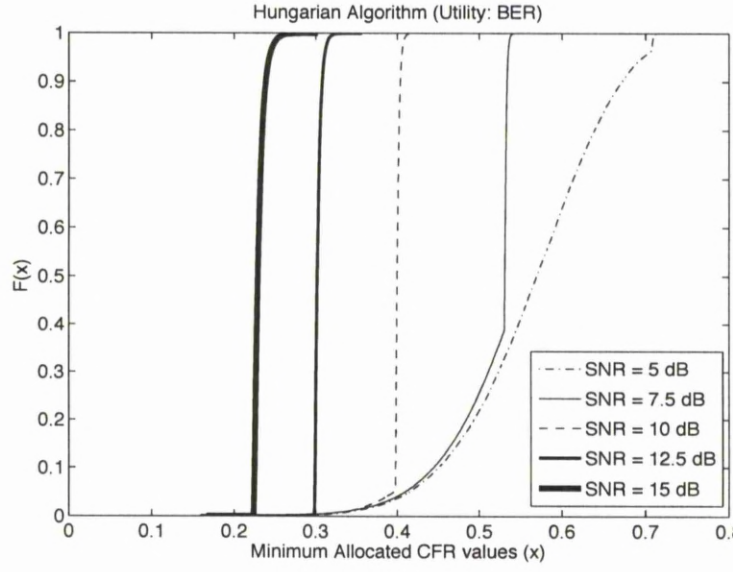

Figure 5.4: The CDFs of the minimum allocated CFR values for the BER utility based Hungarian algorithm at different SNR and $U = 100$ users.

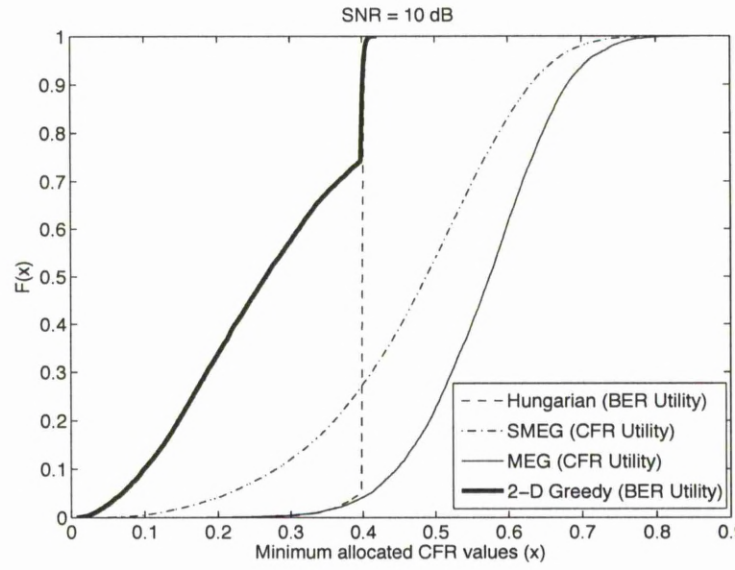

Figure 5.5: The CDFs of the minimum allocated CFR values for different utilities and algorithms at SNR = 10 dB and $U = 100$ users.

a user threshold where most of the minimum allocated PRB CFR are located near this threshold. For example, at 10 dB the Hungarian algorithm has a threshold of about 0.4, with very few PRB values below this threshold. As the SNR increases, the value of the threshold reduces because lower channel gain is required to achieve the same results. These threshold values are closely related to the α value in the f_2 RC.

Figure 5.5 shows the CDF of the minimum allocated PRB CFR values for different algorithms and utilities at SNR = 10 dB. The BER utility based Hungarian algorithm has less than than 5% probability that the minimum allocated PRB has a value lower than 0.4. The CFR utility MEG algorithm has a similar probability, however, it does not show a clear thresholding like the Hungarian algorithm. The SMEG algorithm has approximately a 30% probability that the allocated CFR values lie below the 0.4 threshold, while the BER utility 2-D greedy algorithm has approximately a 70% probability that the allocated PRBs lie below the 0.4 threshold. These differences in the algorithms threshold is responsible for the difference in average BER performances

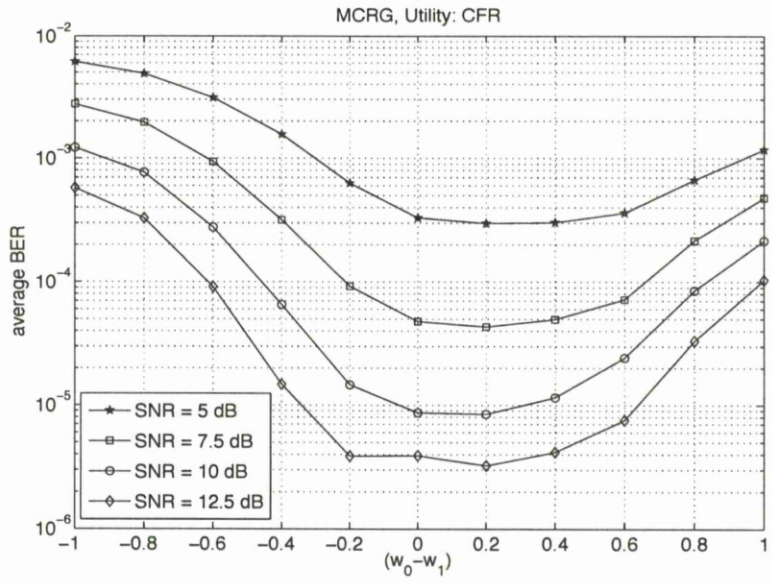

Figure 5.6: Average BER performance of the MCRG algorithm with $U = 100$ users for different SNR values, across a range of criteria weight values $(w_0 - w_1)$.

shown in Figures 4.9 and 4.10.

Table 5.7 shows the best operating parameters for the MCRG (f_0, f_1) algorithm at different number of users settings. These parameters have been found numerically, however, it would be space consuming to include all the graphs, so the best points have been selected and presented in the table. Notice that the 6 users level, all the others have similar weight ranges. Since $w_0 + w_1 = 1$, the range, for example, 0.5 - 0.6 implies that w_0 can take any value between 0.5 and 0.6, while w_1 will be $1 - w_0$. Notice that $w_0 = 0.6$ and $w_1 = 0.4$ have the most amount of occurrence for most user and SNR levels.

Table 5.8 shows the best operating parameters for the MCRG (f_0, f_2, α) algorithm at different number of users settings. Notice that the weights $w_0 = 0.1$ and $w_2 = 0.9$ are the best across all user and SNR levels. The α parameter reduces in values as the SNR increases for each user-level. This corresponds to the effect shown by the

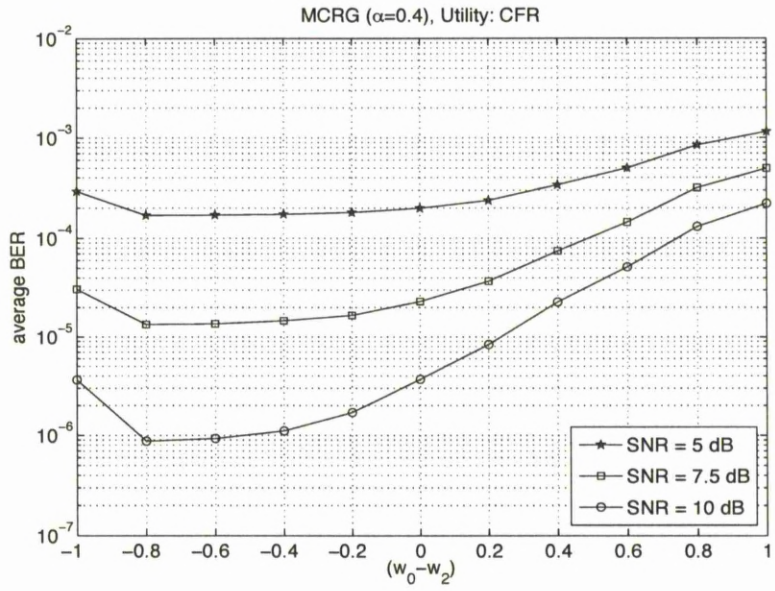

Figure 5.7: Average BER performance of the MCRG algorithm with $U = 100$ users for different SNR values, across a range of criteria weight values $(w_0 - w_2)$, and $\alpha = 0.4$.

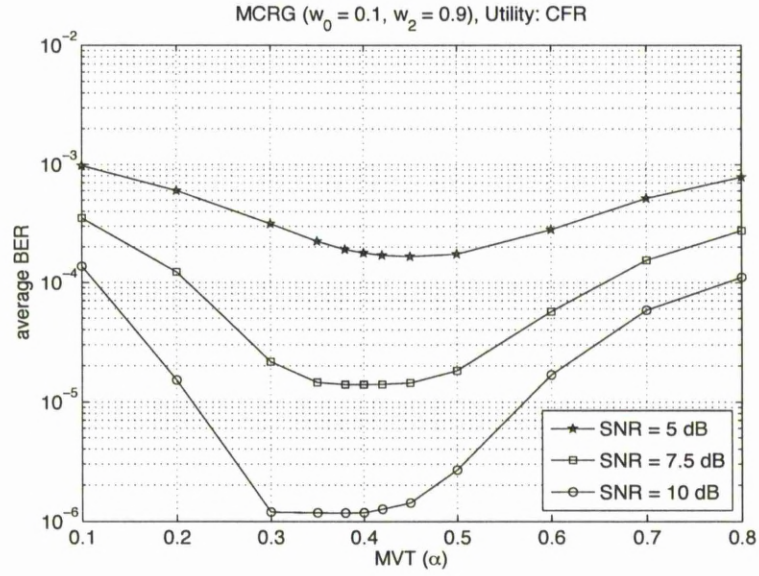

Figure 5.8: Average BER performance of the MCRG algorithm with $U = 100$ users for different SNR values, across a range of MVT values, $0.1 \leq \alpha \leq 0.8$, $w_0 = 0.1$ and $w_1 = 0.9$.

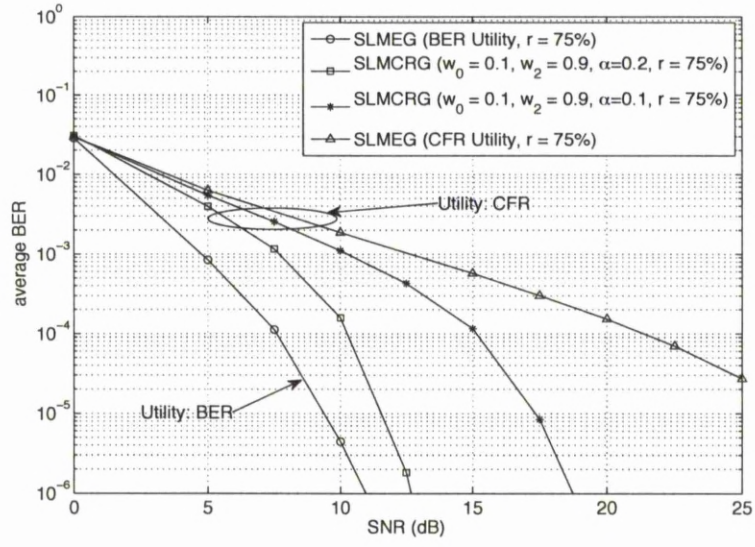

Figure 5.9: Average BER performance of the SLMEG and SLMCRG algorithms with $r = 75\%$ and $U = 100$ users.

Hungarian algorithm in the CDFs of Figure 5.4. The range of α values under some SNR levels can be accounted for by numerical estimation, because the BER, especially at high SNR are close to 10^-6 as shown in the Figure 5.8 for $U = 100$ users.

Figure 5.6 demonstrates the effect of the RC weights on the BER performance of the MCRG (w_0, w_1) algorithm at SNR levels of 5 dB, 7.5 dB, 10 dB and 12.5 dB. The horizontal axis indicates the difference between the two weights w_0 and w_1. Given $w_0 + w_1 = 1$ according to (5.1), it is easy to calculate the two weights at any point in the figure. The best performances occur at $w_0 - w_1 = 0.2$ ($w_0 = 0.6$, $w_1 = 0.4$). At $w_0 - w_1 = 1$,*i.e.*, ($w_0 = 1$, $w_1 = 0$), the MCRG algorithm reduces to the SMEG algorithm. It can be observed that at high SNRs, the weights for different RC have a larger effect on performance of the MCRG(w_0, w_1) algorithm.

Figure 5.7 illustrates the impact of RC weights on the BER performance of the MCRG (w_0, w_2, α) algorithm at SNR levels 5 dB, 7.5 dB and 10 dB. The difference

between the two weights $w_0 - w_2$, is plotted against the average BER, similar to Figure 5.6. In this case, the best performances occurs at $w_0 - w_2 = -0.8$ ($w_0 = 0.1$, $w_2 = 0.9$). This version of the MCRG algorithm also reduces to the SMEG algorithm at $w_0 = 1$ and $w_1 = 0$ and similarly, at high SNRs, the weights for different criteria have a larger effect on performance of the MCRG(w_0, w_2) algorithm.

Figure 5.8 illustrates the effect of the value of α on the BER performance of the proposed MCRG (w_0, w_2, α) algorithm. Notice that the best performances are in the range $0.3 \leq \alpha \leq 0.5$, which closely correspond to the CDF values previously shown in Figure 5.4. It also shows that $\alpha = 0.4$ is a good trade-off across different SNR values, especially in the desired operating region of 7.5 dB to 10 dB, where the BER values are between 10^{-5} and 10^{-6}. This implies that in order to achieve a PRB allocation that results in near optimal average BER, the probability of allocating a PRB CFR value below 0.4 should be minimised. The MCRG (w_0, w_2, α) algorithm achieves this by giving the users with CFR values lower than 0.4 a higher priority, allowing them to be allocated early in the greedy algorithm.

Figure 5.9 illustrates the the performance of the SLMCRG in comparison to that of SLMEG, both with r = 75%. The SLMCRG algorithm uses two RC, f_0 ($w_0 = 0.1$) and f_2 ($w_2 = 0.9$). In this instance, the BER utility based SLMEG has the best performance. The CFR utility based SLMCRG algorithm with $\alpha = 0.2$ and $\alpha = 0.1$ is about 2 dB and 7 dB worse than the BER utility based SLMEG, at BER = 10^{-5}, respectively. The CFR utility based SLMEG algorithm has the worst performance which is over 13 dB and 8 dB worse than both SLMCRG ($\alpha = 0.2$ and $\alpha = 0.1$) configurations, at BER = 10^{-5}, respectively. A comparison between both SLMCRG configurations clearly show that $\alpha = 0.2$ outperforms the case with $\alpha = 0.1$ by over 5 dB at a BER of 10^{-5}.

The best parameters of the SLMCRG algorithm ($w_0 = 0.1$, $w_2 = 0.9$ and $\alpha = 0.2$) were determined by extensive simulations. For each α ($0 \leq \alpha \leq 0.9$) the interaction

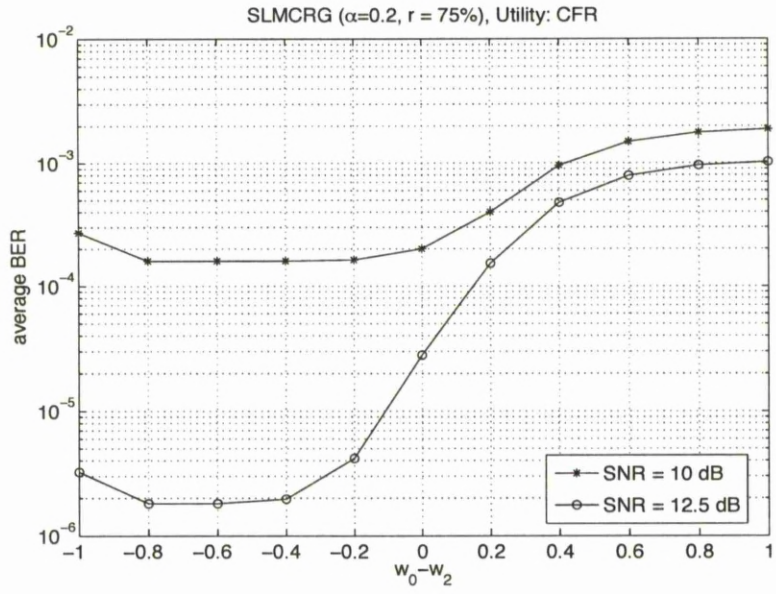

Figure 5.10: Average BER performance of the SLMCRG algorithm with $r = 75\%$ and $\alpha = 0.2$ under various criteria weights with $U = 100$ users and $w_0 + w_2 = 1$

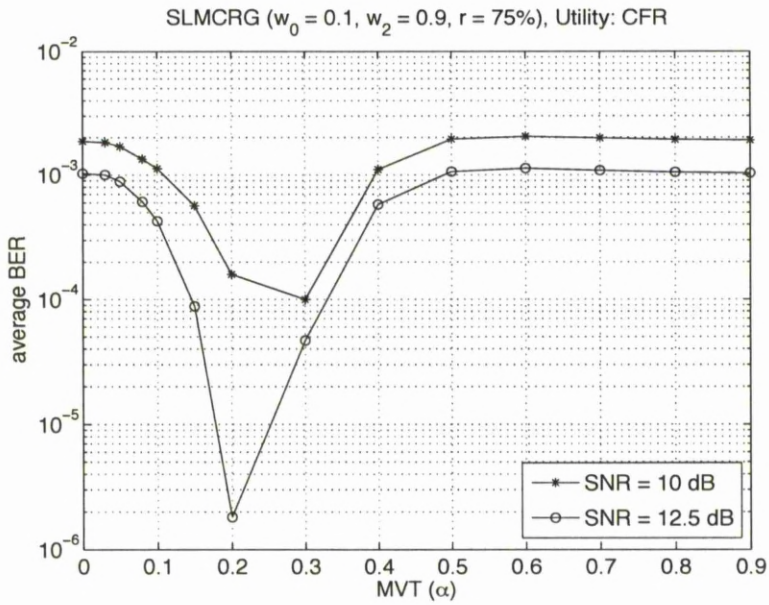

Figure 5.11: Average BER performance of the $r = 75\%$ SLMCRG algorithm under different α values with $U = 100$ users and $w_0 = 0.1$ and $w_2 = 0.9$.

between the RC weights w_0 and w_2 were varied ($-1 \leq w_0 - w_2 \leq 1$). Then the values with the best performances were chosen. Figures 5.10 and 5.11 help to demonstrate this concept.

Figure 5.10 demonstrates the effect of varying the RC weights for the SLMCRG algorithm with $r = 75\%$. Both weights are represented by varying $w_0 - w_2$, since it is already known that $w_0 + w_2 = 1$. At $w_0 - w_2 = 1$, *i.e.*, ($w_0 = 1$, $w_2 = 0$), the SLMCRG greedy algorithm reduces to the CFR based SLMEG algorithm. At SNR =12.5 dB, the BER is close to 10^{-6}, where its best performance is between $-0.8 \leq w_0 - w_2 \leq -0.4$, *i.e.*, ($0.7 \leq w_0 \leq 0.9$ and $0.3 \leq w_2 \leq 0.1$). This implies that f_2 is more important and has a greater impact on delivering a ranking (user-order) that produces acceptable results. It can be observed that at high SNRs, the weights for different criteria have a larger effect on the performance of the SLMCRG algorithm, similar to what was observed in the MCRG algorithm.

Figure 5.11 illustrates the impact of α on the BER performance of the SLMCRG algorithm with $r = 75\%$, $w_0 = 0.1$ and $w_2 = 0.9$. The best performance is $\alpha = 0.2$ for SNR =12.5 dB and $\alpha = 0.3$ for the SNR =10 dB. Nevertheless, $\alpha = 0.2$ is still suitable for SNR = 10 dB, because the performance difference is negligible. Therefore $\alpha = 0.2$ is used in all other simulations. This implies that for near optimal BER performance, the probability of an allocated PRB having a CFR value lower than 0.2, should be minimised.

Figure 5.12 illustrates the performance of the SLMCRG in comparison to that of SLMEG, both with r=50%. The SLMCRG algorithm uses two ranking criteria, f_0 ($w_0 = 0.1$) and f_2 ($w_2 = 0.9$). Notice that the BER utility based SLMEG algorithm does not have the best performance across most SNR values. For this case, a varying α is required for effective performance of the SLMCRG algorithm with r=50% selectivity and CFR utility. Table 5.9 shows the values for α used for this simulation. The fixed $\alpha = 0.1$ SLMCRG mode is shown for comparison, which is approximately 2 dB worse

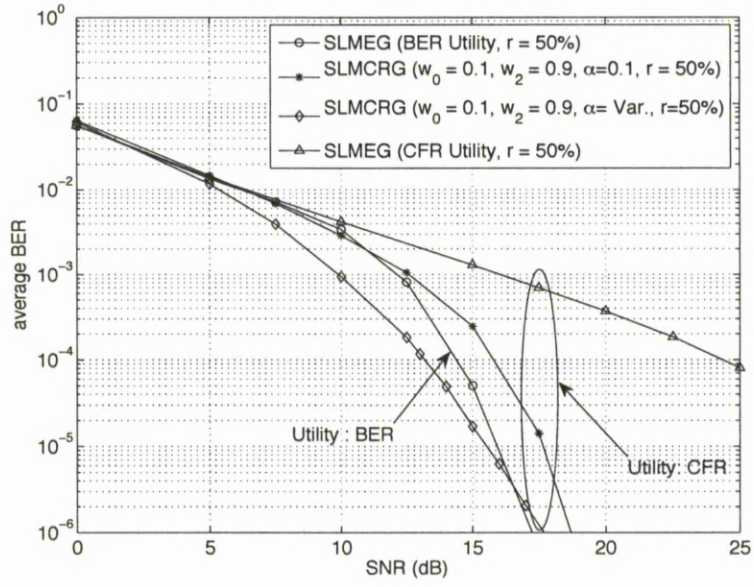

Figure 5.12: Average BER performance of the SLMEG and SLMCRG algorithms with $r = 50\%$ and $U = 100$ users.

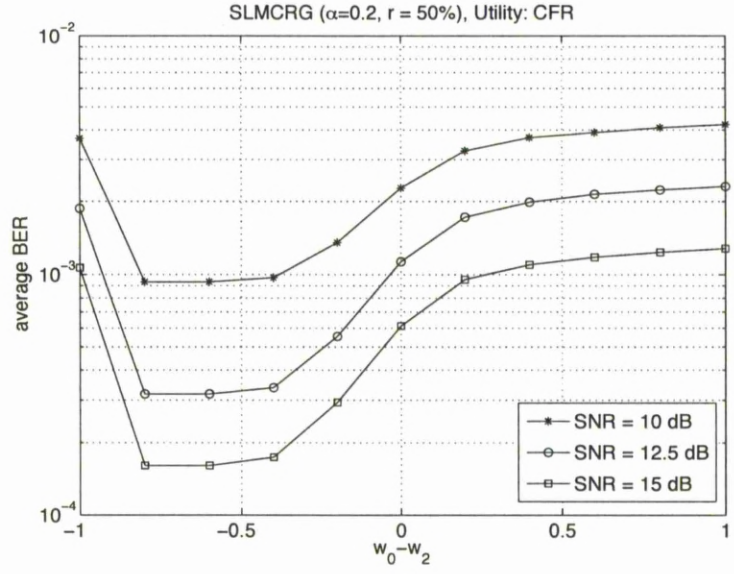

Figure 5.13: Average BER performance of the SLMCRG algorithm with $r = 50\%$ and $\alpha = 0.2$ under varying RC weights with $U = 100$ users and $w_0 + w_2 = 1$.

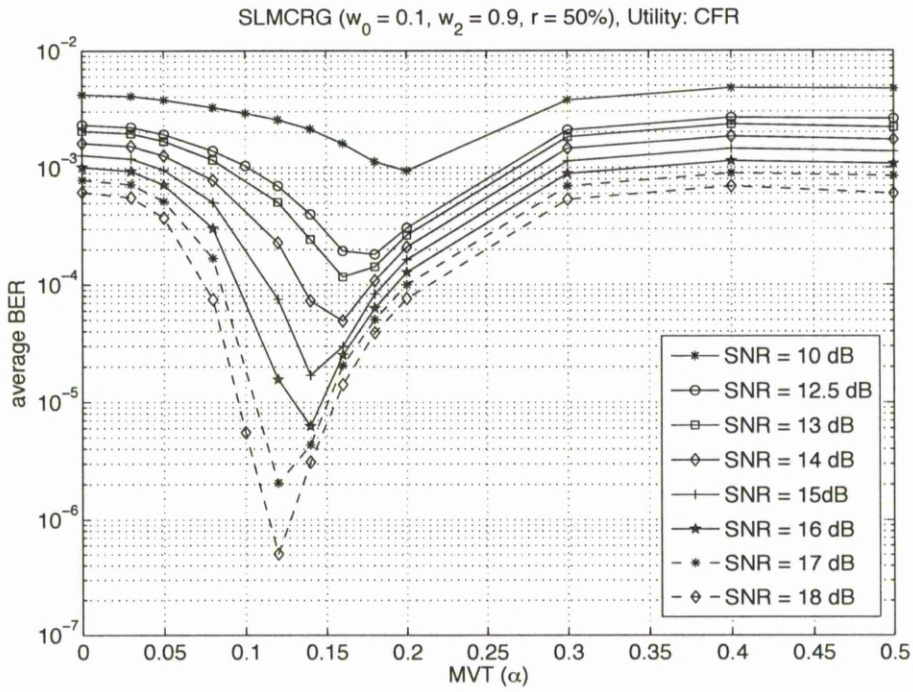

Figure 5.14: Average BER performance of the $r = 50\%$ SLMCRG algorithm under different α values with $U = 100$ users and $w_0 = 0.1$ and $w_2 = 0.9$.

than the BER utility based SLMEG algorithm at a BER of 10^{-5}. The CFR utility based SLMEG algorithm has the worst performance which is approximately 12 dB and 8 dB worse than both SLMCRG (variable α and $\alpha = 0.1$) configurations, at BER $= 10^{-4}$, respectively.

Figure 5.13 demonstrates the effect of varying the RC weights for the $r = 50\%$ SLMCRG algorithm. Similar to Figure 5.10, both weights are represented by varying $(w_0 - w_2)$ with $w_0 + w_2 = 1$. At all the SNR values, the best performance is between $-0.8 \leq w_0 - w_2 \leq -0.4$, *i.e.*, $(0.7 \leq w_0 \leq 0.9$ and $0.3 \leq w_2 \leq 0.1)$. This implies that f_2 is more important and has a greater impact on delivering a ranking (user-order) that produces acceptable results. When $w_0 - w_2 = 1$, *i.e.*, $(w_0 = 1, w_2 = 0)$, the SLMCRG (w_0, w_2) algorithm reduces to the CFR utility based SLMEG algorithm.

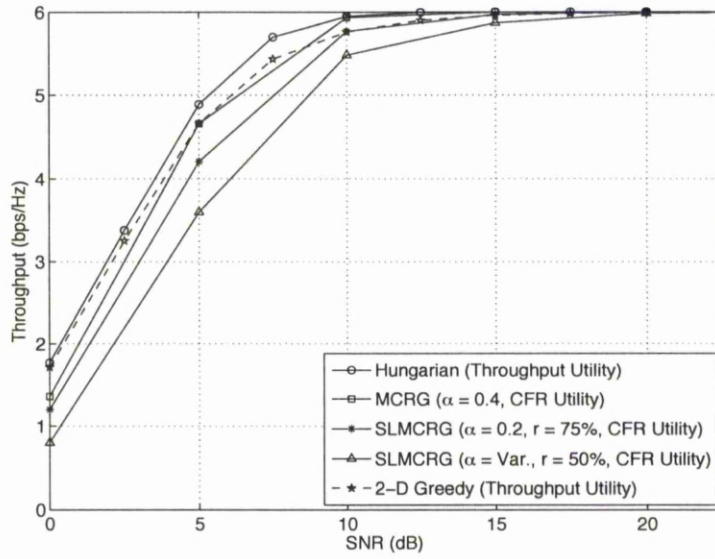

Figure 5.15: Average throughput performance of the algorithms with $U = 100$ users. $w_0 = 0.1$ and $w_2 = 0.9$ for the MCR algorithms.

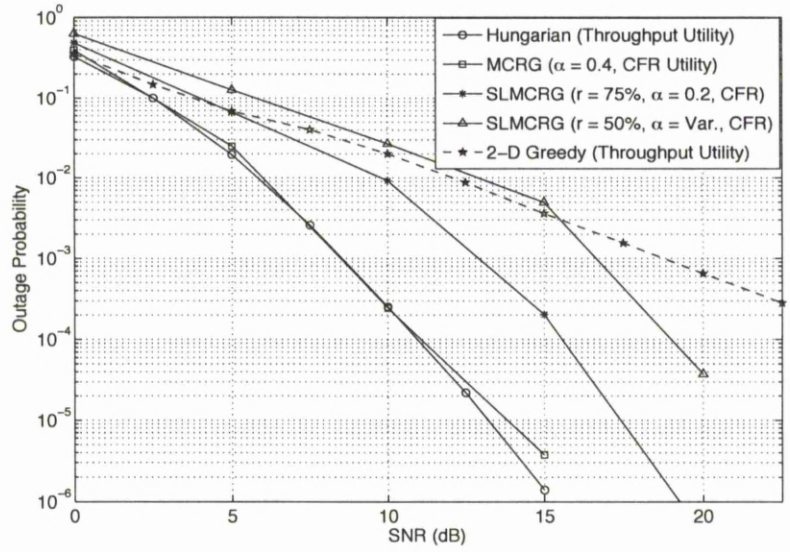

Figure 5.16: Outage probability performance of the algorithms with $U = 100$ users. $w_0 = 0.1$ and $w_2 = 0.9$ for the MCR algorithms.

Figure 5.14 illustrates the impact of α on the BER performance of the CFR based SLMCRG algorithm with $w_1 = 0.1$ and $w_3 = 0.9$. The optimal α value is slightly different for different SNRs. This numerical simulation is used to determine the values of Table 5.9. For lower SNR values, α between 0.15 and 0.2 is acceptable. But at higher SNR values, α lies between 0.1 and 0.15. This implies that as the SNR increases, the required CFR per PRB reduces, which was the same conclusion derived from Figure 5.4.

Figures 5.15 and 5.16 show the average throughput and outage probability performance, respectively, of the CFR utility based MCR algorithms. The optimal throughput utility based Hungarian algorithm and the 2-D greedy algorithm are also shown for comparison. The throughput of the 2-D algorithm achieves near optimal throughput at low SNR, however, the CFR utility based MCRG algorithm achieves a similar performance to the Hungarian algorithm at SNR = 10 dB and above. The outage probability of the MCRG algorithm is similar to the Hungarian algorithm at all SNR values with a much lower computational complexity. The CFR utility based SLMCRG algorithms achieve near optimal throughput performance at high SNR, and outperform the 2-D greedy algorithm in terms of outage probability at high SNR with a much lower computational complexity.

Figures 5.17, 5.18 and 5.19 show the BER, throughput and outage probability performances of the MCRG algorithm under the CFR utility for the WiMAX band AMC settings. These settings have been previously described in Section 4.5.6. The optimal performances, provided by the BER and throughput utility based Hungarian algorithms are included for comparison. The MCRG algorithms provide the same performance trends like the LTE system. The MCRG (w_0, w_2, α) algorithm under the T.U. 6 channel outperforms the MCRG (w_0, w_1) algorithm. However, under the Ped. B channel and at high SNR, the MCRG (w_0, w_1) outperforms the corresponding MCRG (w_0, w_1, α) algorithm under the T.U. 6 channel. This is due to the fact that the mean

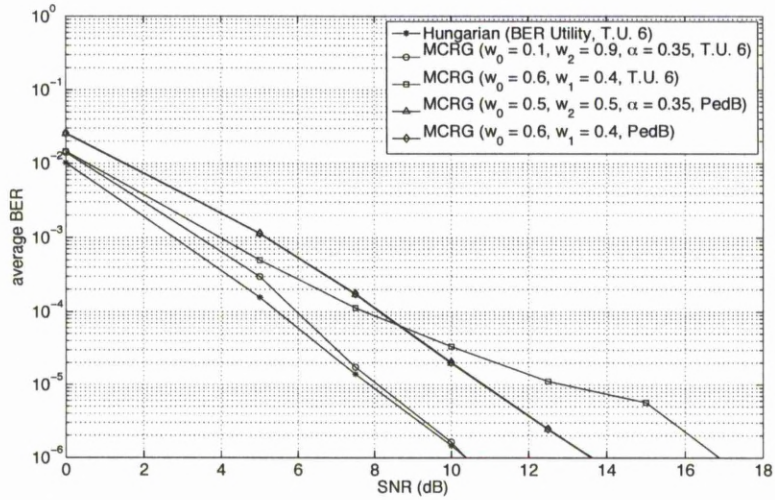

Figure 5.17: Average BER performance of the MCRG algorithms for the WiMAX Band AMC under both the T.U. 6 and Ped. B channels for $U = 48$ users.

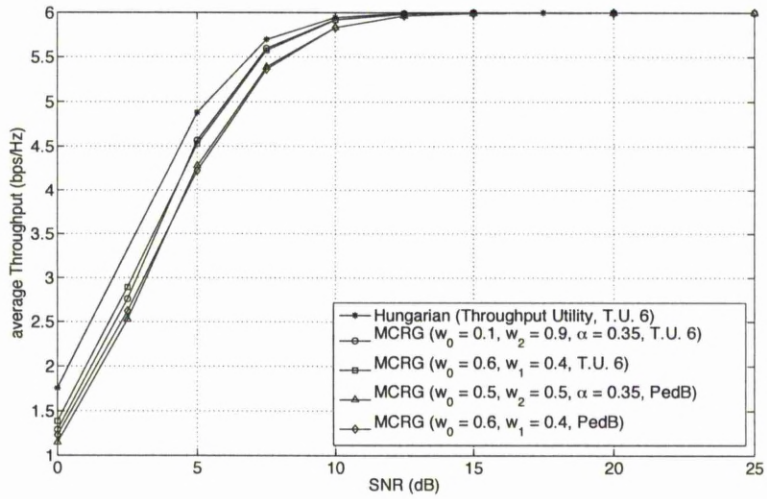

Figure 5.18: Average throughput performance of the MCRG algorithms for the WiMAX Band AMC under both the T.U. 6 and Ped. B channels for $U = 48$ users.

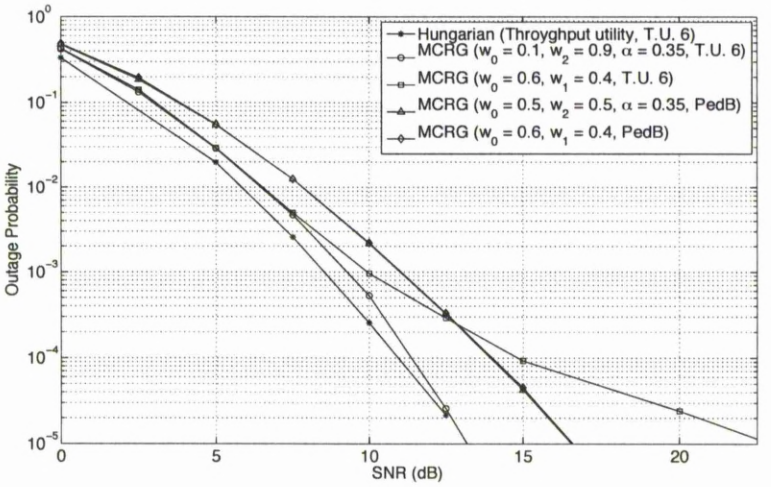

Figure 5.19: Outage probability performance of the MCRG algorithms for the WiMAX Band AMC under both the T.U. 6 and Ped. B channels for $U = 48$ users.

and standard deviation RC do not have the ability to provide a suitable user-order in a channel with high RMS delay spread (high frequency diversity). This implies that the MVT criterion is more efficient at ordering the users in terms of performance in a richly scattered channel, as was the case under the LTE system.

5.7 Summary

In this chapter, MCR based greedy PRB allocation algorithms are proposed. A combination of two MCDA methods, the Electre I and the Promethee II, is used to design a MCR technique that efficiently rank the users' PRB performance before greedy PRB allocation. This ranking is an extension of the single criterion ranking in Chapter 4, because at least two RC are used to find the user-order, with which the greedy algorithm allocates PRBs to users.

A so-called MCRG algorithm is proposed, which always provides near optimal BER, SE and outage probability performance, irrespective of the optimisation utility em-

ployed. This is achieved by using the proposed MCR technique to rank the users, according to multiple RC, simultaneously. The user-order is then used with the 1-D greedy algorithm to complete the PRB allocation process. The CFR utility based MCRG algorithm, particularly benefits from this because the CFR is readily available, and does not require additional computations. Three ranking criteria are proposed: f_0 which is the mean of the users' utility values similar to Chapter 4, f_1 which is related to the STD of the users' utility values and f_2 which is the threshold below (or above for BER) which the PRB CFR value should not be allocated. f_2 is the most suitable for the CFR utility, because the range CFR values are static and do not change with changing SNR. These criteria are used in pairs, (f_0, f_1) and (f_0, f_2) to rank the users' performances, and the resulting user-order is utilised by the 1-D greedy algorithm to provide efficient PRB allocation.

Precise calibration of the parameters needed for the accurate operation of the MCRG algorithm is essential. It is found, using simulation (extensive sensitivity and robustness analysis), that the RC weights are optimal at $w_0 = 0.4$ and $w_1 = 0.6$ for criteria (f_0, f_1) and $w_0 = 0.1$ and $w_2 = 0.9$ for criteria (f_0, f_2). In addition, it is found that an acceptable threshold for the f_2 criterion is about 0.4 across a wide range of SNR values. The performance of the MCRG algorithm provides a near optimal BER performance using the parameters above, especially with a large number of users in the system.

Furthermore, similar to chapter 4, the MCR technique is coupled with the SG algorithm to reduce the complexity of the overall PRB allocation process. The so-called SLMCRG algorithm is proposed which is computationally cheaper than the MCRG algorithm. It is shown that the proposed CFR utility based SLMCRG algorithm has the lowest computational complexity, far lower than its BER utility based SLMEG counterpart, but still provides efficient performances, especially at high SNR levels. Similarly, the sensitivity and robustness simulations are used to determine the efficient

operating values for the parameters in the SLMCRG algorithm. It is shown that the RC weights are best at $w_0 = 0.1$ and $w_2 = 0.9$. $\alpha = 0.2$ is best the best threshold when the greedy algorithm is applied to a selection of r=75% users, while a varying (best value changes with increasing SNR) α is suitable for $r = 50\%$. In general α reduces with increasing SNR.

The complexities of the proposed algorithms are also derived. The complexity of the MCR technique depends on the RC used. It is possible to use more than $C = 2$ RC simultaneously, however, the complexity quickly becomes intractable with an increase in the number of RC. Furthermore, carrying out sensitivity and robustness analysis for $C > 2$ RC is very cumbersome. The total complexity of the MCRG PRB allocation algorithm is the complexity of performing MCR added to the complexity of the 1-D greedy algorithm. The SLMCRG algorithm further reduces the complexity of the overall PRB allocation by combining the efficient MCR with the low complexity SG algorithm. Therefore, the MCRG and SLMCRG algorithms provide efficient PRB allocation, without incurring excessive operational costs.

Table 5.7: Best values of the weights for the MCRG (f_0, f_1) algorithm with different number of users (U) in the system.

Number of Users	SNR (dB)	w_0	w_1
6	5	0.7 - 1	0.3 - 0
	7.5	0.7	0.3
	10	0.6 - 0.7	0.4 - 0.3
	12.5	0.7	0.3
12	5	0.7	0.3
	7.5	0.6 - 0.7	0.4 - 0.3
	10	0.6 - 0.7	0.4 - 0.3
	12.5	0.6	0.4
25	5	0.6 - 0.7	0.4 - 0.3
	7.5	0.5 - 0.6	0.5 - 0.4
	10	0.5 - 0.6	0.5 - 0.4
	12.5	0.6 - 0.7	0.4 - 0.3
50	5	0.6	0.4
	7.5	0.5 - 0.6	0.5 - 0.4
	10	0.5 - 0.6	0.5 - 0.4
	12.5	0.6	0.4
75	5	0.6 - 0.7	0.4 - 0.3
	7.5	0.5 - 0.6	0.5 - 0.4
	10	0.6	0.4
	12.5	0.6	0.4
100	5	0.6 - 0.7	0.4 - 0.3
	7.5	0.6	0.4
	10	0.5 - 0.6	0.5 - 0.4
	12.5	0.6	0.4
48 - WiMAX	5	0.6	0.4
	7.5	0.5 - 0.6	0.5 - 0.4
	10	0.5 - 0.6	0.5 - 0.4
	12.5	0.6	0.4

Table 5.8: Best values of the weights and α parameter for the MCRG (f_0, f_2, α) algorithm with different number of users (U) in the system.

Number of Users (U)	SNR (dB)	α	w_0	w_2
6	5	0.45	0.1	0.9
	7.5	0.4		
	10	0.35 - 0.4		
12	5	0.45	0.1	0.9
	7.5	0.4		
	10	0.35		
25	5	0.4 - 0.45	0.1	0.9
	7.5	0.4		
	10	0.35		
50	5	0.4 - 0.45	0.1	0.9
	7.5	0.35 - 0.4		
	10	0.3 - 0.35		
75	5	0.45	0.1	0.9
	7.5	0.35 - 0.4		
	10	0.3 - 0.4		
100	5	0.45	0.1	0.9
	7.5	0.35 - 0.45		
	10	0.3 - 0.4		
48 - WiMAX	5	0.4 - 0.45	0.1	0.9
	7.5	0.35 - 0.4		
	10	0.3 - 0.35		

Table 5.9: Values of α for each SNR in Figure 5.12

SNR (dB)	0	5	7	10	12.5	13	14	15	16	17	18
α	0.2	0.2	0.2	0.2	0.18	0.16	0.16	0.14	0.14	0.12	0.12

Chapter 6

Conclusions and Future Work

6.1 Conclusions

This thesis has focused on developing high performance, computationally efficient PRB allocation algorithms for the 4G wireless communication systems. The proposed algorithms all have a better trade-off between the BER, SE and performances when compared to the existing 1-D and 2-D greedy algorithms. They also have much lower computational complexity than the optimal Hungarian algorithm.

In Chapter 4, three enhanced ranking greedy algorithms, referred to as the MG, MEG and SMEG algorithms are proposed.

The MG algorithm carefully selects user-orders and performs the 1-D greedy algorithm for all the chosen user-orders. The PRB allocation that corresponds to the best user-order is used. The MG algorithm has scalable computational complexity, however, as the number of selected user-orders increases, the complexity of the MG algorithm rapidly increases, however it is shown that for system with U users, the best out U user-orders always provides satisfactory average BER performances. Its performance is always within a few dB of the Hungarian (optimal) algorithm performance. In terms of optimisation utility, the MG algorithm simultaneously has near optimal BER, SE

and outage probability performances under the BER utility. However, its performances under the other utilities is poor, especially the CFR and OSINR utilities.

The MEG algorithm determines its user order dynamically by always selecting the user that has the lowest mean PRB performance in every iteration. Its computational complexity is fixed and is about 5.5 times lower than the Hungarian algorithm and 69 times higher than the 1-D greedy algorithm, for a 100-user system. The MEG algorithm always provides similar BER, SE and outage probability performances irrespective of the optimisation utility employed. If the cost of estimating the utility is negligible, then the MEG algorithm will have the best performance-complexity trade-off. Nevertheless, the iterative recalculation of the mean makes the complexity grow quickly for a large number of users.

The SMEG algorithm tackles the fairly high computational complexity of the MEG algorithm by calculating and sorting the users' PRB mean performance only once. The sorted user list, is used as the single user-order. This drastically reduces the complexity because only one 1-D greedy algorithm is used (unlike the MG algorithm) and only one mean calculation is required (unlike the MEG algorithm). The SMEG algorithm is just 3 times as complex as the 1-D greedy algorithm. It is 125, 23 and 33 times less complex than the Hungarian, MEG and MG algorithms, respectively. However, it is shown that the SMEG algorithm provides a near optimal BER performance with the BER utility, a reasonable BER performance with the SE utility and poor performance with the CFR and OSINR utilities.

Finally, in chapter 4, based on the enhanced rankings, a so called SLMEG algorithm is proposed, which further reduces the overall complexity of the enhanced ranking based greedy PRB allocation by selectively optimising PRB allocation for a fraction of the available users in the system. It is implemented in a way that the poorly ranked users are selected to optimise their PRB allocation, while the remaining highly ranked users are randomly allocated PRBs. Intuitively, these random PRB allocations do not

incur any cost. Nevertheless, the BER utility based SLMEG algorithm outperforms the 1-D and 2-D greedy algorithm in terms of both the BER and outage probability performances, especially at high SNRs. The SLMEG algorithm is only about 2.5 times as complex as the 1-D greedy algorithm and about 27 times less complex than the 2-D greedy algorithm.

In chapter 5, the issue of varying performances under different optimisation utilities is tackled. A so-called MCRG algorithm is proposed, which provides near optimal PRB allocation, irrespective of the optimisation utility employed. The MCRG algorithm is a combination of a MCR technique and the 1-D greedy algorithm. The MCR is a technique that ranks users according to multiple criteria, simultaneously, which is unlike the single criterion mean ranking in Chapter 4. The MCR technique is created from a combination of two classic MCDA methods, the Electre I and Promethee II. The three RC are considered in this work are the mean (similar to chapter 4), the STD and the MVT. The best pair of RC - the mean with weight, $w_1 = 0.1$ and MVT with weight $w_3 = 0.9$ and threshold $\alpha = 0.4$ - are found by extensive numerical simulations. The computational complexity of the CFR utility based MCRG algorithm is about 9 times more than that of the 1-D greedy algorithm, while the comparable BER utility SMEG algorithm is about 154 times more complex than the 1-D greedy algorithm.

Furthermore, a reduced complexity SLMCRG algorithm is proposed in chapter 5. It is a combination of the MCR technique and the SG algorithm proposed in chapter 4. The superior ranking of the MCR is exploited to provide sufficient BER and outage probability performances with the CFR utility based SLMCRG algorithm. The CFR utility based SLMCRG algorithm outperforms the 1-D greedy algorithm, 2-D greedy algorithm and the CFR utility based SLMEG counterpart, especially at high SNRs. The CFR utility based SLMCRG algorithm BER and outage probability performances is similar to that of the BER based SLMEG algorithm. The CFR utility based SLMCRG algorithm is about 19 times less complex than the BER utility based

SLMEG algorithm.

6.2 Future Work

These PRB allocation algorithms can be extended to multiple input multiple output (MIMO) systems, especially the high performance CFR utility based versions, because the BER of MIMO systems is even more challenging to estimate, particularly in the presence adaptive FEC. Furthermore, the MCR can be used with virtual MIMO (also known as CSM) systems, to select a pair of users that simultaneously share the same time and PRB resources.

The MCDA techniques have been rarely used in wireless communications. There are many case scenarios in wireless communications that could benefit from dynamically selecting algorithms from the various algorithms which exist. For example, if all the users in the system have high channel link quality across the whole bandwidth, then the 1-D greedy algorithm can be selected and if some users have highly varying channel link qualities, then the MCRG algorithm can be selected. Furthermore, in some instances, the ZF equaliser could perform better than the MMSE equaliser and vice versa, so the MCR technique could be used to automatically select an equaliser in one TTI and another equaliser for the next TTI. This dynamic selection of algorithms is made possible by software defined radio, where different algorithms and techniques could be loaded onto the digital signal processing (DSP) and selected for use in real time. Decision aid techniques would certainly benefit resource allocation for cognitive radio.

Extensive simulations should be carried out to determine the suitable operating parameters for all the algorithms under different kinds of wireless channels and systems. In addition, less complex RC can be found, because as shown in this work, estimating the mean and STD for all the users in the system can be quite complex, even more complex than the greedy PRB allocation itself.

Bibliography

[1] 3rd Generation partnership project (3GPP), "Technical specification group radio access network," 2008.

[2] IEEE 802.16 Broadband Wireless Access Working Group, "IEEE 802.16m System Requirements," 2007.

[3] E. Dahlman, S. Parkvall, J. Skold, and P. Beming, *3G Evolution: HSPA and LTE for mobile broadband.* London, UK: Academic Press, 2007.

[4] H. Yaghoobi, "Scalable OFDMA physical layer in IEEE 802.16 wirelessMAN," *Intel technology journal*, vol. 8, no. 3, 2004.

[5] 3GPP TR 36.913, v9.0.0, "Requirements for further advancements for evolved universal terrestrial radio access (E-UTRA) (LTE-advanced)," 2009.

[6] ITU-R Recommendations M.2134, "Requirements related to technical performance for IMT-Advanced radio interface(s)," 2008.

[7] Z. Wang and G. Giannakis, "Wireless multicarrier communications," *Signal Processing Magazine, IEEE*, vol. 17, no. 3, pp. 29 –48, May 2000.

[8] H. Myung, "Single carrier orthogonal multiple access technique for broadband wireless communications," Dissertation, Polytechnic University, New York (NY), 2007.

[9] S. Haykin and M. Moher, *Modern Wireless Communication.* Upper Saddle River, NJ, USA: Prentice-Hall, Inc., 2004.

[10] C. Ciochina, D. Mottier, and H. Sari, "An analysis of OFDMA, precoded OFDMA and SC-FDMA for the uplink in cellular systems," in *Multi-Carrier Spread Spectrum 2007*, ser. Lecture Notes in Electrical Engineering, S. Plass, A. Dammann, S. Kaiser, and K. Fazel, Eds. Springer Netherlands, 2007, vol. 1, pp. 25–36.

[11] X. Huang, "Diversity performance of precoded OFDM with MMSE equalization," in *International Symposium on Communications and Information Technologies Proceedings*, Sydney, Australia, 2007, pp. 802–807.

[12] F. Pancaldi and G. Vitetta, "Block channel equalization in the frequency domain," *IEEE Transactions on Communications*, vol. 53, no. 3, pp. 463 – 471, march 2005.

[13] F. Calabrese, M. Anas, C. Rosa, P. Mogensen, and K. Pedersen, "Performance of a radio resource allocation algorithm for UTRAN LTE uplink," in *IEEE 65th Vehicular Technology Conference, VTC-Spring.*, April 2007, pp. 2895 –2899.

[14] J. Jang and K. B. Lee, "Transmit power adaptation for multiuser OFDM systems," *IEEE Journal on Selected Areas in Communications*, vol. 21, no. 2, pp. 171 – 178, Feb 2003.

[15] C. Wengerter, J. Ohlhorst, and A. von Elbwart, "Fairness and throughput analysis for generalized proportional fair frequency scheduling in OFDMA," in *IEEE 61st Vehicular Technology Conference, VTC-Spring*, vol. 3, May 2005, pp. 1903 – 1907.

[16] Z. Shen, J. Andrews, and B. Evans, "Adaptive resource allocation in multiuser OFDM systems with proportional rate constraints," *IEEE Transactions on Wireless Communications*, vol. 4, no. 6, pp. 2726–2737, Nov. 2005.

[17] G. Song and Y. Li, "Adaptive subcarrier and power allocation in OFDM based on maximizing utility," in *57th IEEE Vehicular Technology Conference, VTC-Spring*, vol. 2, Jelu, Korea, April 2003, pp. 905 – 909.

[18] D. Niyato and E. Hossain, "Adaptive fair subcarrier/rate allocation in multirate OFDMA networks: Radio link level queuing performance analysis," *IEEE Transactions on Vehicular Technology*, vol. 55, no. 6, pp. 1897 –1907, November 2006.

[19] E. Bakhtiari and B. Khalaj, "A new joint power and subcarrier allocation scheme for multiuser OFDM systems," in *IEEE 14th Personal, Indoor and Mobile Radio Communications,*, vol. 2, September 2003, pp. 1959 – 1963.

[20] K. Kim, Y. Han, and S.-L. Kim, "Joint subcarrier and power allocation in uplink OFDMA systems," *IEEE Communications Letters*, vol. 9, no. 6, pp. 526 – 528, Jun 2005.

[21] D. Kivanc, G. Li, and H. Liu, "Computationally efficient bandwidth allocation and power control for OFDMA," *IEEE Transactions on Wireless Communications*, vol. 2, no. 6, pp. 1150 – 1158, Nov 2003.

[22] C. Y. Wong, R. Cheng, K. Letaief, and R. Murch, "Multiuser OFDM with adaptive subcarrier, bit, and power allocation," *IEEE Journal on Selected Areas in Communications*, vol. 17, no. 10, pp. 1747–1758, Oct 1999.

[23] Y. Kwon, K. H. Han and S. Kim, "Efficient subcarrier and power allocation algorithm in OFDMA uplink system," *IEICE Transactions on Communications*, vol. E90-B, no. 2, 2007.

[24] K. A. D. Teo, Y. Otani, and S. Ohno, "Adaptive subcarrier allocation for multiuser OFDM system," *IEICE Trans. Fundam. Electron. Commun. Comput. Sci.*, vol. E89-A, no. 11, pp. 3131–3137, 2006.

[25] C. Y. Wong, C. Tsui, R. Cheng, and K. Letaief, "A real-time sub-carrier allocation scheme for multiple access downlink OFDM transmission," in *IEEE 50th Vehicular Technology Conference, VTC - Fall*, Amsterdam, Netherlands, 1999, pp. 1124–1128.

[26] J. Andrews, A. Ghosh, and R. Muhamed, *Fundamentals of WiMAX*. New Jersey: Prentice Hall, 2007.

[27] Y. Kim and J. Kim, "A 2-D subcarrier allocation scheme for capacity enhancement in a clustered OFDM system," *IEICE Transactions on Communications*, vol. E90-B, no. 7, pp. 1880 – 1883, 2007.

[28] J. Lim, H. Myung, K. Oh, and D. Goodman, "Channel-dependent scheduling of uplink single carrier FDMA systems," in *IEEE 64th Vehicular Technology Conference, VTC-Fall*, Montreal, Canada, Sept 2006, pp. 1–5.

[29] ——, "Proportional fair scheduling of uplink single-carrier FDMA systems," in *IEEE 17th International Symposium on Personal, Indoor and Mobile Radio Communications*, Helsinki, Finland, Sept. 2006, pp. 1–6.

[30] J. Munkres, "Algorithms for the assignment and transportation problems," *Journal of the Society for Industrial and Applied Mathematics*, vol. 5, no. 1, pp. 32–38, 1957.

[31] Y. Wang, F. Chen, and G. Wei, "Adaptive subcarrier and bit allocation for multiuser ofdm system based on genetic algorithm," in *International Conference on Communications, Circuits and Systems*, vol. 1, Hong Kong, China, 27-30 2005, pp. 242 – 246.

[32] W. C. Jakes, *Microwave mobile communications*. New York: John Wiley, 1974.

[33] T. Rappaport, *Wireless Communications: Principles and Practice.* Upper Saddle River, NJ, USA: Prentice Hall PTR, 2001.

[34] J. G. Proakis, *Digital Communications.* Singapore: McGraw-Hill, 2001.

[35] K. Baddour and N. Beaulieu, "Autoregressive modeling for fading channel simulation," *IEEE Transactions on Wireless Communications*, vol. 4, no. 4, pp. 1650 – 1662, July 2005.

[36] A. Pauraj, R. Nabar, and D. Gore, *Introduction to space-time wireless communications.* Cambridge: Cambridge University Press, 2003.

[37] G. Yuan, X. Zhang, W. Wang, and Y. Yang, "Carrier aggregation for LTE-advanced mobile communication systems," *IEEE Communications Magazine*, vol. 48, no. 2, pp. 88 –93, February 2010.

[38] IEEE 802.16 Broadband Wireless Access Working Group, "IEEE 802.16m System Requirements," 2007.

[39] C.-X. Wang, X. Hong, X. Ge, X. Cheng, G. Zhang, and J. Thompson, "Cooperative MIMO channel models: A survey," *IEEE Communications Magazine*, vol. 48, no. 2, pp. 80 –87, february 2010.

[40] K. Balachandran, D. Calin, N. Gopalakrishnan, J. H. Kang, A. Kogiantis, S. Li, L. Ozarow, S. Ramakrishna, A. N. Rudrapatna, and R. Sun, "Design and performance analysis of collaborative spatial multiplexing for ieee 802.16e-based systems," *Bell Lab. Tech. J.*, vol. 13, no. 4, pp. 97–117, 2009.

[41] X. Chen, H. Hu, H. Wang, H. hwa Chen, and M. Guizani, "Double proportional fair user pairing algorithm for uplink virtual mimo systems," *IEEE Transactions on Wireless Communications*, vol. 7, no. 7, pp. 2425 –2429, july 2008.

[42] 3GPP TR 36.814, v9.0.0, "Further advancements for e-utra physical layer," 2010.

[43] W. Forum, "Wimax and the ieee 202.16m air interface standard - april 2010," 2010.

[44] T. Keller and L. Hanzo, "Adaptive multicarrier modulation: a convenient framework for time-frequency processing in wireless communications," *Proceedings of the IEEE*, vol. 88, no. 5, pp. 611 –640, May 2000.

[45] G. Tsoulos, "Experimental and theoretical capacity analysis of space-division multiple access (SDMA) with adaptive antennas," *IEE Proceedings-Communications*, vol. 146, no. 5, pp. 307 –311, oct 1999.

[46] S. Weinstein and P. Ebert, "Data transmission by frequency-division multiplexing using the discrete fourier transform," *IEEE Transactions on Communication Technology*, vol. 19, no. 5, pp. 628 –634, October 1971.

[47] J. Bingham, "Multicarrier modulation for data transmission: an idea whose time has come," *IEEE Communications Magazine*, vol. 28, no. 5, pp. 5 –14, May 1990.

[48] J. Coon, M. Beach, S. Armour, and J. McGeehan, "Adaptive frequency domain equalisation for single carrier multiple-input multiple-output wireless transmissions," *IEEE Transactions on Signal Processing*, vol. 53, no. 8, 2005.

[49] N. Lashkarian and S. Kiaei, "Class of cyclic-based estimators for frequency-offset estimation of OFDM systems," *IEEE Transactions on Communications*, vol. 48, no. 12, pp. 2139 –2149, Dec. 2000.

[50] A. Jayalath and C. Tellambura, "Peak-to-average power ratio of IEEE 802.11 a PHY layer signals," in *Advanced Signal Processing for Communication Systems*, ser. The Kluwer International Series in Engineering and Computer Science, T. A. Wysocki, M. Darnell, and B. Honary, Eds. Springer US, 2002, vol. 703, pp. 83–96.

[51] X. Zhu and R. Murch, "Layered space-frequency equalization in a single-carrier mimo system for frequency-selective channels," *IEEE Transactions on Wireless Communications*, vol. 3, no. 3, pp. 701 – 708, May 2004.

[52] E. Bai and Z. Ding, "Zero-forcing equalizability of FIR and IIR multichannel systems with and without perfect measurements," *IEEE Transactions on Communications*, vol. 48, no. 1, pp. 17 –22, Jan 2000.

[53] X. Zhu and R. Murch, "Performance analysis of maximum likelihood detection in a mimo antenna system," *IEEE Transactions on Communications*, vol. 50, no. 2, pp. 187 –191, Feb. 2002.

[54] M. Bradley and P. Mars, "Application of multiple channel estimators in MLSE detectors for fast time-varying and frequency selective channels," *Electronics Letters*, vol. 32, no. 7, pp. 620 –621, Mar 1996.

[55] M. Tuchler, A. Singer, and R. Koetter, "Minimum mean squared error equalization using a priori information," *IEEE Transactions on Signal Processing*, vol. 50, no. 3, pp. 673 –683, March 2002.

[56] I. Kalet, "The multitone channel," *IEEE Transactions on Communications*, vol. 37, no. 2, pp. 119 –124, Feb 1989.

[57] R. Grunheid, E. Bolinth, and H. Rohling, "A blockwise loading algorithm for the adaptive modulation technique in ofdm systems," in *IEEE 54th Vehicular Technology Conference, 2001. VTC-Fall*, vol. 2, 2001, pp. 948 –951 vol.2.

[58] D. Dardari, "Ordered subcarrier selection algorithm for OFDM-based high-speed WLANs," *IEEE Transactions on Wireless Communications*, vol. 3, no. 5, pp. 1452 – 1458, sept. 2004.

[59] W. Yu and J. Cioffi, "On constant power water-filling," in *IEEE International Conference on Communications*, vol. 6, 2001, pp. 1665 –1669 vol.6.

[60] A. Wyglinski, F. Labeau, and P. Kabal, "Bit loading with ber-constraint for multicarrier systems," *IEEE Transactions on Wireless Communications*, vol. 4, no. 4, pp. 1383 – 1387, July 2005.

[61] J. Campello, "Optimal discrete bit loading for multicarrier modulation systems," in *IEEE International Symposium on Information Theory*, August 1998, p. 193.

[62] A. Goldsmith and S.-G. Chua, "Variable-rate variable-power MQAM for fading channels," *IEEE Transactions on Communications*, vol. 45, no. 10, pp. 1218–1230, Oct 1997.

[63] ——, "Adaptive coded modulation for fading channels," *IEEE Transactions on Communications*, vol. 46, no. 5, pp. 595 –602, May 1998.

[64] S. T. Chung and A. Goldsmith, "Adaptive multicarrier modulation for wireless systems," in *34th Asilomar Conference on Signals, Systems and Computers*, vol. 2, 2000, pp. 1603 –1607 vol.2.

[65] H. Kim and Y. Han, "A proportional fair scheduling for multicarrier transmission systems," *IEEE Communications Letters*, vol. 9, no. 3, pp. 210 – 212, March 2005.

[66] T. Bonald, "A score-based opportunistic scheduler for fading radio channels," in *in Proc. European Wireless*, 2003.

[67] J. Zhu, B. Bing, Y. G. Li, and J. Xu, "An adaptive subchannel allocation algorithm for ofdm-based wireless home networks," in *IEEE Consumer Communications and Networking Conference*, January 2004, pp. 352 – 356.

[68] J. Shi and A. Hu, "Radio resource allocation algorithm for the uplink OFDMA system," in *IEEE International Conference on Communications Workshops*, May 2008, pp. 11 –15.

[69] I. Ahmed and S. Majumder, "Adaptive resource allocation based on modified genetic algorithm and particle swarm optimization for multiuser ofdm systems," in *International Conference on Electrical and Computer Engineering*, Dhaka, Bangladesh, 20-22 2008, pp. 211 –216.

[70] M. Alasti, B. Neekzad, J. Hui, and R. Vannithamby, "Quality of service in WiMAX and LTE networks [topics in wireless communications]," *IEEE Communications Magazine*, vol. 48, no. 5, pp. 104 –111, May 2010.

[71] H. Myung, K. Oh, J. Lim, and D. Goodman, "Channel-dependent scheduling of an uplink SC-FDMA system with imperfect channel information," in *IEEE Wireless Communications and Networking Conference*, April 2008, pp. 1860 –1864.

[72] M. Rinne, M. Kuusela, E. Tuomaala, P. Kinnunen, I. Kovacs, K. Pajukoski, and J. Ojala, "A performance summary of the evolved 3G (E-UTRA) for voice over internet and best effort traffic," *IEEE Transactions on Vehicular Technology*, vol. 58, no. 7, pp. 3661 –3673, September 2009.

[73] I. Wong, O. Oteri, and W. Mccoy, "Optimal resource allocation in uplink sc-fdma systems," *IEEE Transactions on Wireless Communications*, vol. 8, no. 5, pp. 2161 –2165, May 2009.

[74] H. Wang, C. Rosa, and K. Pedersen, "Performance of uplink carrier aggregation in LTE-advanced systems," in *IEEE 72nd Vehicular Technology Conference, VTC-Fall*, September 2010, pp. 1–5.

[75] M. Ehrgott, *Multicriteria Optimization.* Berlin: Springer, 2005.

[76] H. Zhu and J. Wang, "Chunk-based resource allocation in ofdma systems - part i: chunk allocation," *IEEE Transactions on Communications*, vol. 57, no. 9, pp. 2734 –2744, September 2009.

[77] H. Wu and T. Haustein, "Radio resource management for the multi-user uplink using DFT-precoded OFDM," in *IEEE International Conference on Communications*, Beijing, China, May 2008, pp. 4724–4728.

[78] A. Burr, *Modulation and coding for wireless communications.* London: Prentice Hall, 2001.

[79] P. Mathias, W. Udo, and T. Shiau-He, "Quality determination for a wireless communications link," June 2007.

[80] A. Krishnamoorthy, Y. Blankenship, P. Sartori, K. Baum, and B. Classon, "Enhanced link adaptation methods for wireless multi-carrier systems," in *IEEE 65th Vehicular Technology Conference VTC-Spring*, April 2007, pp. 1911 –1915.

[81] H. W. Kuhn, "The hungarian method for the assignment problem," *Naval Research Logistics Quarterly*, vol. 2, pp. 83–97, 1955.

[82] J. A. Bondy and U. S. R. Murty, *Graph Theory with Applications.* London, UK: Macmillan, 1976.

[83] H. A. B. Saip and C. L. Lucchesi, "Matching algorithms for bipartite graphs," Relatorio Tecnico DCC-03, 1993.

[84] J. Klienberg and E. Tardos, *Algorithm Design.* Boston: Pearson Education Inc, 2006.

[85] S. Grant and J. Cavers, "Performance enhancement through joint detection of cochannel signals using diversity arrays," *IEEE Transactions on Communications*, vol. 46, no. 8, pp. 1038–1049, Aug 1998.

[86] J. Figueira, S. Greco, and M. Ehrgott, *Multiple Criteria Decision Analysis: State of the Art Surveys.* Boston, Dordrecht, London: Springer Verlag, 2005.

[87] Y. Collette and P. Siarry, *Multiobjective Optimization, principles and case studies.* Berlin, Germany: Springer, 2003.

[88] S. Roy and P. Vincke, "Multicriteria analysis: Survey and new directions," *European Journal of Operational Research*, no. 8, pp. 207–218, 1981.

[89] P. Brans, J.P. Vincke and B. Mareschal, "How to select and how to rank projects: The promethee method," *European Journal of Operational Research*, no. 24, pp. 228–238, 1986.

[90] E. Chong and S. Zak, *An Introduction to Optimization.* New Jersey: John Wiley, 2008.

[91] V. T'kindt and J.-C. Billaut, *Multicriteria scheduling.* Berlin: Springer-Verlag, 2006.

[92] M. T. Tabucanon, *Multiple criteria decision making in industry.* New York: Elsevier, 1988.

[93] D. Charilas, O. Markaki, J. Psarras, and P. Constantinou, "Application of fuzzy AHP and ELECTRE to network selection," in *Mobile Lightweight Wireless Systems.* Springer Berlin Heidelberg, 2009, vol. 13, pp. 63–73.

[94] J. Mart andnez Morales, U. Pineda-Rico, and E. Stevens-Navarro, "Performance comparison between madm algorithms for vertical handoff in 4g networks," in *7th International Conference on Electrical Engineering Computing Science and Automatic Control*, September. 2010, pp. 309 –314.

[95] F. Bari and V. C. Leung, "Automated network selection in a heterogeneous wireless network environment," *IEEE Networks*, vol. 21, no. 1, pp. 34 –40, Jan.-February 2007.

[96] F. Bari and V. Leung, "Application of electre to network selection in a heterogeneous wireless network environment," in *IEEE Wireless Communications and Networking Conference*, March 2007, pp. 3810 –3815.